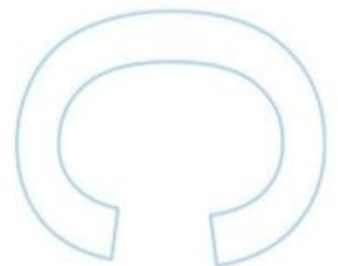
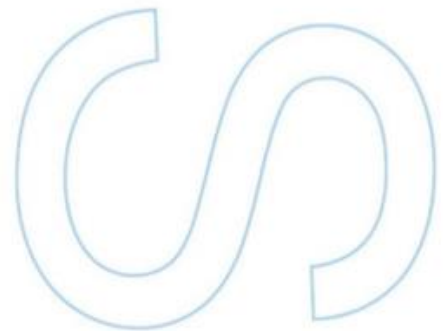
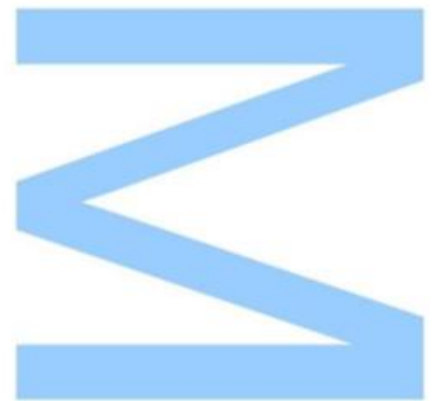


Disclosing the zinc acquisition and homeostatic machinery of *Leishmania* parasites

Teresa Pires de Matos Alves Leão

Dissertação de Mestrado apresentada à
Faculdade de Ciências da Universidade do Porto em
Biologia Celular e Molecular

2019



Disclosing the zinc acquisition and homeostatic machinery of *Leishmania* parasites

Teresa Pires de Matos Alves Leão

MSc in Cell and Molecular Biology

Department of Biology

Faculty of Sciences, University of Porto (FCUP), Portugal

Rua do Campo Alegre 1021/1055, 4169-007 Porto

up201102722@fc.up.pt

2019

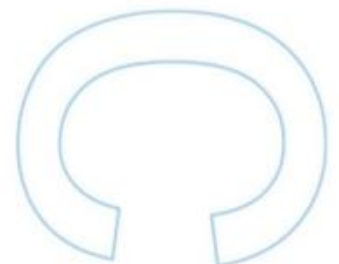
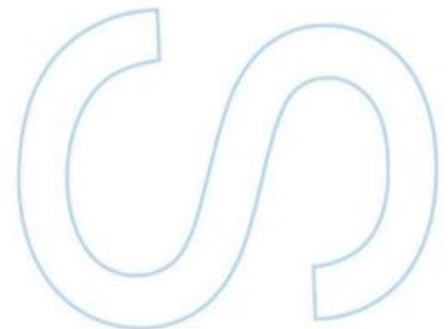
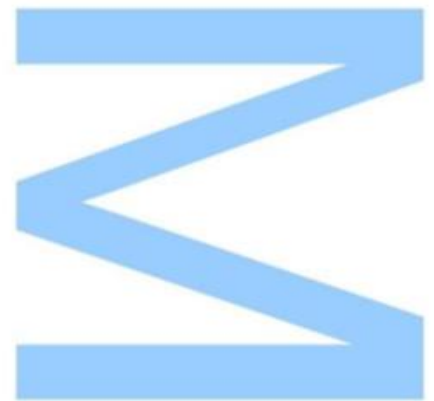
Supervisor:

Ana Maria Luís Ramos Tomás, MSc, PhD

Group Leader, Molecular Parasitology Group, Institute for Molecular and Cell Biology (IBMC), Institute for Research and Innovation in Health, University of Porto (i3S)

Associated Professor, Abel Salazar Institute of Biomedical Sciences, University of Porto (ICBAS)

atomas@ibmc.up.pt

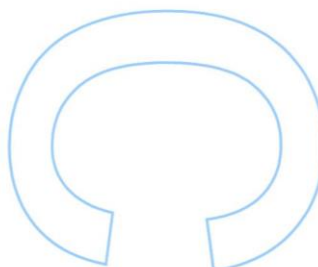
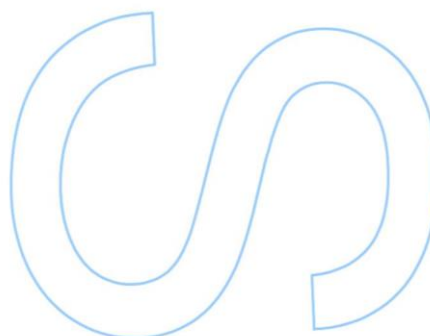
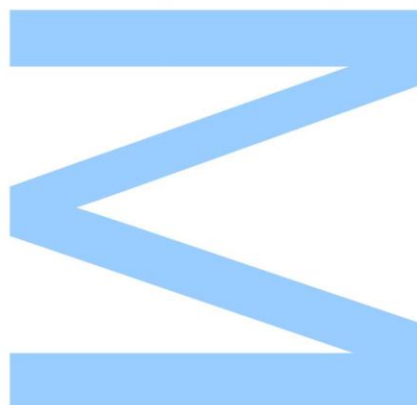




Todas as correções determinadas pelo júri, e só essas, foram efetuadas.

O Presidente do Júri,

Porto, ____/____/____



Authorship declaration

I, Teresa Pires de Matos Alves Leão, student number 201102722 from the Master's Degree in Cell and Molecular Biology, Faculdade de Ciências da Universidade do Porto (2016/2019), hereby declare that I am the sole author of this Dissertation Project and that the contents herein reflect my personal work. I certify that, to the best of my knowledge, this document fully acknowledges every work, published or not, it is based on, in accordance with the standard referencing practices. In such wise, I further declare I understand the consequences of the violation of these conditions.

Teresa Pires de Matos Alves Leão

Porto, September 27, 2019

"To be a scientist is to be naive. We are so focused on our search for truth we fail to consider how few actually want us to find it. But it is always there, whether we see it or not, whether we choose to or not. The truth doesn't care about our needs or wants. It doesn't care about our governments, our ideologies, our religions. It will lie in wait for all time."

Valery Legasov, Chernobyl (HBO, 2019)

Acknowledgments

This project grew with me in the same extent I grew with it, allowing me to achieve one more goal towards my future as a scientist.

There are not enough words to express my gratitude and fulfillment after these years as a young researcher. To all of those who gave me their support throughout this cumbersome journey, those who did not stop believing in me and did not let me give up, to those who assisted me in keeping my focus and determination as sharp as I needed to. I wouldn't accomplish an infinitesimal part of my ambitions if it wasn't for you.

To the Molecular Parasitology Group, IBMC-i3S, for embracing me and constantly teach me way more than protocols. To everyone that constitute(d) the Group and accompanied me through this project, directly or not. I apologize for all the conversations that unintendedly (I swear!), whether I was present or not, were shifted to discussions about zinc. In particular, to Helena Castro and Margarida Duarte, my eternal co-supervisors, for the invaluable knowledge they transmit me, always sparing time to help and support me since I was a naïve Bachelor trainee.

To Professor Ana Tomás, for always believing I will be up to the challenge. For compelling me to push my limits through every opportunity she presents me. For being my scientific role model and support. For sharing this fascinating story with me and walking by my side through it.

To my grandparents, Fernando and Dulce. For the everlasting support of my growth as a human, as a woman, as a student and as a professional. Know my constitutive challenge and goal is to make both of you endlessly honored and proud.

To my mother. A day where I think I deserve you is never to come. I am perpetually grateful for you, and for you never curtailing my dreams. All I am, all I ambition and all I accomplish, I dedicate to you.



This work was financed by Norte-01-0145-FEDER-000012 - Structured program on bioengineered therapies for infectious diseases and tissue regeneration, supported by Norte Portugal Regional Operational Programme (Norte 2020), under the PORTUGAL 2020 Partnership Agreement, through the European Regional Development Fund (FEDER) through the COMPETE 2020 - Operational Program for Competitiveness).

Abstract

Trypanosomatids of the genus *Leishmania* are the agents of the leishmaniasis, a group of neglected chronic diseases affecting millions worldwide, for which there are no vaccines and chemotherapy is problematic. To design innovative therapies, it is imperative to identify the mechanisms enabling parasites to thrive in their hosts. This project focused on the parasite's requirement to scavenge essential nutrients, specifically zinc, from its host.

Transition metals such as zinc are essential for *Leishmania*, yet they can be deleterious if in excess. This dichotomy is often exploited by mammalian hosts to fight infections, in processes collectively designated as "nutritional immunity". To prevail, it is imperative that pathogens rapidly sense host-induced changes in metal bioavailability and translate these into adaptive responses. The Molecular Parasitology Group at i3S endeavours to identify and characterize the players implicated on *Leishmania*'s zinc homeostasis, to which this project contributes to by studying three *Leishmania infantum* proteins: *LZIP1*, *LZIP2* and *LZIP3*.

LZIP3 was the first zinc importer characterized in *Leishmania*¹. Recent studies employing *LZIP3*-null mutants (*LZIP3*^{-/-}) suggested this protein could be required for parasite survival under low zinc conditions and exposed the existence of a second zinc transporter at the parasites' membrane. Following on these preliminary observations, this project i) performed an extensive phenotypic characterization of *LZIP3*^{-/-} parasites to establish the exact conditions in which it becomes essential ii) investigated if *LZIP1* and *LZIP2*, two other ZIP proteins encoded in the *Leishmania* genome, can function as a second zinc importer and iii) addressed the role played by *LZIP3* in visceral leishmaniasis animal models. The results gathered in this project suggest that alternative zinc uptake mechanisms might sustain parasite growth at initial phases of murine infection but, as disease progresses, *LZIP3* expression becomes essential for parasite survival in the spleen. These observations imply that zinc withholding mechanisms are employed by the host to control infection, posing *LZIP3* as a virulence factor of *Leishmania*.

This project ambitions to unveil the importance of zinc and zinc transporters for *Leishmania*, from a fundamental biology perspective and, most importantly, in the context of infection. Data gathered here is expected to impact the current state of knowledge regarding *Leishmania* nutrient acquisition, and how these parasites surpass the nutritional hindrances imposed by its hosts' immune system, both processes being amenable to be targeted by immune- or chemotherapeutic-based approaches.

Keywords: *Leishmania*, zinc, zinc transporters, metal homeostasis, nutritional immunity.

Resumo

Os tripanossomatídeos do género *Leishmania* são os agentes das leishmanioses, um grupo de doenças crónicas negligenciadas. Coletivamente, as leishmanioses afetam globalmente milhões de humanos e cães, não existindo vacinas nem quimioterapias eficientes. De forma a projetar terapias inovadoras, é imperativo identificar os mecanismos que permitem aos parasitas prosperarem nos seus hospedeiros. Os estudos apresentados nesta Tese concentraram-se no facto de estes parasitas terem obrigatoriamente de obter certos nutrientes, nomeadamente zinco, do seu hospedeiro.

Metais de transição como o zinco são essenciais para a *Leishmania*, podendo tornar-se prejudiciais quando em excesso. Esta dicotomia é frequentemente explorada por hospedeiros vertebrados para combater infeções, que podem ativar mecanismos coletivamente designados como "imunidade nutricional". Para prevalecer, é imperativo que os patógenos detetem rapidamente alterações induzidas pelo hospedeiro na biodisponibilidade do metal e as traduzam em respostas adaptativas. O Grupo de Parasitologia Molecular do i3S procura identificar e caracterizar os fatores envolvidos na homeostasia do zinco presentes em *Leishmania*. Este projeto contribuiu para este objetivo estudando três proteínas de *Leishmania infantum*: *LZIP1*, *LZIP2* e *LZIP3*.

A proteína *LZIP3* foi o primeiro transportador de zinco caracterizado em *Leishmania*¹. Estudos prévios com mutantes nulos de *LZIP3* (*LZIP3*^{-/-}) sugeriram que esta proteína poderia ser necessária para a sobrevivência do parasita em condições limitantes em zinco, e expôs a existência de um segundo importador do metal. Com base nestas observações preliminares, este projeto i) realizou uma extensa caracterização fenotípica de parasitas *LZIP3*^{-/-}, para estabelecer as condições exatas em que a proteína se torna essencial, ii) investigou se a *LZIP1* e a *LZIP2*, duas outras proteínas ZIP codificadas no genoma de *Leishmania*, podem funcionar como importadores de zinco e iii) abordou o papel desempenhado pela *LZIP3* durante a infeção de modelos animais de leishmaniose visceral. Os resultados reunidos neste projeto indiciam que mecanismos alternativos de captação de zinco podem sustentar o crescimento do parasita nas fases iniciais da infeção. Contudo, ao longo da progressão da doença, a expressão de *LZIP3* torna-se essencial para a sobrevivência do parasita no baço. Estas observações sugerem que, para controlar a infeção, o hospedeiro pode ativar mecanismos de retenção de zinco e que, neste contexto, a *LZIP3* poderá constituir um fator de virulência de *Leishmania*.

Este projeto pretendeu revelar a importância do zinco e das moléculas que o transportam, tanto da perspetiva da biologia fundamental do parasita como, principalmente, no contexto da infeção. Espera-se que os dados aqui reunidos impactem o estado atual do

conhecimento sobre a aquisição de nutrientes em *Leishmania*, bem como a forma como estes parasitas suplantam as restrições nutricionais impostas pelo sistema imunológico dos seus hospedeiros, sendo ambos os processos passíveis de serem direcionados para abordagens imunológicas ou quimioterapêuticas.

Palavras-chave: *Leishmania*, zinco, transportadores de zinco, homeostasia de metais, imunidade nutricional.

List of contents

List of figures.....	9
List of tables.....	11
List of abbreviations	12
Chapter 1: Introduction.....	16
1.1. <i>Leishmania</i> and the Leishmaniases	17
1.1.1. <i>Leishmania</i> life cycle	17
1.1.2. The Leishmaniases	18
1.1.3. Nutrient acquisition and <i>Leishmania</i> infection.....	19
1.2. Zinc.....	21
1.2.1. Physiological properties of zinc	21
1.2.2. Zinc-related cellular toxicity	22
1.3. Cellular zinc homeostasis:	24
1.4. Zinc in human physiology.....	26
1.4.1. Zinc and the immune system.....	26
1.4.2. Zinc at the host-pathogen interface: nutritional immunity versus nutritional virulence.....	27
1.5. Zinc transport in protozoa parasites	35
1.5.1. Zinc homeostasis in <i>Leishmania</i>	35
1.6. Genomic engineering and the CRISPR-Cas9 system	38
1.6.1. CRISPR-Cas9 as a genome editing tool.....	38
1.6.2. Genome editing in <i>Leishmania</i> parasites	40
Chapter 2: Objectives.....	43
Chapter 3: Materials and methods	45
3.1 <i>Leishmania infantum</i> strain and culture medium.....	46
3.2 Plasmid construction for parasite transfection.....	46
3.3 gRNA and primer design and synthesis.....	46
3.4 <i>L. infantum</i> transfection	47

3.5 Zinc quantification in <i>L. infantum</i> parasites	47
3.6 Protein extracts and western blotting	48
3.7 Indirect immunofluorescence	48
3.8 <i>In vivo</i> assays	48
3.9 Statistical analysis	49
Chapter 4: Results	50
4.1 Phenotypic characterization of <i>LiZIP3</i> ^{-/-} parasites:.....	51
4.1.1 <i>LiZIP3</i> is dispensable in standard conditions but essential under zinc limitation 51	
4.1.2 <i>LiZIP3</i> ^{-/-} parasites retain the capacity of internalizing zinc.....	53
4.1.3 The zinc deficiency phenotype is reverted in add-back strains	55
<i>Generation of LiZIP3 add-back parasites – ribosomal locus integration</i>	55
<i>Construction of the pLEXSYZIP3 vector and introduction in LiZIP3</i> ^{-/-} <i>parasites</i>	55
<i>Phenotypic analysis</i>	58
<i>Protein analysis following parasite mouse passage</i>	59
<i>Generation of LiZIP3 add-back parasites – episomal complementation</i>	59
<i>Phenotypic analysis</i>	60
<i>Protein analysis following parasite mouse passage</i>	60
4.2 Disclosing the second zinc transporter	63
4.2.1 <i>LiZIP1</i> protein expression analysis	63
4.2.2 CRISPR-Cas9-mediated ablation of <i>LiZIP1</i>	65
<i>Generation of WT and ZIP3</i> ^{-/-} <i>promastigote lines carrying the Cas9 nuclease, the T7 RNA polymerase and a vector for episomic expression of LiZIP1</i>	65
<i>Single guide RNA and donor DNA design and production</i>	67
4.2.3 Characterization of <i>LiZIP2</i>	69
<i>CRISPR-Cas9-mediated tagging of LiZIP2</i>	69
4.2.4 Overexpression analysis	74
4.3 Addressing the role of <i>LiZIP3</i> in the course of an infection of an animal model.....	76
Chapter 5: Discussion	79
5.1 Phenotypic characterization of <i>LiZIP3</i> ^{-/-} parasites.....	81

5.2 Disclosing the second zinc transporter.....	82
5.3 Addressing the role of <i>LZIP3</i> in the course of an infection of an animal model.....	87
Chapter 6: Final considerations and future work	89
Chapter 7: References	92
Chapter 8: Appendix	106
8.1 Supplementary Figures.....	107
8.2 Supplementary Tables.....	116

List of figures

Fig. 1. Life cycle of <i>Leishmania</i> parasites.	18
Fig. 2. Predicted membrane topologies of the ZIP and CDF family of transporters.	24
Fig. 3. Schematic representation of targeted genome editing using CRISPR-Cas9.	39
Fig. 4. Schematic representation of the Crispr-Cas9-mediated <i>Leishmania</i> genome editing methodology used in this work.	41
Fig. 5. Parasites lacking LiZIP3 do not survive in zinc-depleting conditions.	52
Fig. 6. LiZIP3^{-/-} growth contraction in the presence of 2.5 μM TPEN is specifically due to zinc restriction.	52
Fig. 7. LiZIP3^{-/-} parasites bypass the absence of LiZIP3 in standard and zinc surplus conditions.	53
Fig. 8. Schematic representation of the pLEXSYZIP3 ribosomal locus integration plasmid.	56
Fig. 9. Generation of LiZIP3^{-/-} revertant strains by ribosomal locus integration.	57
Fig. 10. LiZIP3 expressed from the ribosomal locus reverts the defective phenotypes of the LiZIP3^{-/-} mutant.	58
Fig. 11. The ZIP3^{-/-}_pLEXSYZIP3 revertant strain lost LiZIP3 expression following mouse passage.	59
Fig. 12. The ZIP3^{-/-}_pXGZIP3 revertant strain expresses LiZIP3.	60
Fig. 13. LiZIP3 expressed from the pXGZIP3 episome reverts the defective phenotypes of the LiZIP3^{-/-} mutant.	61
Fig. 14. The ZIP3^{-/-}_pXGZIP3 revertant strain expresses LiZIP3 following mouse passage.	61
Fig. 15. LiZIP1 expression pattern along the WT and ZIP3^{-/-} promastigote growth curve.	64
Fig. 16. Schematic representation of the LiZIP1 locus targeting, deletion and substitution by a donor template carrying a drug resistance gene, using CRISPR-Cas9, in <i>L. infantum</i>.	66
Fig. 17. WT and ZIP3^{-/-} parasites carrying the pXGZIP1 episome are able to overexpress LiZIP1.	67
Fig. 18. Schematic representation of the knock-in of a mNeonGreen-carrying cassette at the N-terminus of LiZIP2, using CRISPR-Cas9, in <i>L. infantum</i>.	70
Fig. 19. Schematic representation of the knock-in of a mNeonGreen-carrying cassette at the C-terminus of LiZIP2, using CRISPR-Cas9, in <i>L. infantum</i>.	71

Fig. 20. Production of mNeonGreen-LiZIP2 and LiZIP2-mNeonGreen chimeras was unsuccessful. 73

Fig. 21. Zinc content analysis of LiZIP1- and LiZIP2-overexpressing parasites..... 75

Fig. 22. LiZIP3 expression is essential for full infectivity of *Leishmania infantum* in the spleen. 78

Fig. 23. Predicted topologies of the LiZIP2 protein and of the mNeonGreen-tagged LiZIP2 proteins..... 86

Fig. 24. Schematic representation of the mechanisms that might take place during *Leishmania intramacrophagic* infection. 91

Fig. S 1. Schematic representation of the LiZIP3 locus targeting, deletion and substitution by a *Ble* cassette using CRISPR-Cas9 in *L. infantum*.108

Fig. S 2. Schematic representation of the pXGZIP3 expression plasmid.....109

Fig. S 3. LiZIP3^{-/-} growth contraction in the presence of 2.5 μM TPEN is specifically due to zinc restriction.110

Fig. S 4. Sequencing results from the assembled pLEXSYZIP3 construct.111

Fig. S 5. Sequencing results from the assembled pLEXSYZIP3 construct.112

Fig. S 6. Schematic representation of the pXGZIP1 expression plasmid.....113

Fig. S 7. Gel electrophoresis of the sgRNAs and donor DNA cassettes used to abrogate the LiZIP1 locus.....114

Fig. S 8. Gel electrophoresis of the sgRNAs and donor DNA cassettes used to knock-in the mNeonGreen-carrying cassette into the N-/C-terminus of LiZIP2.115

List of tables

Table 1. Zinc-related virulence factors described in human pathogens. 31

Table S 1. Oligonucleotides used in this work..... 117

List of abbreviations

AB: Add-back

BLAST: Basic local alignment search tool

BSD: Blasticidin

BSD^R: Blasticidin resistance gene

Bp: Base pairs

Cas9: CRISPR-associated protein 9

CDF: Cation diffusion facilitator

CL: Cutaneous leishmaniasis

CRISPR: Clustered regularly interspaced short palindromic repeats

Cys: Cysteine

DAPI: 4',6'-diamino-2-phenylindole

DC: Dendritic cell

DMT: Divalent metal transporter

DNA: Deoxyribonucleic acid

DSB: Double strand break

Dpi: Days post-infection

FAAS: Flame atomic absorption spectroscopy

FBSi: Inactivated Fetal Bovine Serum

G418: Geneticin

GP63: *Leishmania* glycoprotein of 63 kDa

gRNA: Guide RNA

HDR: Homologous directed repair

HEPES: 4-(2-hydroxyethyl)-1-piperazineethanesulfonic acid

HF: Homology flanks

HIV: Human immunodeficiency virus

HR: Homologous recombination

Hyg: Hygromycin

ICP-MS: Inductively coupled plasma mass spectrometry

IFN: Interferon

IL: Interleukin

IP: Intraperitoneal

IREG: Iron-regulated transporter

IV: Intravenous

K_d: Dissociation constant

kDa: KiloDalton

KO: Knockout

LPS: Lipopolysaccharide

LiCDF1: *Leishmania infantum* cation diffusion facilitator 1

LiZIP1: *Leishmania infantum* ZRT-/IRT-like protein 1

LiZIP2: *Leishmania infantum* ZRT-/IRT-like protein 2

LiZIP3: *Leishmania infantum* ZRT-/IRT-like protein 3

MCL: Mucocutaneous leishmaniasis

MMEJ: Microhomology-mediated end joining

mRNA: Messenger RNA

MT: Metallothionein

Neo^R: Neomycin resistance gene

NET: Neutrophil extracellular trap

NHEJ: Non-homologous end joining

NMRI: National Marine Research Institute

NRAMP: Natural resistance-associated macrophage protein

Nt: Nucleotide

ORF: Open reading frame

PAM: Protospacer-adjacent motif

PBS: Phosphate buffer saline

PCR: Polymerase chain reaction

pH: Potential of hydrogen

PFA: Paraformaldehyde

Puro: Puromycin

Puro^R: Puromycin resistance gene

RING: Really interesting new gene

RNA: Ribonucleic acid

ROS: Reactive oxygen species

rRNA: Ribosomal ribonucleic acid

SDS-PAGE: Sodium dodecyl sulfate polyacrylamide gel electrophoresis

sgRNA: Single guide RNA

siRNA: Small interfering RNA

SLC: Solute carrier family

SOD: superoxide dismutase

Th: T-helper

TLR: Toll-like receptor

TNF: Tumor necrosis factor

TPEN: N, N, N', N'-tetrakis (2-pyridylmethyl)ethylenediamine

UTR: Untranslated region

VL: Visceral leishmaniasis

WHO: World Health Organization

WT: Wildtype

ZIP: Zrt-/Irt-like protein

Zn: Zinc

ZnT: Zinc transporter

Chapter 1: Introduction

1.1. *Leishmania* and the Leishmaniases

The Leishmaniases are neglected vector-borne tropical infections caused by parasitic protozoa of the genus *Leishmania*. Of the more than 30 species that have been described, at least 20 are pathogenic for mammals, affecting primarily humans and dogs (WHO, 2015). These organisms cause significant morbidity and mortality in the 98 countries and territories where the disease is endemic, with higher incidence in tropical and subtropical areas, including the Mediterranean basin. The real global burden of leishmaniasis remains unknown, but an estimated 350 million people are at risk of infection with 2 million new cases and 500.000 associated deaths annually. The incidence of human leishmaniases has increased over the past decades due to failing preventing and therapeutic measures, human migration caused by conflicts and political instability, malnutrition, global warming and the emergence of drug-resistant parasites in developing countries²⁻⁵. The prevalence of the leishmaniases, among protozoan parasitic diseases, is only surpassed by malaria, placing them in the top 10 of the largest disease burdens among individual infectious diseases².

1.1.1. *Leishmania* life cycle

Leishmania is a digenetic parasite that alternates between an insect vector, more precisely a hematophagous female sandfly, and a mammalian host. The life cycle begins when infected sandflies inoculate infective (metacyclic) flagellated promastigotes while taking a bloodmeal. The sandfly bite induces a local inflammatory response, leading to rapid recruitment of several types of leukocytes. Promastigotes are ingested by phagocytes, where they differentiate to an aflagellate, non-motile stage - the amastigote. This intracellular location shields parasites from the majority of the host immune responses. Inside the macrophage, amastigotes reside and replicate within the phagolysosome while actively evading the microbicidal activity of the phagocyte. New cycles of infection occur mainly through increase of amastigote density inside the phagolysosome, that may result in overburdening and rupture of the host macrophage, followed by reinvasion of local phagocytes. The transmission cycle is complete when parasite-harboring cells or free amastigotes are ingested by a sandfly feeding on an infected host. In the insect's midgut, through a period of 4-25 days, these parasitic organisms differentiate back to the infective promastigote stage (Fig. 1)⁶.

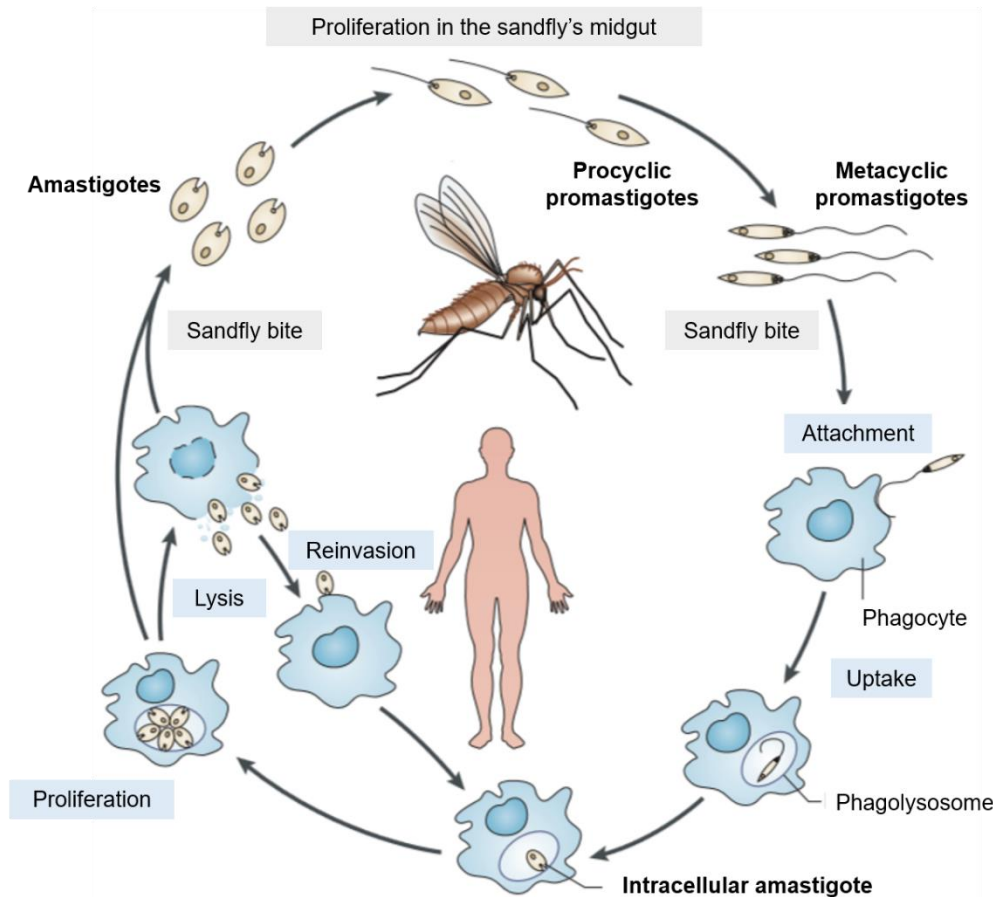


Fig. 1. Life cycle of *Leishmania* parasites. The protozoan assumes two forms, depending on its host: promastigotes, which can be found in the sandfly vector and amastigotes, which thrive inside mammalian macrophages. See main text for detailed description. Adapted from Kaye, P. (2011)⁶.

1.1.2. The Leishmaniasis

The clinical presentation of leishmaniasis depends on both the parasite species, their tropism and the immunological response of the host⁶. Briefly, the disease manifests mainly as self-healing skin ulcers (cutaneous leishmaniasis, CL), as disfiguring lesions that result from the destruction of cutaneous and subcutaneous tissues (mucocutaneous leishmaniasis, MCL), or as an internal organ disease, affecting mainly the liver and the spleen (visceral leishmaniasis, VL). While CL is the most common form of the disease, VL is the most severe syndrome amongst the leishmaniasis. VL is caused by *Leishmania infantum* and *Leishmania donovani*, which reside mainly within reticuloendothelial organs (liver and spleen). This form of the disease can be fatal if left untreated (in 95% of the cases within 2 years after the onset of the disease), accounting for 50.000 deaths per year alone².

Other factors, such as the parasite load and persistence, number, localization and duration of lesions, age, pregnancy, host genetic background, drug metabolism, irregular treatment, co-morbidities, co-infection and immunosuppression can influence the host cellular immune

response and, consequently, the establishment, outcome and severity of the disease⁷. Importantly, the host's nutritional status can greatly influence leishmaniasis settlement and progression, due to the tight relationship between the immune system and nutrition. In agreement with this, it is pertinent to consider that over 500 million adults and children are undernourished, and that a substantial part of this population intersects with endemic areas of leishmaniasis (WHO 2018).

Despite the many efforts carried out in the drug/vaccine development, diagnosis techniques and vector control fields aiming to control and eliminate the leishmaniasis, their outcomes are still not satisfactory. Namely, currently available chemotherapies are associated with poor efficacy, life-threatening toxicity, prolonged administration, high costs or widespread resistance^{8,9}. Liposomal amphotericin B has presently the best safety profile, being used with increasing frequency to treat VL and HIV/VL co-infection, although most exclusively in developed countries¹⁰. New antileishmanial drug development has been stalled by a scarcity of robustly validated drug targets in these parasites. Consequently, emerging strategies are shifting their focus into targeting *Leishmania* viability indirectly through host-parasite interactions, *i.e.*, into exploiting the host cell (the macrophage) in parallel with the parasites' biology. One of the processes amenable to interfere with is the dependence of the parasite on the host, to meet its own nutritional and metabolic needs.

1.1.3. Nutrient acquisition and *Leishmania* infection

Central to the ability of a parasite to be transmitted, infect a mammal and cause disease is its capacity to scavenge nutrients from its hosts. While all organisms acquire nutrients from their environment, the parasitic way of life of *Leishmania* imposes several peculiarities regarding nutrient uptake. First, the fact that their life cycle entails two different hosts obligates these microbes to cycle between physiologically distinct milieus with pronounced alterations not only in pH, temperature and ionic composition, but also in nutrient composition/availability. Second, the parasite must compete with its hosts in order to acquire essential compounds. As outlined before, inside the mammalian macrophage, *Leishmania* lives within phagolysosomes. This implies that nutrients must reach the lumen of these organelles so that the parasite can access them. *Leishmania* parasites should therefore i) present efficient nutrient uptake systems that keep up with the profound environmental alterations they are subjected to, and ii) employ regulatory mechanisms to adjust import/export according to nutrient availability (which will likely differ in the two life cycle stages), in order to maintain homeostasis and avoid toxicity¹¹.

Zinc is among the most important nutrients for *Leishmania* parasites. An example of a biologically relevant *Leishmania* protein that requires zinc for its activity is GP63, a glycoprotein of 63 kDa with metalloprotease activity that is involved in parasite development and virulence^{12,13}. Despite the importance of zinc, studies concerning the impact of its availability on the physiology and survival of *Leishmania* parasites are still sparse. Recently, alterations in intracellular labile zinc levels were related to activation of apoptosis-like death mechanisms, proposing zinc deprivation as an effective means of disease control^{14,15}.

As mentioned above, the leishmaniases pose an unacceptable threat to millions of people and domestic dogs worldwide, and their so-far unsuccessful eradication results in inestimable human misery and economic loss. To overcome the challenge imposed by *Leishmania*, it is crucial to understand better not only the host response to the parasites, but also the *Leishmania* biology itself and the adaptations that enable these organisms to give rise to long-lived infections. Studying the relationship between the essential nutrient zinc and *Leishmania* parasites can retrieve novel information - not only at the molecular level, about the zinc transport and homeostatic machinery in *Leishmania*, but also regarding the role of this metal at the host-pathogen interface throughout the infection course.

1.2. Zinc

Transition metals ions such as manganese, iron, cobalt, nickel, copper and zinc occupy a central position in biological systems. They are ubiquitously found in all organisms almost exclusively as protein constituents, and their functional roles can be broadly assorted into non-catalytic functions, redox catalysis and non-redox catalysis. Ergo, transition metals are incorporated into metalloproteins including storage proteins, transcription factors and metalloenzymes¹⁶. However, the same heightened activity of transition metals that makes them essential to biological systems also renders them toxic at conditions where these metal ions are present in excess or found in the wrong cellular location. Today, the concept of trace metal homeostasis, in which various cellular actions preserve the fine balance between nutrition and toxicity, is well established. The following sections will focus on the numerous roles of zinc, either at the cellular and molecular level or as a central player in integrated biological systems.

1.2.1. Physiological properties of zinc

Among the physiologically relevant first-row, late *d*-block metals, the chemical properties of zinc ensure that this essential trace micronutrient enrolls in nearly every major metabolic process/pathway within a cell. Biological systems exploit the unique chemistry of zinc by using it as a stabilizing factor for many transcription factors and structural domains, including RING fingers, LIM domains, Zn-fingers and Zn-clusters, which are involved in cellular regulation, signal transduction networks, and metabolic control¹⁷. Concurrently, zinc is a cofactor of enzymes among all six major functional classes¹⁸⁻²⁰, playing a role in the activity of approximately 50% of these proteins in eukaryotes. Additionally, eukaryotic cells rely on a substantial number of zinc-dependent transcription factors (44% of the zinc-containing proteins), demonstrating that zinc plays an important part in gene regulation in these organisms^{16,20,21}. Furthermore, zinc was recently shown to be a signalling molecule, serving as an intracellular second messenger in various signalling pathways²²⁻²⁴.

The extensive biological involvement of zinc as compared to other transition metals is related to its peculiar chemical properties²⁵. Unlike other biologically relevant transition metals (iron, manganese, copper and nickel), zinc has a filled *d* orbital, which makes it a redox-stable ion. Zinc is the most common non-redox transition metal²¹, being often the cofactor of choice for enzymatic reactions due to its prowess to attract or stabilize negative charges. Additionally, zinc can activate substrates as a consequence of its strong Lewis acid properties²⁶: as it is able to accept electron pairs, it can generate an hydroxide ion for the attack of a substrate when bound to water, or it can also be involved in generating the

attacking nucleophile and in enhancing the electrophilicity of the substrate which undergoes a nucleophilic attack²⁷.

The binding of zinc to proteins is facilitated by its highly versatile coordination chemistry: its coordination number varies from 4 to 6, with the corresponding geometries being tetrahedral, square pyramidal, trigonal bipyramidal or octahedral²⁵. Zinc can form both stable and exchangeable chemical bonds with nitrogen, oxygen and sulphur atoms, and thus the principal ligands that coordinate Zn ions are usually a combination of histidines, cysteines, acidic residues, water molecules and, more rarely, tyrosines, serines and threonines²⁸⁻³⁰. Hence, zinc has the ability to irreversibly bind protein structural components or catalytic cofactors but also regulates signaling, trafficking and storage through reversible protein bonds²⁸.

The metal is maintained in the Zn²⁺ state under all biologically relevant redox potential and pH conditions²⁸. Accordingly, it is not directly involved in physiological redox reactions but can act as an ancillary antioxidant factor. Zinc is a co-factor of superoxide dismutases in almost all eukaryotes (Zn-Cu-SODs), thus playing a central role in the cellular antioxidant defenses. Additionally, zinc plays a role against oxidative damage as it can interact with protein thiol groups precluding their oxidative inactivation. Zinc also reduces intracellular ROS formation by preventing the interaction of iron and copper with proteins: by competing and displacing these redox-active metal ions from their binding locations, zinc diverts sites of recurring production of free radicals, thereby limiting damage from localized Fenton and Haber-Weiss reactions³¹⁻³³. Furthermore, even if zinc is not redox-active *per se*, zinc proteins are not redox-inert. As Cys is redox-active, zinc coordination with this amino acid has a noteworthy property: sulphur ligands can be oxidized and reduced with release and binding of zinc, respectively, conferring redox properties to the complex, which links some zinc proteins to redox signaling³⁴.

The biophysical and biochemical aspects of zinc explain the multifarious roles of this ion as a structural, signalling and catalytically relevant divalent metal. However, the same properties that secure an essential role for zinc can be, in some circumstances, detrimental to cells.

1.2.2. Zinc-related cellular toxicity

Metal-related toxicity can arise from a faulty protein-metal interaction process known as mismetallation. When this happens, a given metal is erroneously incorporated into apo-proteins, being invariably unproductive and thus rendering proteins inactive. In the specific case of zinc this occurs because, as predicted by the Irving-Williams series, Zn²⁺ forms

more stable complexes with proteins than other transition metals do, being only surpassed by cupric ions³⁵. Thus, zinc toxicity can result from displacing the cognate cations in essential enzymes, thereby blocking their activity^{36,37}. In addition, it is described that zinc can compete with manganese and copper uptake systems, leading to metal nutritional deficiencies^{38,39}.

Intracellular zinc misbalance is also described to be involved in lipid peroxidation, DNA bases' modification and disruption of calcium and sulfhydryl homeostasis^{40,41}. Furthermore, the abovementioned beneficial zinc relation with thiol groups can have negative impacts, as the inadvertent binding of zinc to free Cys residues may interfere with the cellular redox homeostasis⁴². Ergo, both zinc deficiency and overload can elicit cellular oxidative stress, being imperative to maintain its concentration within a tight physiological range.

To circumvent zinc-associated toxicity, cells evolved metal acquisition and accessibility mechanisms to maintain optimal, pro-antioxidant zinc concentrations while keeping competitive metals out of mismetallation-prone binding sites. In fact, correct metallation *in vivo* is privileged because the cytoplasm is a metal-controlled environment due to the action of the highly regulated transport of metals into and out of the cytosol – processes known as “muffling”. In line with this, cells can take advantage from storage organelles to extrude zinc from the cytosol to sustain metal homeostasis^{43,44}. Although plant and yeast vacuoles are the most well-known metal sequestering structures, compartments such as acidocalcisomes and other lysosome-related organelles are emerging as central mediators of the fine tuning of metal balance in several organisms, both in metal-excess or metal-deficient situations⁴⁴.

Intracellular metal pools are further managed by the binding of metal ions to a myriad of macromolecules, which is known as “buffering”. Indeed, zinc is found in one of two forms within cells: i) protein-bound, comprising zinc complexes both tightly and loosely bound (such as to metallothioneins), and ii) “free” zinc ions, which are conceivably bound by unknown (non-protein) ligands^{17,45}. Hence, although the average total cellular zinc concentration can range between tens and hundreds of micromolar⁴⁵⁻⁴⁷, cells present a high zinc-chelating capacity and the cytosolic labile zinc pool is small, fluctuating between the picomolar and low nanomolar^{45,48,49}. Nevertheless, these metal concentrations are adequate for steady-state cellular functions, such as the synthesis of zinc-containing proteins and zinc-mediated signaling processes.

1.3. Cellular zinc homeostasis:

The modulation of zinc metabolism is grounded on an equilibrium of uptake, distribution, utilization, storage and efflux that ensures metal availability in accordance with physiological needs⁵⁰. Cellular zinc fluctuations result mainly from metal uptake and efflux controlled by transporter proteins, since the hydrophilicity of zinc ions renders their diffusion across membranes unfeasible⁵¹. Among the proteins mediating zinc import and homeostasis along biological systems, ZIP [Zrt-/Irt-like proteins, also termed Solute Carrier 39 (SLC39)] transporters, involved in zinc translocation into the cytosol from either the extracellular environment or intracellular storage vesicles, constitute one of the most important families⁵² (Fig. 2A). On the other hand, the cation diffusion family (CDF, also named ZnT transporters or SLC30) includes proteins responsible for metal cytosolic efflux, either out of the cell or towards the lumen of organelles⁵³ (Fig. 2B). The cellular spatial and temporal distribution of these proteins controls zinc concentration in the cytosol and intracellular organelles including the Golgi, mitochondria, nucleus and storage vesicles. Furthermore, other nondedicated divalent cation transporters were described to transport zinc, including NRAMP1 (SLC11A1), NRAMP2 (DMT1, SLC11A2) and ferroportin (IREG1, SLC40A1)⁵⁴.

In bacteria, in addition to the abovementioned families of transporters, other categories of zinc transporters can be found, including high affinity ABC-type transporters (ZnuABC in Gram-negative bacteria^{55,56}, AdcBCA in Gram-positive streptococci⁵⁷), homologs of the eukaryotic NRAMP transporter family^{58,59} and P-type ATPases⁶⁰.

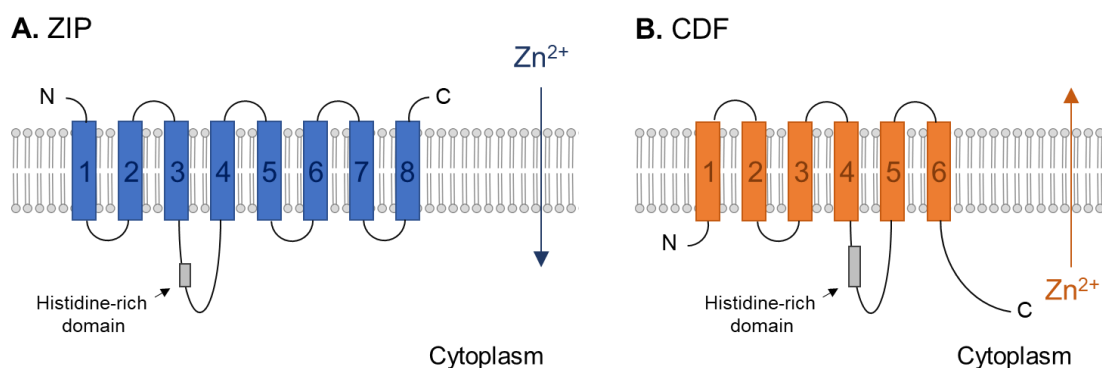


Fig. 2. Predicted membrane topologies of the ZIP and CDF family of transporters. The number of domains, the location of the N- and C-termini, the location of the histidine-rich domains (postulated to serve as the metal binding sites) and the direction of zinc transport are depicted. Adapted from Eide, D.J. (2006)⁶¹

It is of note that, together with specific membrane transporters, cellular zinc homeostasis is complemented by metallothioneins (MTs). These proteins comprise a class of cytosolic metal-binding structures that are able to coordinate up to 7 zinc atoms with picomolar

affinity, chelating around 5-15% of the cytosolic zinc pool⁶². These proteins act as a redox-dependent exchangeable labile zinc pool that buffers the cytosolic metal concentration^{34,63,64}. These proteins are known to play an immunomodulatory role and to undergo dynamic expression changes in response to ROS or pathogens^{65,66}, including *Leishmania*⁶⁷⁻⁷⁰.

The regulation of zinc homeostasis requires the coalition of signaling, membrane transport and protein sequestration concertedly with variations in transcription, translation, post-translational modifications and trafficking. Each transporter and zinc-binding protein has distinct induction patterns, expression profiles, subcellular localization and tissue distribution, that can be altered in response not only to intracellular zinc but also to ROS, inflammatory signaling and pathogen recognition. These disparate activities and locations provide each protein a unique role in zinc metabolism that reflects the need for strict equilibrium in face of different biologic stimuli in an organelle-, cell- and tissue-specific manner.

1.4. Zinc in human physiology

The essentiality of zinc for living organisms was first recognized in 1869 in the fungus *Aspergillus niger*⁷¹. Subsequently, zinc was found to be essential for the normal development of plants⁷², rats⁷³ and birds⁷⁴. However, not until the 1960s was zinc identified as an essential micronutrient for humans, with symptoms of severe anemia, growth retardation, hypogonadism, skin abnormalities and mental lethargy attributed to nutritional zinc deficiencies^{75,76}.

The human body contains about 2-3g of zinc, making it the second most abundant transition metal after iron⁷⁷. Despite being systemically plentiful, zinc is primarily sequestered within cells. The concentration of zinc in the circulation varies between 1-16 μM , accounting for only 0,1% of the total body zinc content⁷⁸, being mostly protein-bound: approximately 80% of this metal ion is loosely bound to albumin ($K_d=1\mu\text{M}$)⁷⁹, the remainder being tightly bound to other proteins such as $\alpha 2$ -macroglobulin and transferrin⁸⁰. Of note, the general zinc distribution among tissues differs largely. Skeletal muscles and bones contain most of the total body zinc (~80%), rendering visceral organs poorer in terms of metal content. Of particular interest to this project, the liver of an adult human is reported to contain about 100-250 μg zinc /g dry weight, whereas the spleen presents around 55-65 μg zinc /g dry weight⁸¹.

Since its discovery as a component of carbonic anhydrase in 1939⁸², it has been estimated that approximately 3000 proteins, or 10% of the proteins encoded by the human genome, contain a putative zinc binding motif, which can be translated in either structural or catalytic activity purposes²⁰. Consequently, zinc is involved in numerous cellular functions, from cell proliferation and differentiation, RNA and DNA synthesis, cell structure and cell membrane stabilization, to complex mechanisms in differentiated cell types⁸³. Of special interest is the multifaceted role of zinc in the regulation of the immune system⁸⁴.

1.4.1. Zinc and the immune system

One of the factors known to affect immunological innate and adaptive functions and, thus, alter resistance to infection is zinc bioavailability⁸⁵. The immunomodulatory attributes of this metal have long been appreciated: aberrant zinc regulation in the circulation is described to impact phagocytosis, leukocyte recruitment, cytokine production, glycolysis and oxidation driven by immune signals⁸⁶. It is particularly crucial for normal development and function of neutrophils and natural killer cells, and for the development and activation of T and B cells impairing, consequently, Th1 cytokine and antibody production⁸⁷. In summary, an intact, robust immune response requires strict zinc regulation.

Systemic zinc deficit can skew predominantly type 1 responses to type 2 responses⁸⁸. In particular, macrophages are adversely affected by zinc deficiency, due to dysregulated cytokine production, phagocytosis and intracellular killing due to their type 2 response-associated M2 polarization. In the particular case of the leishmaniasis a type 2 response, associated with IL-4, IL-5, IL-10 and TGF- β production, suppresses a leishmanicidal immune response⁸⁹⁻⁹⁴. In summary, zinc deficiency and its role in type 1/type 2 response balance has the potential of giving intracellular pathogens “free rein” to proliferate due to the lack of effective immune functions⁹⁵⁻⁹⁹. Hence, pathogenic infections are likely more prone to subsist in the setting of malnutrition¹⁰⁰⁻¹⁰².

Appropriate zinc levels are required not only to the proper functioning of the immune system, but also to the growth and survival of invading pathogens. This presents the host the opportunity to either harness antimicrobial properties of the metal or limit its availability as defense strategies, directly regulating microbial growth and survival by modulating zinc abundance.

1.4.2. Zinc at the host-pathogen interface: nutritional immunity versus nutritional virulence

The first studies pertaining zinc homeostasis and macrophage antimicrobial functions focused on the ability of peritoneal macrophages to eradicate *Trypanosoma cruzi* infection. The aptitude to recognize and kill internalized parasites was impaired in macrophages from mice subjected to mild/severe zinc deficiency, which was reversed upon zinc (but not copper, nickel or manganese) supplementation⁹⁶. These results gave rise to the first insights on the crucial role zinc plays on macrophagic microbicidal functions. Since then, the field of “zinc immunology” established that an aberrant zinc homeostasis affects clearance of numerous pathogens, either bacterial (e.g. *E. coli*, *Salmonella*, *Staphylococcus*, *Pseudomonas*, *Yersinia*, *Klebsiella*), fungal (e.g. *H. capsulatum*, *C. neoformans*, *C. albicans*, *A. fumigatus*), or viral¹⁰³.

The concept of active nutrient withholding/intoxication mechanisms at organism, tissue and/or cellular levels, with the purpose of limiting microbial proliferation and bolster pathogen elimination, is designated “nutritional immunity”¹⁰⁴. The underlying mechanisms can involve the control of the availability of essential nutrients such as amino acids, lipids and transition metals. While the host-pathogen arms-of-race for iron is well-established¹⁰⁵⁻¹¹⁰, the implication of other metals, such as manganese, copper and zinc, has emerged on the literature only more recently. In order to thwart these mechanisms, successful pathogens have evolved strategies to either scavenge essential nutrients in the host’s

restrictive environment, or to defend themselves from the harmful effects of being overexposed to metal ions. Indeed, numerous metal homeostasis-related factors have been shown to be essential for pathogen “nutritional virulence”^{16,111}.

Even though zinc is of paramount importance for immune defence, the bioavailability of zinc ions on the host, even in steady-state conditions, is quite limited. As outlined before, only 0.1% of the total body zinc is found in the plasma where it is most entirely bound to proteins, further reducing the accessibility to this metal. The same is valid for the intracellular, cytosolic labile zinc pool in host cells. In the context of an infection, sequestering the already paltry free (unbound) zinc is an ingenious way of depriving invading pathogens of this essential nutrient.

Redistribution of zinc during inflammation, at the systemic level, has been extensively studied¹¹²⁻¹¹⁵. Typically, the acute phase response of the immune system includes production of inflammatory cytokines, such as IL-6, that cause the upregulation of the ZIP14 zinc transporter in hepatocytes, mediating the influx of the metal from circulation to an intracellular location, where it is bound to an inflammatory-mediated expanded number of MTs¹¹⁶⁻¹²⁰ and, thus, no longer available for pathogens to acquire. The overall deprivation of seric zinc (hypozincaemia) is concomitantly assisted by the activation of epithelial cells and neutrophils, both of which release metal-binding proteins with antimicrobial functions. The majority of these proteins are from the S100 family of proteins, namely psoriasin (S100A7), calgranulin C (S100A12) and calprotectin [a heterodimer of calgranulin A (S100A8) and calgranulin B (S100A9)]¹²¹⁻¹²⁶. Neutrophils, when recruited during an immune response, release NETs that contain a large amount of calprotectin, a high-affinity zinc- and manganese-chelating protein whose levels are augmented in the context of an infection^{16,111,122,127}. Calprotectin-mediated extracellular zinc sequestration is well-described as a bactericidal and fungicidal mechanism (e.g. *E. coli*, *K. pneumoniae*, *S. aureus*, *S. typhimurium*, *S. epidermidis*, *B. burgdorferi*, *A. baumannii*, *C. neoformans*, *C. albicans*, *A. fumigatus*, *M. furfur*, *M. canis*, *T. mentagrophytes*, as well as the model yeast *S. cerevisiae*)^{122,128-133} that, together with other microbicidal insults, undermines the pathogen.

If, for extracellular pathogens, calprotectin is one of the dominant challengers in terms of zinc bioavailability, other mechanisms of zinc deprivation oppose intracellular organisms. The “tug-of war” over zinc continues after pathogens are phagocytosed by a macrophage, and the plasticity of these cells allows them to either use metal intoxication or deprivation to promote pathogen clearance.

Several reports support the role of host-mediated zinc sequestration as a means to restrict pathogen viability upon an immune response. For example, the TLR4-agonist LPS, from

Gram-negative bacteria, was reported to reduce intracellular zinc concentration within murine DCs, suggesting that zinc export may occur in response to some microorganisms¹³⁴; ZIP8 is described to decrease phagosomal zinc levels in macrophages and IFN- γ -stimulated T cells, by transporting the metal into the cytoplasm in the context of bacterial infections¹³⁵; neutrophils infected with *C. neoformans* enhance the production of calprotectin¹³⁶; additionally, the transcriptional response signature of some fungi upon phagocytosis by macrophages supports a state of nutrient deprivation within these cells¹³⁷. Recently it was reported that macrophages infected with *H. capsulatum* and polarized towards an M1 phenotype, albeit upregulating the membrane transporter ZIP2 (thus augmenting zinc import to the cytosol), limit the pathogen's access to zinc. Two mechanisms account for this: first, metal ions are tightly bound to MT-1 and MT-2, constricting the metal labile pool; second, zinc is distributed to intracellular organelles (such as the Golgi, mediated by ZnT4 and ZnT7 transporters' action), away to the phagosome. Since zinc is required by fungal antioxidant defence proteins, this two-fold metal sequestration, coordinated with enhanced ROS production (cytosolic zinc reduction augments the macrophage's oxidative burst), creates a highly antimicrobial environment¹³⁸.

A contrasting mechanism in the battle for metals at the host-pathogen interface involves directed metal intoxication. Host-mediated copper toxicity against bacterial pathogens is a well-documented microbicidal mechanism¹³⁹⁻¹⁴². Regarding zinc, there is less documentation. A report showed that *S. pneumoniae* is exposed to extracellular zinc intoxication; the metal competes with manganese for binding to a manganese-binding protein, and thus acts as an antimicrobial mechanism through inhibition of the bacterial manganese uptake¹⁴³. On another report, activation of macrophages with TNF- α and IFN- γ promoted toxic zinc overaccumulation in *M. avium*-containing phagosomes¹⁴⁴. Additionally, the poisoning of intra-macrophagic *M. tuberculosis* (and *E. coli*) with excess zinc and copper has been described¹⁴⁴⁻¹⁴⁶. The specific mechanisms by which this mechanism is bactericidal remains unknown, but is thought to involve inactivation of essential proteins (for e.g., by Fe-S cluster destruction)¹⁴⁷ or starvation of essential metal ions due to competition¹⁴³. Importantly, these studies showed that the expression of metal efflux systems is essential for these bacteria to alleviate heavy metal poisoning.

Although it is consensual that that the immune system capitalizes on divergent zinc sequestration or intoxication mechanisms to restrain an infection, it is not yet completely clear how immune cells preferentially use these opposing stratagems against different pathogens, as well as the molecular signals that govern this decision. However, it is becoming clear that the pathogen's nature alone may not be a sufficient condition to elicit a specific nutrient withholding/overdose response. For example, group A *Streptococcus*

seems to be challenged with zinc toxicity during nasopharynx colonization, although it faces zinc depletion on the skin¹⁴⁸. Other decisive factors may rely on the presence or absence of specific cytokines, the tissue and cell type, intracellular trafficking of the pathogen and the time point in the infection cycle¹⁶. Independently of the signals governing this decision, in order to successfully colonize the host, invading organisms must swiftly sense and react to the ever-changing metal levels of the host during the course of infection: species which have evolved pathogenic potential must also have evolved efficient, highly sensitive regulatory factors, controlling uptake mechanisms and detoxification systems, to circumvent the metal-centric assault of the nutritional immune response and ensure their physiological needs in these nutrients. Therefore, the ability to deal with host nutritional immunity is considered a virulence trait. Some of the zinc-trafficking and zinc-sensing factors described to be involved in pathogenic virulence are listed in Table 1.

Compared with the extensive body of literature that exists regarding the zinc tug-of-war at the host-bacteria/host-fungi interface, descriptions of nutritional immunity processes taking place at parasitic protozoa infections are rare. Conversely, little is known about parasite zinc transporter systems, let alone nutritional virulence factors employed by these organisms to undermine such processes. Lessons learned from how the host capitalizes on zinc during infection, and from the characterization of opposing virulence factors of pathogenic organisms, can pave the way to the discovery of zinc-related host/pathogen factors modulating the course of parasitic infections.

Table 1. Zinc-related virulence factors described in human pathogens.

Kingdom	Organism	Location	Described implications in virulence	Referenc
Bacteria	<i>Acinetobacter baumannii</i>	Extracellular	ZnuB (part of ZnuABC zinc uptake system) deletion mutants show decreased infectivity in mouse lung infection models	149
	<i>Brucella abortus</i>	Intracellular (facultative)	ZnuA (part of ZnuABC zinc uptake system) deletion mutants show decreased infectivity in mice	150, 151
	<i>Campylobacter jejuni</i>	Intracellular (facultative)	ZnuA (part of ZnuABC zinc uptake system) deletion mutants show decreased infectivity in chick gastrointestinal tract	152
	<i>Escherichia coli</i> (non- pathogenic)	Intracellular (facultative)	ZntA (zinc exporter) is required for survival at the phagosomes of infected human macrophages	146
	<i>Escherichia coli</i> (enterohemorrhagic)	Intracellular (facultative)	ZnuA (part of ZnuABC (zinc uptake system) deletion mutants show decreased ability to adhere to epithelial cells; ZinT (zinc-binding protein) deletion mutants show decreased infectivity in a rabbit model	153, 154
	<i>Escherichia coli</i> (uropathogenic)	Intracellular (facultative)	ZnuABC (zinc uptake system) and ZupT (zinc transporter) deletion mutants show decreased infectivity in mouse ascending UTI models	155, 156
	<i>Francisella tularensis</i>	Intracellular (facultative)	ZnuA (part of ZnuABC zinc uptake system) is required for survival at the cytosol of infected macrophage-like cells	157

Table 1. Zinc-related virulence factors described in human pathogens (continued).

Kingdom	Organism	Location	Described implications in virulence	Referenc
Bacteria	<i>Haemophilus ducreyi</i>	Extracellular	ZnuA (part of ZnuABC zinc uptake system) deletion mutants show decreased infectivity in chancroid rabbit models	158
	<i>Haemophilus influenzae</i>	Extracellular	ZevAB (zinc uptake system) deletion mutants show decreased infectivity in a mouse lung infection model	159
	<i>Helicobacter pylori</i>	Extracellular	CznABC (zinc efflux system) deletion mutants show decreased infectivity in mice	160
	<i>Listeria monocytogenes</i>	Intracellular (facultative)	ZurAM (zinc uptake system) and ZinA (part of ZinABC zinc uptake system) deletion mutants show decreased infectivity in an oral infection mouse model	161
	<i>Moraxella catarrhalis</i>	Extracellular	ZnuABC (zinc uptake system) deletion mutants show decreased infectivity in mice	162
	<i>Mycobacterium smegmatis</i> (avirulent)	Intracellular	ZntA (zinc exporter) is required for survival at the phagosomes of infected human macrophages	163
	<i>Mycobacterium tuberculosis</i>	Intracellular	CtpC (zinc exporter) is required for survival at the phagosomes of infected human macrophages	146

Table 1. Zinc-related virulence factors described in human pathogens (continued).

Kingdom	Organism	Location	Described implications in virulence	Referenc
	<i>Pasteurella multocida</i>	Extracellular	ZnuABC (zinc uptake system) deletion mutants show decreased infectivity in mice	164
	<i>Proteus mirabilis</i>	Extracellular	ZnuC (part of ZnuABC zinc uptake system) deletion mutants show decreased infectivity in mouse ascending UTI models	165
	<i>Salmonella typhimurium</i>	Intracellular (facultative)	ZnuABC (zinc uptake system) deletion mutants show decreased infectivity in mice; ZntA, ZitB and FieF (zinc exporters) deletion mutants show decreased infectivity in NRAMP1-positive mice	166-169
Bacteria	<i>Staphylococcus aureus</i>	Extracellular	CntABCDF (zinc uptake system) and staphylopin (broad-spectrum metallophore) deletion mutants show decreased infectivity in mice	170
	<i>Streptococcus pneumoniae</i>	Extracellular	AdcB (from the AdcABC zinc uptake system) deletion mutants show decreased infectivity in mice; AdcA/AdcAll (zinc-binding proteins) double deletion mutants show decreased infectivity in mouse models of nasopharyngeal carriage, pneumonia and sepsis	171
	<i>Streptococcus pyogenes</i>	Extracellular	AdcA (from the AdcABC zinc uptake system), Lmb (zinc-binding protein) and CzcD (zinc exporter) deletion mutants show decreased infectivity in mice	148,172

Table 1. Zinc-related virulence factors described in human pathogens (continued).

Kingdom	Organism	Location	Described implications in virulence	Referenc
Bacteria	<i>Yersinia pestis</i>	Intracellular (facultative)	ZnuABC and YbtX [yersiniabactin (siderophore-like zinc binding protein) biosynthesis] deletion mutants show decreased infectivity in bubonic and pneumonic plague mouse models	173
	<i>Aspergillus fumigatus</i>	Extracellular /Intracellular	ZafA (transcription factor - response to zinc starvation) deletion mutants show decreased infectivity in invasive aspergillosis mouse models	174
Fungi	<i>Candida albicans</i>	Intracellular (facultative)	Pra1 (a siderophore-like zinc binding protein) deletion mutants show inability to damage/colonize host cells in the absence of zinc; Zrt2 (membrane zinc importer) and Zrc1 (zincosome zinc importer) deletion mutants show decreased infectivity in mice	175,176
	<i>Cryptococcus gattii</i>	Extracellular	Zap1 (transcription factor - response to zinc starvation) deletion mutants show decreased virulence in cryptococcosis infection mouse models	177

1.5. Zinc transport in protozoa parasites

The completion of many parasite genome projects has facilitated the identification of putative zinc transporters by sequence similarity to proteins with known functions in other organisms^{178,179}. However, although numerous transporter proteins are annotated in parasitic genomes, most remain uncharacterized. Few exceptions include the identification and characterization of ZIP family homologues in *Trichomonas vaginalis* (zinc transport)¹⁸⁰ and *Plasmodium berghei* (iron/zinc transport)¹⁸¹, and a CDF-like protein in *Toxoplasma gondii* (zinc transport)¹⁸².

The abovementioned approach allowed the Molecular Parasitology group to identify ZIP family homologues in *L. infantum*, among which were two pairs of identical genes and one single-copy gene. One pair of the identical genes (*LinJ31.3180* and *LinJ31.3190*) specifies the orthologue of the *L. amazonensis* ferrous-ion transporter LIT-1^{183,184} and was renamed *LiZIP1*. The single copy gene (*LinJ33.3350*) was designated *LiZIP2*. The second pair of identical genes (*LinJ28.2050* and *LinJ28.2060*) encodes a protein that is referred to as *LiZIP3*¹. In addition, a single copy CDF family homologue gene (*Linj31.2470*) found in the *L. infantum* genome was named *LiCDF1*.

1.5.1. Zinc homeostasis in *Leishmania*

As mentioned before, *Leishmania* parasites may face drastic changes concerning zinc availability during their life cycle. Hence, in order to cope either with zinc shock or deficiency, parasites must resort to resistance mechanisms similar to those mentioned for other organisms. Namely, storage organelles and high-affinity transporters are likely to play pivotal roles in the homeostasis of parasite intracellular zinc, which may impact its survival and, ultimately, its virulence upon infection.

In *Leishmania*, one intracellular compartment implicated in intracellular metal homeostasis is the acidocalcisome. These lysosome-related organelles have been linked with several functions, including polyphosphate metabolism, calcium homeostasis, maintenance of intracellular pH homeostasis, osmoregulation and storage of divalent cations^{185,186}, including zinc¹⁸⁷⁻¹⁹¹. Central to the ability of this organelle to house zinc is the existence of divalent cation transporters on its membrane. In line with this, *LiCDF1* was confirmed to locate to the membrane of acidocalcisomes, where it is postulated to transport cytosolic zinc into the lumen of the organelle¹⁹². Although it is accepted that acidocalcisomes contain zinc, the physiological role of this zinc pool in *Leishmania* metal biology is still unclear. Concretely, it is not known if zinc deposition in this organelle is part of a defense mechanism

against zinc toxicity, a zinc-storing process to support growth during extracellular metal shortage, or both. Such questions, although relevant to entirely comprehend zinc homeostasis in *Leishmania*, were not addressed in the scope of this thesis.

LizIP3 is the first high-affinity zinc transporter reported in *Leishmania* parasites¹. Functional complementation in the yeast *Saccharomyces cerevisiae* and radiotracer assays in RNA-injected *Xenopus laevis* oocytes first showed that *LizIP3* displays zinc transport activity. The protein was demonstrated to locate at the parasite cell surface, and to be tightly regulated at the mRNA level by the concentration of zinc in the medium. Specifically, its expression is upregulated when the parasite faces zinc-limiting conditions and downregulated when the metal is available, “disappearing” from the parasites’ membrane 6-12h following a zinc stimulus. Messenger RNA destabilization in response to zinc surplus is thought to occur through a pathway that requires a short-lived protein to interact with a *cis*-acting zinc-sensing element in the 3’ untranslated region (UTR) of the transcript^{1,193}. The importance of the gene for *L. infantum* survival and establishment of a successful infection in mammalian hosts remained elusive in these first studies¹, as consecutive efforts towards generating parasites lacking functional copies of *LizIP3* were unsuccessful. These fruitless attempts were all carried out with classical homologous recombination strategies which, up to recently, were the only available means to ablate genes in *Leishmania* spp. (of notice, the siRNA-mediated gene downregulation approach is not functional in these organisms). Recently, however, *LizIP3* abrogation was achieved resorting to CRISPR-Cas9, a genome editing system successfully adapted to trypanosomatids¹⁹⁴⁻¹⁹⁷.

Successful generation of *LizIP3* homozygous knockout parasites¹⁹⁸ gave important insight regarding not only the relevance of the protein but also the zinc uptake mechanisms present in *Leishmania*. Firstly, it was acknowledged that *LizIP3* is not essential for promastigotes in standard (zinc-replete) culture conditions. This observation suggested that an alternative zinc transporter, possibly of low-affinity, co-existed in *L. infantum*. Preliminary evidence supporting the presence of a second zinc acquisition system was the observation that *LizIP3*^{-/-} parasites retain the ability to accumulate zinc when this metal is provided in high amounts (in zinc-surplus conditions). Dual-transport systems for acquisition of a given substrate are common in biology. High-affinity transporters, like *LizIP3*, are expressed under low substrate concentration as part of a nutrient-specific starvation response, *i.e.*, are an attempt of the organism to restore nutrient homeostasis. On the other hand, low-affinity transporters are constitutively expressed or regulated only to a small extent, internalizing substrates when these are abundant¹⁹⁹. A second important conclusion retrieved from the phenotypic analysis of the *LizIP3*^{-/-} mutants was that the transporter becomes essential

when zinc is made a limiting factor, for instance, by addition of the zinc chelator TPEN to the culture medium.

In summary, the finding that *L. infantum* promastigotes are able to express at least two zinc transporters appears to constitute a physiologic advantage, as these provide parasites a means to adequately acquire zinc even in face of drastic environmental changes in nutrient availability¹⁹⁹. Defining the identity of this alternative zinc uptake mechanism is important, constituting one of the objectives of this project. Also relevant is to address the significance of *LIZIP3* upon infection, being the main purpose of the present project. The macrophage environment in which the amastigote stage lives may present or impose nutrient restrictions^{69,200} and this can also be the case of zinc. If so, *LIZIP3* knockouts are unlikely to replicate or, at least, not to do so to the same extent of wildtype parasites, giving rise to decreased parasite burdens in infected animals. Importantly, if amastigotes prove to be incapable of overcoming *LIZIP3* absence, this transporter can be regarded as a putative drug target. Such a result would set stage to further studies on macrophage zinc-limiting mechanisms as leishmanicidal strategies employed by these immune cells.

1.6. Genomic engineering and the CRISPR-Cas9 system

Genetics is a powerful tool to perceive the molecular mechanisms that modulate *Leishmania* life cycle progression and host-pathogen interactions. The effect of the ablation of a given gene can be evaluated by assessing the ability of a mutant to replicate as procyclic promastigotes and to differentiate into metacyclic promastigotes or amastigotes in culture, or by infection studies in macrophages, animals or sandflies. Also, by means of genomic engineering it is now possible to introduce tags, such as fluorescent proteins or small epitopes, fused to a given protein's gene in order to facilitate their characterization and subsequent functional studies. However, the full potential of genome manipulation in *Leishmania* was hitherto deterred by technical hurdles. The recently described CRISPR-Cas9 system^{201,202} has the power to break the enduring bottleneck of genetic tailoring in underexplored organisms as *Leishmania*, enabling researchers to tackle questions that, due to methodological impediments, remained unresolved.

1.6.1. CRISPR-Cas9 as a genome editing tool

The CRISPR-Cas system is a prokaryotic adaptive immune system^{203,204} present in many bacteria (>50%) and most archaea (>80%)²⁰⁵. A comprehension of its features and natural functions has set the stage for a broad array of applications, from building resistance to viruses in industrial structures, to cutting-edge genome engineering. Although CRISPR *loci* were first described in 1987²⁰⁶, their biological role remained elusive until 2005²⁰⁷⁻²⁰⁹. Since then, many reports delved into the molecular characterization of the CRISPR-Cas genetics, mechanisms and applications. The findings that this system was i) RNA-mediated and protein dependent, akin to the RNA interference mechanism in eukaryotes²¹⁰, that ii) DNA is its primary target²¹¹ and that iii) interference occurs through sequence-specific target DNA cleavage^{212,213} supported the potential of the CRISPR-Cas system (particularly of the type II) as a fast, low-cost, efficient and customizable technology for manipulating genomic sequences with nearly-surgical precision.

The CRISPR-Cas9 gene editing tool (Fig. 3A) was adapted from the *Streptococcus piogenes* type II system^{201,202}. Its two key components are the Cas9 nuclease and a single guide RNA (sgRNA). The sgRNA consists on a custom-designed 20-nt sequence guide RNA (gRNA), responsible for directing the enzyme to a chosen, specific DNA target, followed by an 82-nt chimeric sequence responsible for Cas9 stable binding. To edit a particular region of a given genome, the gRNA must be designed in order to be complementary to the DNA sequence of interest. Importantly, that sequence must be flanked by a 5'-NGG-3' PAM, and be as unique as possible in the genome to avoid off-site

targeting. When Cas9 and the sgRNA are co-expressed in the same cell, the Cas9 forms a trimeric complex along with the sgRNA and the cognate DNA. The enzyme, through its nuclease HNH and RuvC domains²¹⁴, cleaves both DNA strands that are complementary and non-complementary to the gRNA, respectively^{201,215}, exactly 3 bp upstream of the PAM motif²⁰¹.

In most species, repair of the double strand breaks (DSBs) (Fig. 3B) occurs by the non-homologous end-joining (NHEJ) pathway, creating insertions or deletions (indels) that result in point mutations, leading to frameshift disruption of the targeted gene. Alternatively, if in the presence of an appropriate DNA template with arms homologous to the targeting site (homologous flanks, HF), homology-directed recombination (HDR) can occur, which introduces any desired sequence in the genome^{202,216-218}.

As of this writing, nearly 8000 papers related to CRISPR/CRISPR-Cas9 have been published, illustrating the impact of this system in the molecular biology field. It has already been applied in plants, fungi²¹⁹⁻²²³, fruit flies^{224,225}, zebra fish^{226,227}, nematodes²²⁸, mice²²⁹⁻²³¹, rats^{232,233}, and human cells^{202,234,235}, among others. More recently, implementation of this system was reported in several pathogenic protozoa^{194-197,236-238}, including three species of *Leishmania*: *Leishmania major*^{196,238}, *Leishmania donovani*¹⁹⁷ and *Leishmania mexicana*²³⁸.

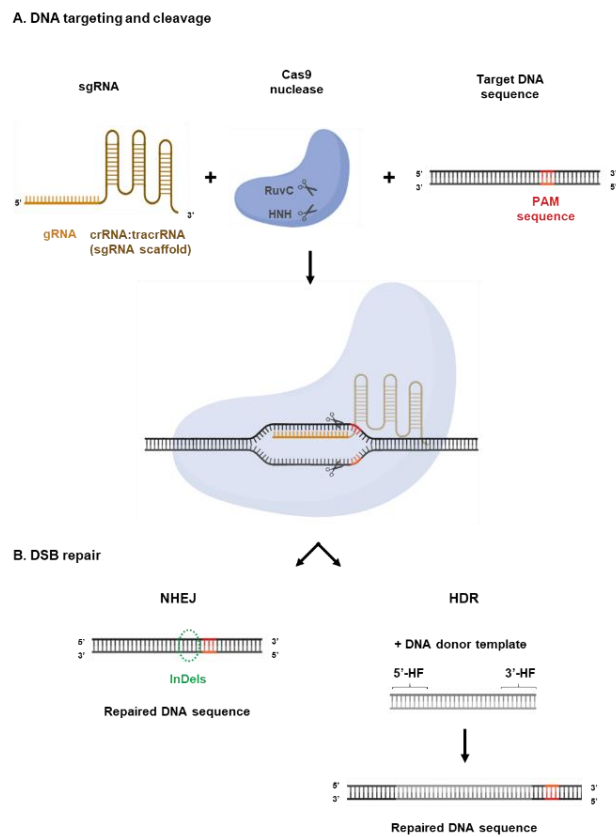


Fig. 3. Schematic representation of targeted genome editing using CRISPR-Cas9. The technology relies in site-specific double-stranded break generation (A), followed by repair of the cleaved DNA (B). See main text for detailed description.

1.6.2. Genome editing in *Leishmania* parasites

Knockout generation by homologous recombination in *Leishmania*, a diploid organism, typically required two successive rounds of transfection with at least two different constructs carrying disparate selective markers. These constructs needed long HFs (150–200 bp) flanking the selectable marker to achieve double-crossover replacement.^{236,239,240} As shown by the efficient adaptation to several trypanosomatids and by the Molecular Parasitology Group's successful implementation of the system in *L. infantum*, the use of CRISPR-Cas9 provides not only a simpler methodology but also a highly efficient approach when compared to the former available genome engineering tools for *Leishmania*²⁴⁰. The so-far laborious gene deletion procedure, as well as the introduction of epitopes, tags, drug markers, frame shifts or point mutations, is becoming no more than regular protocols through the use of this technology. Nevertheless, since the first descriptions of CRISPR-Cas9-based genome editing in *Leishmania*^{196,197}, continuous optimization attempts emerge on the literature.

Recently a new, high-throughput genome editing CRISPR-Cas9-based toolkit for *Leishmania* was described²³⁸. This protocol presents an elegant sgRNA delivery method using PCR-amplified DNA templates harboring a T7 promoter, which are transcribed *in vivo* by cells expressing T7 RNA polymerase along with the system's key protein, Cas9 (Fig. 5A). It furthermore permits rapid tagging and knock-out generation as i) these can be achieved in a single-round of transfection and ii) do not involve time-consuming DNA cloning steps as all donor DNA cassettes (harboring drugs, epitopes or fluorescent tags) are assembled by PCR from the same set of template plasmids (pT and pPLOT plasmids, Fig. 5B), using appropriate primers to produce 30 nt-long, target-specific HFs.

The aforementioned CRISPR-Cas9-mediated genome editing methodology will be employed in the present project to serve two general purposes: i) to knock-in fluorescent (mNeonGreen) and small-epitope (cmyc) tags fused to a target protein's gene, for both functional and localization analysis and ii) to knockout zinc-related genes, in order to gain insight on their function in parasites and overall role on zinc homeostasis.

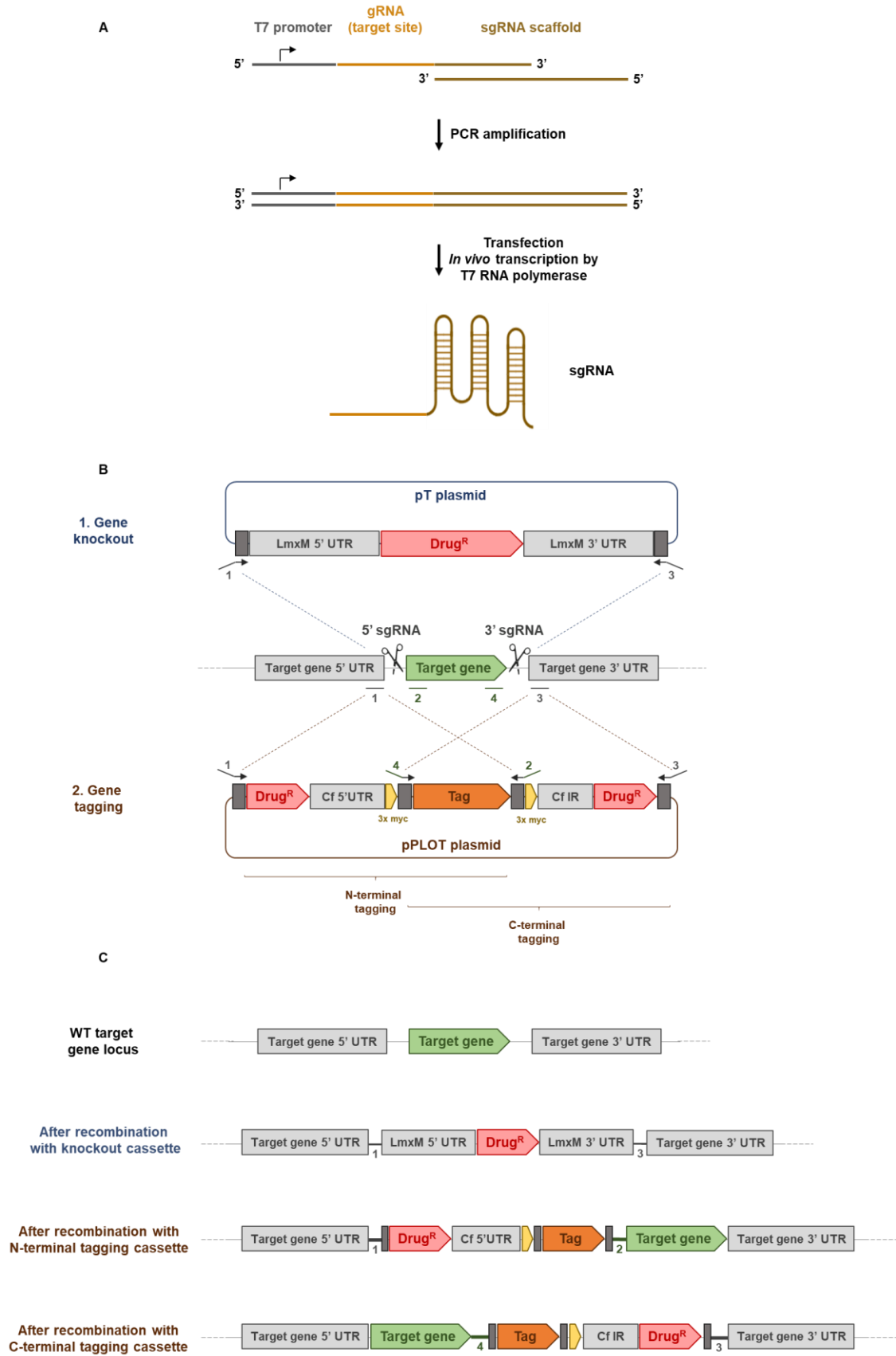


Fig. 4. Schematic representation of the Crispr-Cas9-mediated *Leishmania* genome editing methodology used in this work. (continues in the next page).

Fig. 4. (Continued) (A) Strategy for sgRNA production and delivery: the sgRNA template is PCR-amplified using a forward primer encoding the T7 RNA polymerase promoter, the 20 nt gRNA (defining the target DNA site) and a sequence complementary to the 3' end of the reverse primer, which comprises the sgRNA scaffold. The resulting amplicon is transfected into *Leishmania* promastigotes expressing the T7 RNA polymerase (and the Cas9 nuclease), that drives in vivo transcription of the complete sgRNA. (B) Strategy for donor DNA template production, either for gene knockout (blue) or knock-in (brown) purposes. These donor DNA templates promote HDR of Cas9-induced DSBs, allowing precise modification of target loci. To delete a target gene (B1), two sgRNAs direct Cas9 to sites immediately upstream (5'-sgRNA) and downstream (3'-sgRNA) of the target gene/locus. Donor DNA cassettes harbouring a drug-selectable marker gene (DrugR, red) and 30 nt sequences homologous to the target sites are PCR-amplified from pT plasmids with primers 1 and 3; To tag a target gene (B2), one sgRNA directs Cas9 to a site to sites immediately upstream or downstream of the target gene, to fuse tags to the N- or to the C-terminus of a protein, respectively. Donor DNA cassettes harbouring the desired tag (orange), a cmc tag (yellow) and a drug-selectable marker gene and 30 nt sequences homologous to the target sites are PCR-amplified from pPLOT plasmids. Primer pair 1-2 is used to amplify the cassette for N-terminal tagging, and primer pair 3-4 to amplify the cassette for C-terminal tagging. (C) Schematic representation of a target gene locus before and after the insertion of knockout/tagging repair cassettes. Adapted from Beneke, T (2017)²³⁸

Chapter 2: Objectives

This project accommodates several lines of investigation, their cornerstone being the endeavor to expose the molecular machinery enabling *Leishmania* parasites to maintain zinc homeostasis. Concretely, this study contemplates the *LZIP3* zinc transporter, previous studies conducted at the Molecular Parasitology Group constituting the foundation of the outlined work. The aim of the project is to establish the role of this protein for the parasite's growth and virulence, both in *in vitro* and in *in vivo* assays. Specifically, this project sets to:

- i) Perform an extensive characterization of *LZIP3* knockout mutants, to establish the conditions in which the transporter becomes essential;
- ii) Investigate if *LZIP1* and *LZIP2*, two other ZIP proteins encoded in the *Leishmania* genome, function as a second zinc import system;
- iii) Address the role played by *LZIP3* during a *Leishmania* animal infection.

The conclusions drawn from this thesis should refine the current knowledge on *Leishmania*'s metal homeostasis and elucidate how this parasite is able to cope with disparate environments throughout its life cycle that, pertaining to zinc bioavailability, can be adequate, restricted or toxic. Such findings might pave the way for the development of novel means to overcome the global threat posed by the neglected leishmaniases.

Chapter 3: Materials and methods

3.1 *Leishmania infantum* strain and culture medium

Unless otherwise indicated, *L. infantum* promastigotes (strain MHOM/MA/67/ITMAP-263) were routinely cultivated at 25°C in complete RPMI medium, *i.e.*, RPMI 1640 GlutaMAX™-I medium supplemented with 10% (v/v) heat-inactivated fetal bovine serum (FBSi), 50 U mL⁻¹ penicillin, 50 µg mL⁻¹ streptomycin (all from Gibco) and 20 mM HEPES pH 7.4. For each assay, parasites were first synchronized through 3-5 daily refreshments of culture medium and seeded at 10⁶ mL⁻¹ at the beginning of the experiments. Parasite density was evaluated by cell counting in a Neubauer chamber.

3.2 Plasmid construction for parasite transfection

The pLEXYZIP3 ribosomal *locus* integration plasmid was generated as follows. First, the pLEXY-mCherry-Hyg plasmid²⁴¹ (kindly provided by Rafael Balaña-Fouce) was sequentially digested with *NotI* and *BglII*, to excise the *mCherry* ORF and accommodate the *LiZIP3* ORF. The *LiZIP3* ORF (1389 bps) was PCR amplified from the pUC19_*LiZIP3*¹⁹⁸ with primers P1 and P2 that insert the *BglII* and *NotI* restriction sites at the 5' and 3' termini, respectively. The resulting PCR amplicon was sequentially digested with *BglII* and *NotI* and cloned into the corresponding sites of pLEXY_Hyg. To confirm that no mutations were introduced in the *LiZIP3* ORF, accuracy of the assembled pLEXYZIP3 construct constructs was verified by DNA sequencing at Eurofins Genomics (Germany) using primers P3, P4, P5 and P6 (Fig. S5 and S6). Finally, pLEXYZIP3 was digested with *SwaI*, to generate the ribosomal *locus* integration cassette (Fig. 9).

The pTB007, pTPuro, pTBlast and pPLOT-mNG-blast-blast plasmids²³⁸ were kindly provided by Eva Gluenz.

All constructions involved transformation of and plasmid DNA isolation from DH5α/XL1-Blue competent *Escherichia coli*. Confirmation of positively transformed *E. coli* was carried out by PCR-colony, followed by restriction of the isolated plasmids.

3.3 gRNA and primer design and synthesis

The gRNA-targeting sequences were selected using LeishGEdit (www.leishgedit.net)²³⁸ and EuPaGDT (<http://grna.ctegd.uga.edu>)²⁴², followed by a manual analysis using a BLAST tool (<http://tritypdb.org>)²⁴³.

The sgRNA templates were produced by PCR using an oligonucleotide (forward primer) encoding the T7 promoter, 20 nt defining the target site and a sequence complementary to

the 3'-end of the second oligonucleotide (reverse primer), comprising the sgRNA scaffold (P11). The resulting PCR products were transfected into pTB007-harboring cells for T7 RNAP-driven transcription of the sgRNAs.

The donor cassettes were obtained from the pTPuro, pTBlast or pPLOT-mNG-blast-blast plasmids²³⁸ by PCR amplification using oligonucleotides containing 30 nt to promote specific HDR at the target locus.

All oligonucleotides used in this study (Supplementary Table 1) were synthesized and purchased from Sigma–Aldrich Corp.

3.4 *L. infantum* transfection

Promastigotes in the logarithmic phase of growth were electroporated using the Amaxa Nucleofactor System with the X-001 program, as described elsewhere²³⁸. Briefly, 10^7 parasites were washed in Tb-BSF electroporation buffer (90 mM sodium phosphate, 5 mM KCl, 0.15 mM CaCl_2 , 50 mM HEPES pH 7.3) and electroporated with 5-10 μg of plasmid DNA or 4-6 μg of purified PCR products. Parasites were allowed to recover in culture medium for 24h at 25°C in the absence of selective drugs. When indicated, transfected cultures were spread on agar plates containing the appropriated drugs. Individual clones were then picked from the agar plates and transferred into selective liquid medium. Unless otherwise indicated, geneticin (G418; Sigma), hygromycin (Hyg; Invitrogen) and blasticidin (Bsd, CAYLA-InvivoGen) were used at 15 $\mu\text{g}/\text{mL}$ and puromycin (Puro, Sigma) at 17.5 $\mu\text{g}/\text{mL}$.

3.5 Zinc quantification in *L. infantum* parasites

To analyze the zinc content in *L. infantum*, promastigotes were seeded at 10^6 mL^{-1} in fresh medium. At specific time points, aliquots of approximately 10^8 parasites were harvested at 3000 rpm for 10 min at 4°C, washed twice in ice-cold 1xPBS (4.3 mM $\text{Na}_2\text{HPO}_4 \cdot 7\text{H}_2\text{O}$, 1.5 mM KH_2PO_4 , 2.7 mM KCl, 140 mM NaCl) and the resulting pellets dried at 37°C and stored at -80°C until further use. Prior to analysis, parasite pellets were dissolved in 65% (v/v) HNO_3 for 2h at 65°C. Zinc was quantified by atomic absorption spectrometry (flame atomization) using the Atomic Absorption Spectrometer PU 9200X (Phillips), or by inductively coupled plasma-mass spectrometry using an iCAP™ Q ICP-MS equipment (Thermo Fisher Scientific).

3.6 Protein extracts and western blotting

Parasites were harvested at 3000 rpm for 10 min at 4°C and washed twice in ice-cold PBS. The pellet was resuspended at 6.25×10^8 cells/mL in 4% (w/v) SDS/50mM Tris-HCl pH 7.4. The suspension was stored at -20°C until further use. Before loading into SDS PAGE gels, samples were treated with 4 M urea and 1% (v/v) β -mercaptoethanol, without boiling or heating. Samples were then resolved on 10% SDS-PAGE and transferred to nitrocellulose blotting membranes. Membranes were incubated in a blocking solution of 5% (w/v) skim milk and probed with the primary and secondary antibodies.

Antibodies and respective dilutions were as follows: α -LIZIP3 antibody^{1,244}, 1:200 dilution; α -LIZIP1 antibody^{1,244}, 1:500 dilution; α -mTXNPx antibody, 1:2000 dilution; α -GP63 antibody, 1:2000 dilution; α -myc antibody, 1:250 dilution; α -rabbit IgG antibody conjugated with horseradish peroxidase (HRP) antibody, 1:10 000 dilution; α -sheep IgG antibody conjugated with HRP, 1:4000 dilution; α -mouse IgG antibody conjugated with HRP, 1:4000; α -rat IgG antibody conjugated with HRP, 1:5000. Detection was performed with the BIORAD Clarity™ chemiluminescence kit (BioRad Laboratories) using Chemidoc (BioRad Laboratories).

3.7 Indirect immunofluorescence

Promastigotes were harvested, washed in ice-cold 1xPBS, fixed in 4% paraformaldehyde (w/v) and adhered to Superfrost™ Ultra Plus Adhesion slides (Thermo Fisher Scientific). Cells were dried, rehydrated with 1xPBS and incubated with 0.1 M glycine for 15 minutes. Parasites were then permeabilized with 0.1% (w/v) Triton X-100 in 0.05 M glycine. DNA was stained with 4', 6-diamidino-2-phenylindole (DAPI). Slides were mounted in 30% (v/v) glycerol in PBS. Promastigotes were visualized with the fluorescence microscope Zeiss Axio Imager Z1 (Carl Zeiss, Germany) with a 63x glycerol-immersion objective. Images were acquired using the Axiovision 4.8 (Carl Zeiss, Germany) software.

3.8 *In vivo* assays

Animals and Ethics Statement: C57BL/6 and National Marine Research Institute (NMRI) mice were obtained from the i3S Animal Facility and were raised under specific-pathogen-free conditions. Experimental animal procedures were approved by the Local Animal Ethics Committee of i3S and licensed by DGAV (Direção Geral de Alimentação e Veterinária, Government of Portugal). The i3S Animal Facility is certified by DGAV. Animals were handled in strict accordance with good animal practice as defined by national authorities (DGAV, Directive 113/2013 from 7th August) and by the International Guiding Principles for

Biomedical Research Involving Animals, issued by the Council for the International Organizations of Medical Sciences (EC Directive 86/609/EEC).

Animal infection and parasite burden determination: Male C56BL/6 mice (around 6 weeks old) were used in all experiments. The animals were housed in groups of 2-6 animals per cage, and the experimental groups were randomized as to mouse age, cage and cage location. Mice were restrained and intravenously (IV) injected in the tail vein with 2×10^7 stationary phase promastigotes using a 26G needle. Animals were euthanized at defined time points by an overdose of isoflurane inhalation followed by cervical dislocation. The liver and spleen were excised, weighted and homogenized in Schneider's medium (Sigma) supplemented with 10% (v/v) FBSi, 100 U/mL penicillin, 100 mg/mL streptomycin, 5 mM HEPES (pH 7.4) and 5 mg/mL phenol-red (Sigma). The number of parasites per gram of organ (parasite burden) was calculated as described elsewhere²⁴⁵. Briefly, homogenates were diluted to 10 mg/mL and subsequently titrated in quadruplicate across a 96-well plate in serial fourfold dilutions. After 2 weeks of growth at 25°C, the last dilution containing promastigotes was recorded, and the parasite burden was calculated.

All parasite lines were passaged through NMRI mice before the C57BL/6 infection experiments (infected intraperitoneally with 1×10^8 stationary promastigotes). Parasites were then recovered from the spleen one week after infection.

3.9 Statistical analysis

All the data obtained in this work was organized and analysed using the GraphPad Prism 6 software. Statistical tests are registered in the descriptions of the figures. The significance was defined as $P \leq 0.05$.

Chapter 4: Results

4.1 Phenotypic characterization of *LZIP3*^{-/-} parasites:

To fully characterize *LZIP3* in *Leishmania infantum*, the single zinc transporter reported so far in these parasites, it is essential to address the relevance of this protein in both promastigotes and amastigotes. As a step towards this objective, *L. infantum* mutants devoid of both *LZIP3* loci, *i.e.*, homozygous knockouts, were previously produced using CRISPR-Cas9 genome editing¹⁹⁸. The fact that ablation of *LZIP3* from the genome was successful, *per se* demonstrated that this protein is not essential for promastigotes in standard culture conditions. Preliminary results suggested, however, that *LZIP3* might be essential under zinc limitation. The first objective of this thesis was to investigate this premise in depth, by performing a detailed analysis of *LZIP3*^{-/-} parasites.

4.1.1 *LZIP3* is dispensable in standard conditions but essential under zinc limitation

To assess the performance of *LZIP3*^{-/-} cells in standard and zinc-limiting culture conditions, the growth pattern of these parasites was compared to that of WT. To that end, promastigotes were seeded at 10⁶ cells/mL and allowed to grow in unaltered culture medium (complete RPMI + 10% FBSi) or in the presence of increasing concentrations of the zinc chelator TPEN, and parasite number evaluated at defined times. As illustrated in Fig. 1, *LZIP3*^{-/-} parasites presented cell densities similar to the WT line, when in normal culture medium over the 7 days of the experiment. However, a statistically significant contraction of growth was observed in parasites lacking *LZIP3* relative to WT cells, when these were cultured in the presence of 2.5 μM of TPEN. Noticeably, this growth defect became more evident from day 3 onward, coincident to KO parasites starting to present a stress-related morphology (data not shown). At days 6 and 7, no living parasites were detected in the 2.5 μM TPEN-supplemented culture. Parasites, including WT, could not cope with 5 μM TPEN and died after 2-3 days.

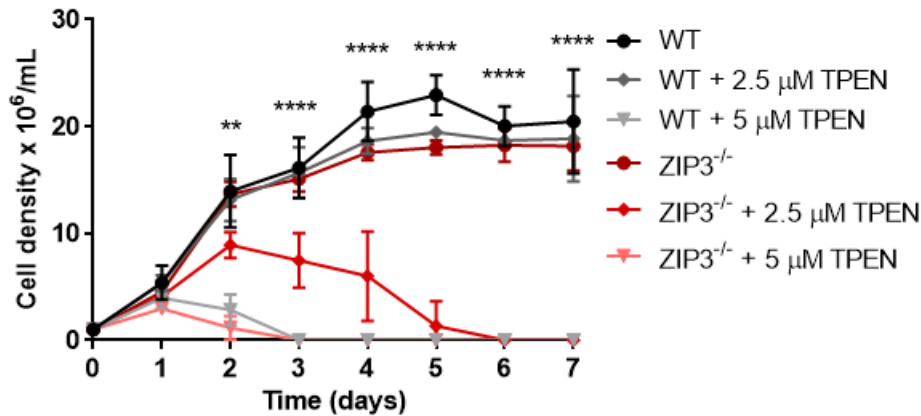


Fig. 5. Parasites lacking LiZIP3 do not survive in zinc-depleting conditions. Growth curves of WT and ZIP3^{-/-} promastigotes in absence or in the presence of two concentrations of TPEN. Parasites were synchronized prior to the beginning of the experiment and, at day 0, cells were seeded at 10⁶ cells/mL. Cell counting was performed in the indicated time points. Stars represent significant differences observed between untreated WT and ZIP3^{-/-} + 2.5 μM TPEN (**P ≤ 0.01, ****P ≤ 0.0001) at different time points analysed by Two-way repeated measures ANOVA with Tukey multiple comparison test. Data represent the mean ± S.D. from three independent experiments.

In short, results shown in Fig. 5 corroborate preliminary data indicating that ZIP3^{-/-} parasites are incapable of growing in medium made zinc limited by addition of TPEN, suggesting that these cells cannot scavenge zinc from the extracellular milieu in an efficient way. One hypothesis is that metal storages are drained over the first two days and parasites become increasingly starved, inducing a stressing situation that would otherwise be met by the LiZIP3 high-affinity zinc transporter.

To confirm that ZIP3^{-/-} growth defect in zinc-limiting conditions is indeed due to specific nutrient restriction and not to a cytotoxic effect of the employed zinc chelator, this cell line was seeded in culture medium containing 2.5 μM TPEN and, when cell densities started to clearly decline (between day 4-5), cultures were supplemented with 50 μM ZnCl₂.

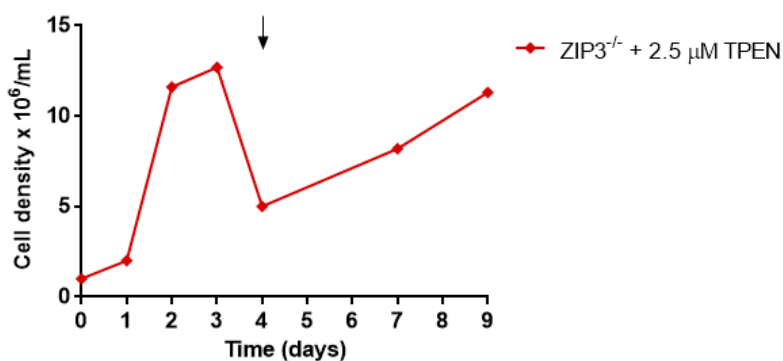


Fig. 6. LiZIP3^{-/-} growth contraction in the presence of 2.5 μM TPEN is specifically due to zinc restriction. Growth curves of ZIP3^{-/-} promastigotes in the presence of 2.5 μM TPEN. Cultures were supplemented with 50 μM ZnCl₂ when cell density declined (arrow). After zinc supplementation, parasite growth resumed. Parasites were synchronized prior to the beginning of the experiment and, at day 0, cells were seeded at 10⁶ cells/mL. Cell counting was performed in the indicated time points. One representative experiment is shown. See Fig. S3 for two additional independent experiments.

As shown in Fig. 6 and Fig. S3, parasite growth was resumed upon zinc addition. This result shows that the TPEN-induced growth defect in *L*ZIP3^{-/-} cells is due to lack of zinc in the culture.

4.1.2 *L*ZIP3^{-/-} parasites retain the capacity of internalizing zinc

As referred to above, ZIP3^{-/-} and WT parasites show no differences in growth when in normal culture medium. To evaluate whether the lack of ZIP3 expression impacts on zinc acquisition, the zinc content of WT and ZIP3^{-/-} and promastigotes was compared.

Parasites grown for 96h were used as a starting point, as at this moment all zinc in the medium was consumed and, therefore, cells were in zinc-limiting conditions¹. Cultures were then supplemented with 50 μM ZnCl₂, a concentration ~20 times higher than that determined to be present in normal, fresh culture medium. Aliquots were harvested before (96h), immediately after (0h) and 2h, 6h and 24h following zinc addition. Cellular zinc content was then analysed by Flame Atomic Absorption Spectrometry (FAAS). Simultaneously, ZIP3 expression was analysed by western blotting using an α-ZIP3 antibody (Fig. 7).

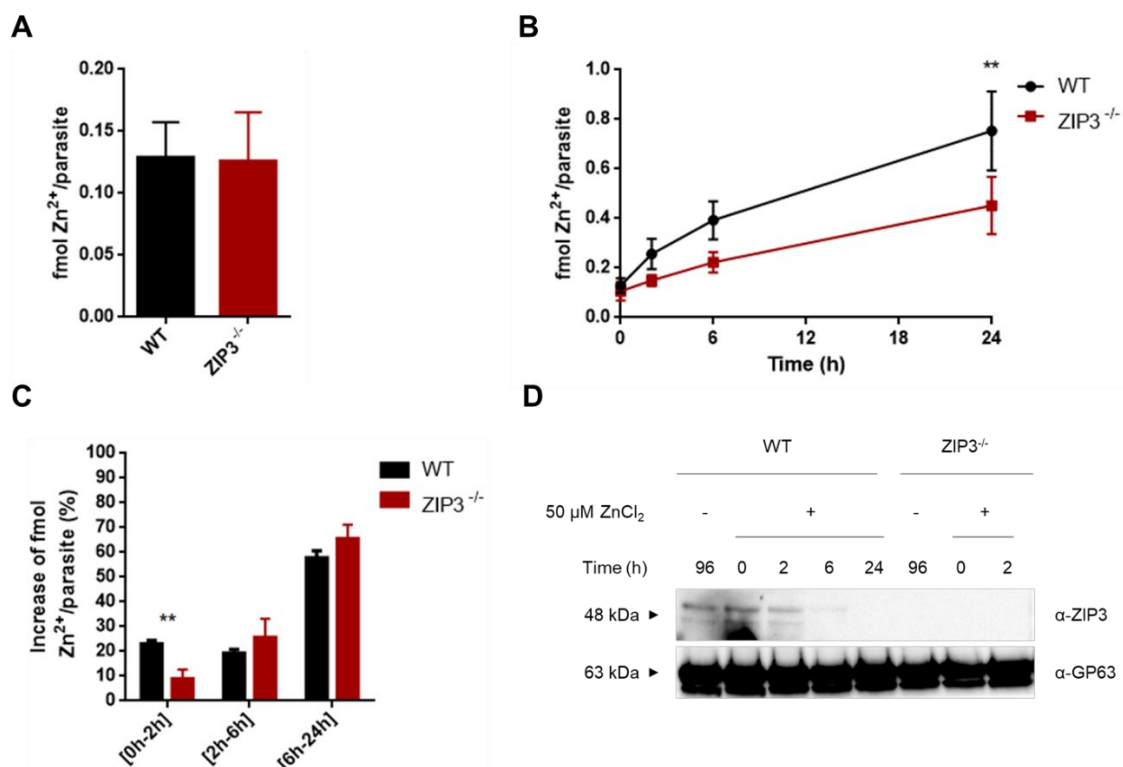


Fig. 7. *L*ZIP3^{-/-} parasites bypass the absence of *L*ZIP3 in standard and zinc surplus conditions. **A** – Zinc content of parasites after 96h of growth in standard culture medium, measured by FAAS. **B** – Zinc content of parasites at defined time-points after the addition of zinc, measured by FAAS. **C** – Percentage of increment in zinc internalization during different intervals of time upon zinc addition. **D** – ZIP3 expression levels, analysed by western blotting. Membranes were hybridized with α-ZIP3 (upper panel). Loading control (lower panel) was performed with α-GP63. (Continues in the next page)

Fig. 7. (Continued) Parasites were synchronized prior to the beginning of the experiments and, at day 0, cells were seeded at 10^6 cells/mL and allowed to grow for 96h. Parasites samples for both zinc measurements and protein analyses were harvested before (96h), immediately (0h) and 2h, 6h and 24h after addition of 50 μ M ZnCl₂ to the culture medium. Stars represent significant differences between WT and ZIP3^{-/-} (**P \leq 0.01) analysed by Two-way repeated measures ANOVA with Sidak multiple comparison test. Data represent the mean \pm SD from three independent experiments.

As shown in Fig. 7A, 96h-grown parasites had approximately the same zinc content, in agreement to being under zinc limitation. A significant difference (P \leq 0.01) between these lines was nonetheless observed upon zinc supplementation, ZIP3^{-/-} cells presenting consistently less zinc than WT parasites. This disadvantage of ZIP3^{-/-} parasites is particularly significant at the farthest analysed time point after zinc addition to the cultures (24h) (Fig. 7B). This shows that absence of *L*ZIP3 impacts on intracellular zinc content within the considered timeframe of the experiment.

Zinc measurements represented in Fig. 7 also show that zinc content of ZIP3^{-/-} parasites continued to increase along the 24h following zinc supplementation, albeit never reaching that of WT cells, indicating that parasites possess an alternative means to internalize zinc. Interestingly, data suggests that the differential accumulation kinetics is restricted to the first hours that follow zinc addition to the cultures. To directly assess this hypothesis, the differences in parasite zinc content during specific intervals of time was modeled for the two lines. For this, the equation below was used, in which A_t , $A_{(t+1)}$, A_n and A_0 correspond to the amount of zinc (fmol/parasite) in a given time point, in the following time point, in the final time point and in the first time point, respectively.

$$\% \text{ increase } \frac{\text{Zn}^{2+}}{\text{parasite}} = \frac{A_{(t+1)} - A_t}{A_n - A_0} \times 100, t \in \{0, 1, \dots, n\}$$

This analysis shows that there is a statistically significant difference between the cell lines (P \leq 0.01) regarding metal uptake velocity in the first 2h following zinc addition (Fig. 7C), WT parasites acquiring the metal faster than ZIP3^{-/-} during that considered time frame. After this initial period WT zinc internalization kinetics seem to decelerate, levelling that of ZIP3^{-/-}. This likely occurs because, after this time, the level of *L*ZIP3 in the membrane of WT cells is drastically reduced¹ (Fig. 7D), acquisition of the metal in these cells being ascribed to a different protein which likely is also functional in ZIP3^{-/-} parasites.

Collectively, analysis of ZIP3^{-/-} parasites give an insight into the existence of a second transporter that translocates zinc from the environment to the *L. infantum* cytosol, with a slower transport kinetics/lower affinity for Zn²⁺ than *L*ZIP3. This transporter could be responsible for survival of ZIP3^{-/-} promastigotes under standard and zinc-surplus conditions. Also, a lower affinity of this second transporter could explain parasite growth ceasing in

zinc-limiting conditions (Fig. 5), as under these circumstances parasites might be unable to import the metal. Attempts to identify the second zinc importer will be described in Section 4.2 – Disclosure of the second zinc transporter.

4.1.3 The zinc deficiency phenotype is reverted in add-back strains

Reintroduction of ablated genes in a knockout cell line is essential to ensure that any observed phenotype is ascribed to loss of that particular gene and not to unexpected events, namely mutations in other genes. Hence, to prove that i) the growth defect of *L*ZIP3^{-/-} parasites in zinc-restricted conditions and ii) the slower kinetics of zinc internalization in zinc-surplus conditions are due to the absence of this transporter, *L*ZIP3 was inserted back in the homozygous knockout cells, *i.e.*, revertant/add-back lines were generated. Production of an add-back strain is also imperative to appreciate the relevance of ZIP3 in the amastigote form of *L. infantum*, specifically in the context of *in vivo* experiments with ZIP3^{-/-} parasites.

To produce an add-back line, two approaches were followed, i) introduction of the *ZIP3* ORF in the ribosomal *locus* of *L*ZIP3^{-/-} cells and ii) episomal complementation. It is of note that in none of these strategies the *ZIP3* ORF was accompanied by its 3'UTR, hence the expressed protein would not be regulated, differing from a WT situation.

Generation of LiZIP3 add-back parasites – ribosomal locus integration

The first approach to create a *L. infantum* ZIP3^{-/-} add back strain made use of a pLEXY vector that allows recombination of a DNA cassette harbouring the gene of interest in the ribosomal *locus* of *Leishmania*²⁴¹. The first step towards this strategy implied the introduction of the ZIP3 ORF in the pLEXY vector.

Construction of the pLEXYZIP3 vector and introduction in LiZIP3^{-/-} parasites

The pLEXYZIP3 plasmid containing the ZIP3 ORF (Sequencing – Fig. S5 and S6), a drug-selectable marker and the required sequences to allow integration in the ribosomal *locus* of *L. infantum* through homologous recombination (5' SSU and 3' SSU) was constructed (Fig. 8; See Materials and Methods).

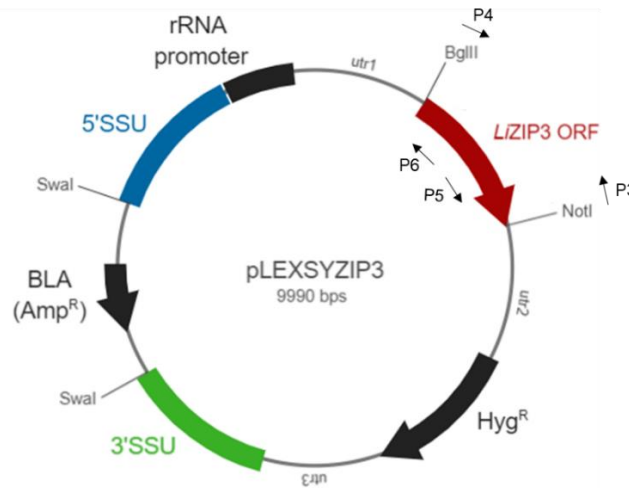


Fig. 8. Schematic representation of the pLEXSYZIP3 ribosomal locus integration plasmid. 5' SSU: start of 18S rRNA of *Leishmania* spp.; rRNA promoter: *Leishmania donovani* rRNA promoter fragment; utr1: 5' non-translated region of adenine phosphoribosyltransferase (apt) gene of *Leishmania tarentolae* with splice acceptor site for target gene; utr2: 1.4 kb intergenic region from calmodulin (cam) operon from *Leishmania tarentolae* with polyA site for target gene and splice acceptor site for marker gene; Hyg^R: Hyg marker gene encoding hygromycin phosphotransferase; utr3: *Leishmania major* DNA region for divergent RNA region upstream of dihydrofolate reductase-thymidylate synthase with polyA site for marker gene; 3' SSU: 3' part of rRNA of *Leishmania* spp.; BLA: beta-lactamase marker gene.

The assembled pLEXSYZIP3 plasmid was digested with Swal, and the resulting 7126 bp linear fragment (Fig. 9A) was electroporated into ZIP3^{-/-} promastigotes, resulting in hygromycin-resistant polyclonal cell cultures. Transfected parasites were plated, and isolated colonies picked and cultured in hygromycin-containing medium. From these, one clonal cell culture was chosen for subsequent analysis. This line will be, from now on, referred to as ZIP3^{-/-}_pLEXSYZIP3.

Genomic DNA isolated from the ZIP3^{-/-}_pLEXSYZIP3 culture was used to confirm the correct integration of the Swal-Swal fragment into the 18S rRNA locus of ZIP3^{-/-} parasites' genome. Fig. 9B shows a schematic representation of the expected replacement. As shown in Fig. 9C, use of primer pair P7+P8 amplified a product of ~1.8 kb in the ZIP3^{-/-}_pLEXSYZIP3 line, compatible with the correct integration of the Swal-Swal fragment in the ribosomal locus. Furthermore, use of primer pair P3+P4 led to the amplification of a ~1.4 kb band in ZIP3^{-/-}_pLEXSYZIP3 (and WT), corresponding to the ZIP3 ORF (Fig 9D) (See Fig. 8, 9 and Fig. S1 for primer location). WT and ZIP3^{-/-} genomic DNA were used as controls.

To confirm that ZIP3 expression was restored in ZIP3^{-/-} cells, total protein was extracted from cells, separated by SDS-PAGE, transferred onto a membrane and hybridized with an α-ZIP3 antibody¹. WT, ZIP3^{-/-} and parasites overexpressing ZIP3¹ (i.e., cells with an ectopic copy of ZIP3, WT_pXGZIP3; See Fig. S2) were used as controls. Fig. 5E shows that ZIP3^{-/-}_pLEXSYZIP3 cells were able to express ZIP3, contrary to ZIP3^{-/-} parasites. The relatively high expression in ZIP3^{-/-}_pLEXSYZIP3 parasites, comparatively to WT, can tentatively be

ascribed to multiple integration events of the Swal-Swal fragment in several 18S rRNA *loci*, which would result in numerous copies of ZIP3.

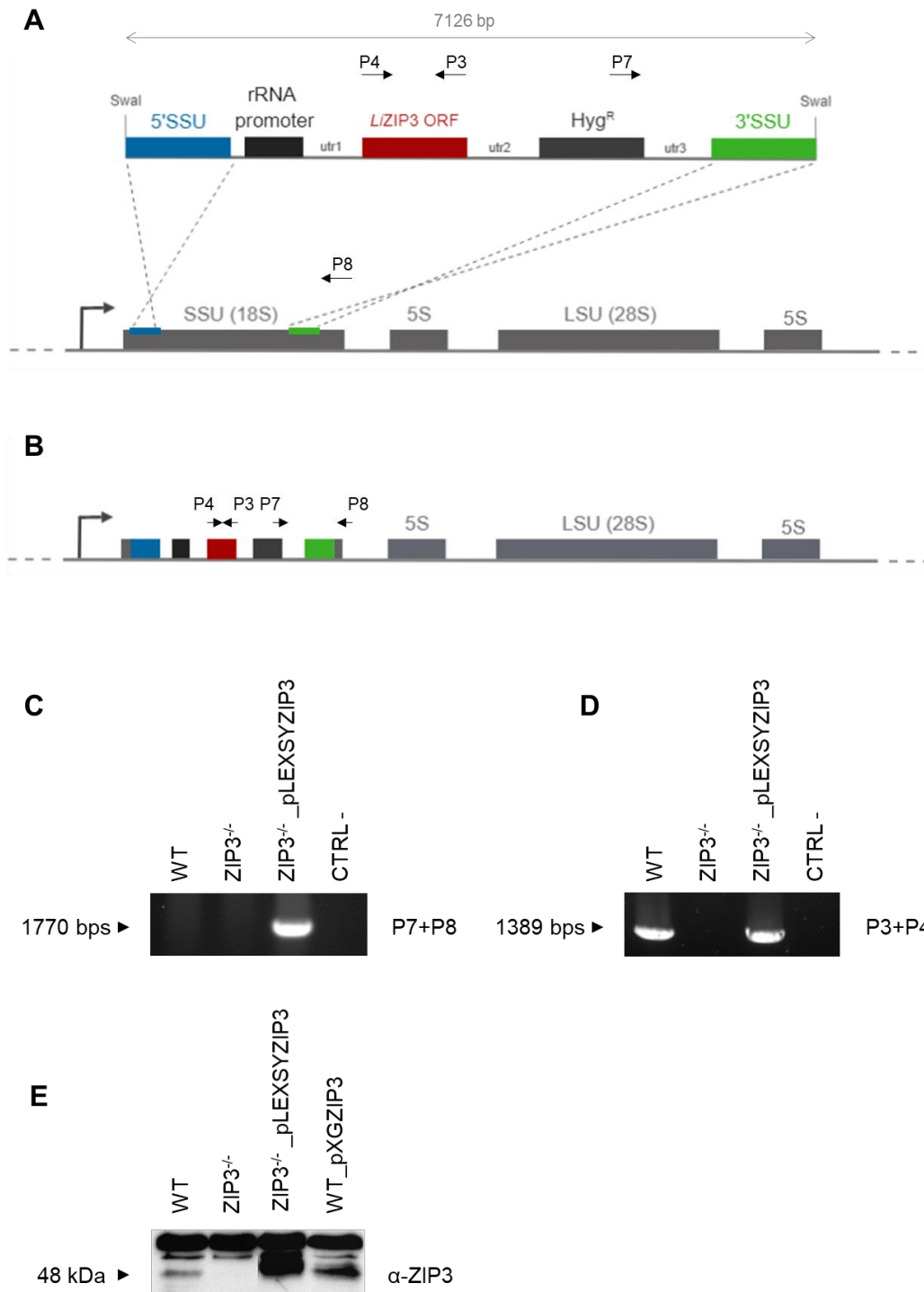


Fig. 9. Generation of LiZIP3^{-/-} revertant strains by ribosomal locus integration. (A) Schematic representation of the Swal-linearized pLEXSYZIP3 cassette and (B) its integration into the *Leishmania* 18S rRNA locus. Genomic analysis of hygromycin-resistant ZIP3^{-/-} parasites obtained upon transfection of the Swal-linearized pLEXSYZIP3 fragment, by PCR, show (C) correct integration of the cassette in the ribosomal locus and (D) presence of the ZIP3 ORF. (E) Protein analysis of ZIP3^{-/-}_pLEXSYZIP3 parasites by western blotting shows that ZIP3^{-/-}_pLEXSYZIP3 parasites are able to express LiZIP3. Membranes were hybridized with α-ZIP3. Parasites were synchronized, seeded at 10⁶ cells/mL and allowed to grow for 96h prior to being harvested for protein analysis.

Phenotypic analysis

To assess if the ZIP3 protein expressed from ribosomal *loci* was functional, the levels of zinc internalization in ZIP3^{-/-}_pLEXSYZIP3 cells were first addressed. For this, parasites that had been growing for 96h were incubated with 50 μM ZnCl₂ for a 24h period. Aliquots of parasites harvested before (96h) and after zinc supplementation (96h + 24h) were then analysed by ICP-MS. Wildtype and ZIP3^{-/-} cells were used as controls.

As can be seen in Fig. 10A, reintroduction of the gene restored zinc acquisition in the add-back cells. Next, it was investigated if hypersensitivity to TPEN addition was lost in ZIP3^{-/-}_pXGZIP3 cells. Fig. 10B shows that the ZIP3^{-/-}_pLEXSYZIP3 line grows as WT in the presence of 2.5 μM TPEN, confirming that expression of ZIP3 from the ribosomal *locus* allows the reversion of growth hindrance observed in the knockout background. Furthermore, it corroborates the hypothesis that abrogation of ZIP3 is the sole responsible for loss of parasite viability in zinc-limiting conditions.

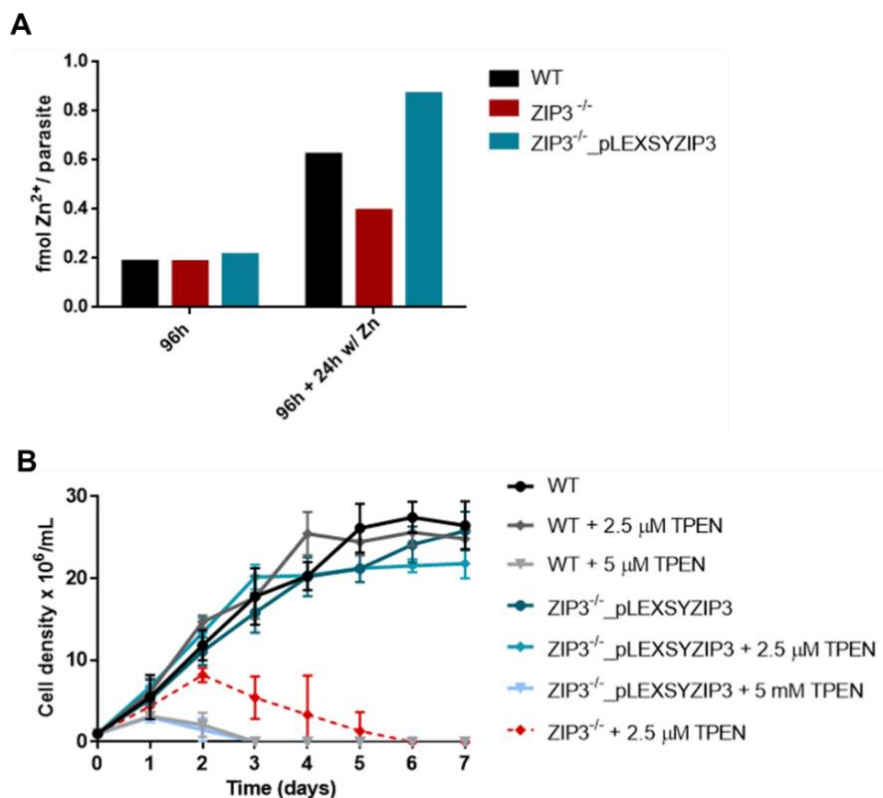


Fig. 10. LiZIP3 expressed from the ribosomal locus reverts the defective phenotypes of the LiZIP3^{-/-} mutant. (A) Zinc content of WT, ZIP3^{-/-} and ZIP3^{-/-}_pLEXSYZIP3 parasites before and after zinc supplementation, measured by ICP-MS. Parasites were synchronized prior to the beginning of the experiment and, at day 0, cells were seeded at 10⁶ cells/mL and allowed to grow for 96h. Parasites samples zinc measurements were harvested before (96h) and 24h after addition of 50 μM ZnCl₂ to the culture medium. (B) Growth curves of WT, ZIP3^{-/-} and ZIP3^{-/-}_pLEXSYZIP3 promastigotes in absence or in the presence of two concentrations of TPEN. Parasites were synchronized prior to the beginning of the experiment and, at day 0, cells were seeded at 10⁶ cells/mL. Cell counting was performed in the indicated time points. Data represents three independent experiments.

Protein analysis following parasite mouse passage

Genome integration is generally considered to be stable even in an *in vivo* situation, where drug pressure is not applied. Nevertheless, there are reports of loss of ribosomal-integrated fragments in *Leishmania*. Hence, expression of ZIP3 in ZIP3^{-/-}_pLEXSYZIP3 cells was assessed after murine infection.

A single NMRI male mouse was intraperitoneally infected with 2x10⁷ ZIP3^{-/-}_pLEXSYZIP3 stationary promastigotes. Parasites were recovered from the infected spleen one week later and cultured in the presence of the selective drug (Hyg). Unexpectedly, ZIP3^{-/-}_pLEXSYZIP3 promastigotes collected from splenic tissue showed remarkable reduction of ZIP3 expression (Fig. 11), not only compared to WT parasites subjected to the same procedure but also relatively to the expression that these cells presented before mouse passage (Fig 9E). This result suggested that integration of the ZIP3 ORF in the ribosomal *locus* of ZIP3^{-/-} parasites was highly unstable, and that many copies of the gene were apparently lost following a 7-days *in vivo* experiment.

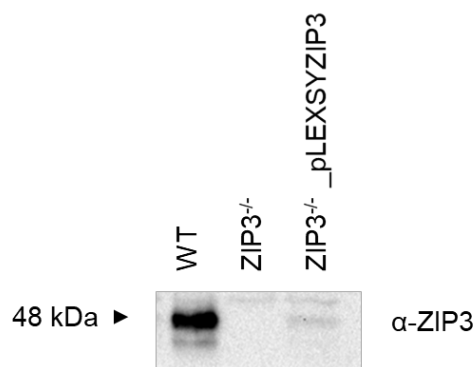


Fig. 11. The ZIP3^{-/-}_pLEXSYZIP3 revertant strain lost LiZIP3 expression following mouse passage. Protein analysis by western blotting shows that ZIP3^{-/-}_pLEXSYZIP3 parasites recovered from the spleen of infected NMRI mice, seven days post-infection, are not able to express LiZIP3 as before the mouse passage. Membranes were hybridized with α-ZIP3. Parasites were allowed to grow in liquid culture medium for 96h prior to being harvested for protein analysis.

As previously mentioned, a major reason to re-introduce ZIP3 expression in ZIP3^{-/-} parasites was to address the role of this protein in the context of a leishmaniasis animal model, using the add-back line as a control. Hence, an alternative method to generate an add-back line was pursued, consisting on the expression of an ectopic copy of ZIP3 from an episome.

Generation of LiZIP3 add-back parasites – episomal complementation

As a second approach to produce a ZIP3^{-/-} add-back line, protein expression from an episome was considered. For this, the vector pXGZIP3^{1,244} carrying the ZIP3 ORF and a

neomycin resistance gene (Fig. S2) was electroporated into ZIP3^{-/-} parasites, giving rise to a neomycin-resistant cell line. This line will be, from now on, referred to as ZIP3^{-/-}_pXGZIP3. Expression of ZIP3 from the pXGZIP3 episome in transformed parasites was confirmed by western blotting with an α -ZIP3 antibody^{1,251}. WT, ZIP3^{-/-} and WT_pXGZIP3 cells were used as controls. The results revealed that ZIP3^{-/-}_pXGZIP3 cells were able to express ZIP3 (Fig. 12).

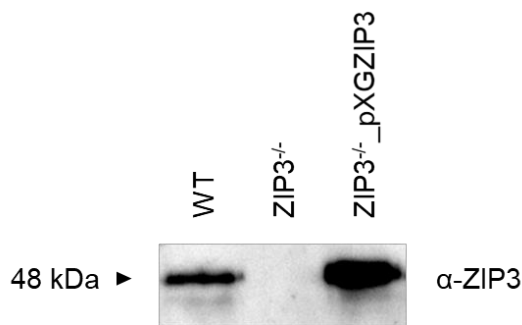


Fig. 12. The ZIP3^{-/-}_pXGZIP3 revertant strain expresses LiZIP3. Protein analysis by western blotting confirms that ZIP3^{-/-}_pXGZIP3 parasites express LiZIP3 from the episome. Membranes were hybridized with α -ZIP3. Parasites were synchronized, seeded at 10⁶ cells/mL and allowed to grow for 96h prior to being harvested for protein analysis.

Phenotypic analysis

To understand if the ZIP3 protein expressed from the pXGZIP3 plasmid was functional, zinc internalization in ZIP3^{-/-}_pXGZIP3 promastigotes was evaluated. For this, parasites grown for 96h were incubated with 50 μ M ZnCl₂ for 24h, and aliquots of parasites were harvested before (96h) and after zinc supplementation (96h + 24h) were analysed by ICP-MS. Wildtype and ZIP3^{-/-} cells were used as controls. As shown in Fig. 13A, ectopic expression of ZIP3 restored zinc acquisition in the add-back line. Next, analysis of growth of ZIP3^{-/-}_pXGZIP3 promastigotes with and without TPEN was pursued. Fig. 13B shows that, as expected, the ZIP3^{-/-}_pXGZIP3 line grows as WT in the presence of 2.5 μ M TPEN, confirming that re-expression of ZIP3 from the episome in mutant cells enables parasites to recover the capacity to grow in the presence of TPEN.

Protein analysis following parasite mouse passage

Similarly to what was performed with the ZIP3^{-/-}_pLEXSYZIP3 add-back line, it was important to address whether ZIP3 expression from the ectopic vector was maintained after murine infection. For this, a single NMRI male mouse was intraperitoneally infected with 2x10⁷ ZIP3^{-/-}_pXGZIP3 stationary promastigotes and, one week later, parasites were recovered from the infected spleen. Following western blotting analysis (Fig. 14), it was considered that ZIP3^{-/-}_pXGZIP3 promastigotes collected from splenic tissue expressed close to normal levels of ZIP3 expression, compared to WT parasites subjected to the same procedure and to add-back parasites before mouse passage (Fig 12).

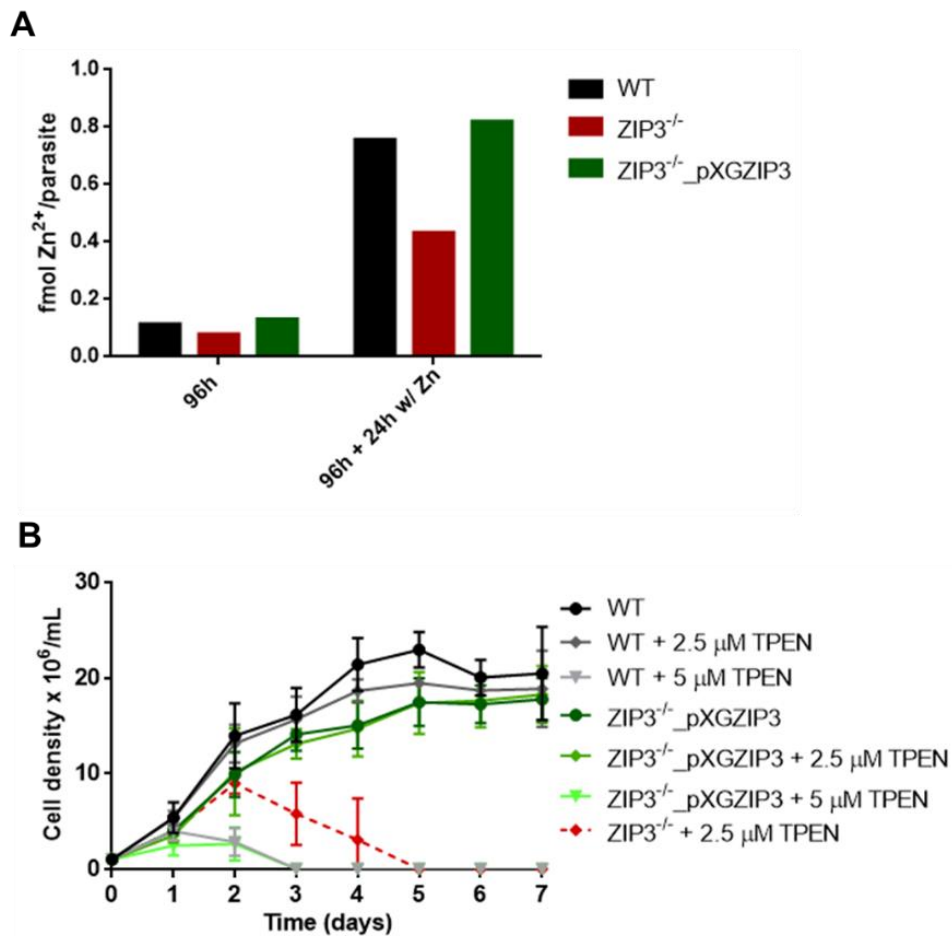


Fig. 13. LiZIP3 expressed from the pXGZIP3 episome reverts the defective phenotypes of the LiZIP3^{-/-} mutant. (A) Zinc content of WT, ZIP3^{-/-} and ZIP3^{-/-}_pXGZIP3 parasites before and after zinc supplementation, measured by ICP-MS. Parasites were synchronized prior to the beginning of the experiment and, at day 0, cells were seeded at 10⁶ cells/mL and allowed to grow for 96h. Parasites samples zinc measurements were harvested before (96h) and 24h after addition of 50 μM ZnCl₂ to the culture medium. (B) Growth curves of WT, ZIP3^{-/-} and ZIP3^{-/-}_pXGZIP3 promastigotes in absence or in the presence of two concentrations of TPEN. Parasites were synchronized prior to the beginning of the experiment and, at day 0, cells were seeded at 10⁶ cells/mL. Cell counting was performed in the indicated time points. Data represents three independent experiments.

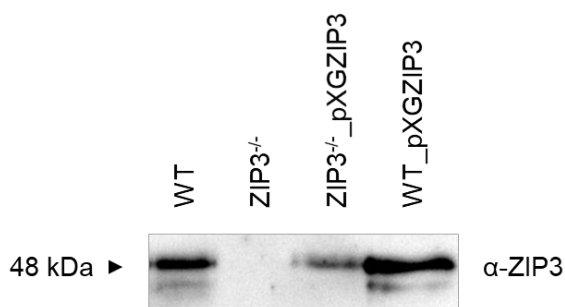


Fig. 14. The ZIP3^{-/-}_pXGZIP3 revertant strain expresses LiZIP3 following mouse passage. Protein analysis by western blotting shows that ZIP3^{-/-}_pXGZIP3 parasites recovered from the spleen of infected NMRI mice, seven days post-infection, are able to express LiZIP3. Membranes were hybridized with α-ZIP3. Parasites were allowed to grow in liquid culture medium for 96h prior to being harvested for protein analysis.

Collectively, studies on ZIP3^{-/-}_pXGZIP3 parasites both *in vitro* and *in vivo* met all the conditions not only to prove that the observed phenotypes are most certainly exclusively due to ZIP3 *loci* ablation, but also to be used in experiments focusing on the importance of ZIP3 in a leishmaniasis infection animal model. The latter will be addressed in Section 4.3 – Addressing the role of *Liz*ZIP3 in the course of an infection of an animal model.

4.2 Disclosing the second zinc transporter

As discussed in Section 4.1, successful generation of *LZIP3* homozygous knockout parasites gave important insights not only on the importance of the ZIP3 protein but also on zinc uptake mechanisms in *Leishmania*. Namely, the acknowledgment that ZIP3 is not essential for promastigotes in standard culture conditions suggests that an alternative zinc transporter, possibly of low affinity, co-exists in *L. infantum*. Supporting the presence of a second zinc acquisition system is the observation that ZIP3^{-/-} parasites retain the ability to accumulate zinc when this metal is provided in high amounts (in zinc-surplus conditions).

The finding that *L. infantum* promastigotes are able to express at least two zinc uptake systems appears to constitute a physiologic advantage, as these would likely provide a means for the parasite to adequately acquire zinc even in face of drastic environmental changes in nutrient availability¹⁹⁹. Defining the identity of this alternative zinc uptake mechanism is important, constituting the premise of the work presented in this section.

For a protein to be candidate for the alternative zinc transporter function, it has to meet at least two conditions, i) to be expressed in the parasite membrane and ii) to be able to mediate zinc internalization. As a starting point to disclose the molecular player(s) behind the alternative zinc transport system, the two other ZIP family proteins encoded in the *Leishmania* genome, *LZIP1* and *LZIP2*, were considered as obvious candidates.

To dissect if *LZIP1* can function as an alternative zinc transport system, its expression pattern in *L. infantum* promastigotes was first analysed. Secondly, efforts to abrogate *LZIP1* expression were conducted. Finally, metal uptake in *LZIP1*-overexpressing parasites was addressed. In what concerns *LZIP2*, the knock-in of a fluorescent tag fused to the endogenous protein was attempted. Furthermore, as for *LZIP1*, metal uptake in *LZIP2*-overexpressing parasites was analysed.

4.2.1 *LZIP1* protein expression analysis

LZIP1 was previously object of preliminary studies in the Molecular Parasitology lab, namely in what concerns its metal transport specificity and subcellular localization²⁴⁴. It was ascertained that *LZIP1* is expressed in the parasite cellular membrane^{1,244}, meeting *a priori* one of the requirements to, theoretically, being capable of acting as an alternative zinc importer. It is of note that an orthologue of *LZIP1*, named LIT1, was described in *L. amazonensis* as a ferrous iron transporter^{183,184}. However, despite the high degree of homology between *LZIP1* and LIT1 (BLASTn – 88% identities, 92% positives)²⁴⁴, studies

on the Molecular Parasitology Lab were not conclusive about role of the former on iron uptake in *L. infantum*.

To investigate if *LiZIP1* could act as a second zinc import system, protein expression throughout the promastigote stage was first analyzed. These studies were conducted in WT cells to assess if *LiZIP1* expression responds to progressive metal deficiency in the culture media along the growth curve of parasites, as it is the case of *LiZIP3*. Additionally, protein expression in WT cells was compared to that in *ZIP3^{-/-}* parasites, to explore the possibility of *LiZIP1* expression being altered in the latter background. These analyses were possible due to the existence of an α -ZIP1 antibody previously produced in the lab^{1,244}.

Parasites were grown in standard conditions, aliquots of lag (0h, 24h), early log (48h) and late log (120h, 142h) phase parasites were harvested, and total protein extracts were analyzed by western blotting (Fig. 15).

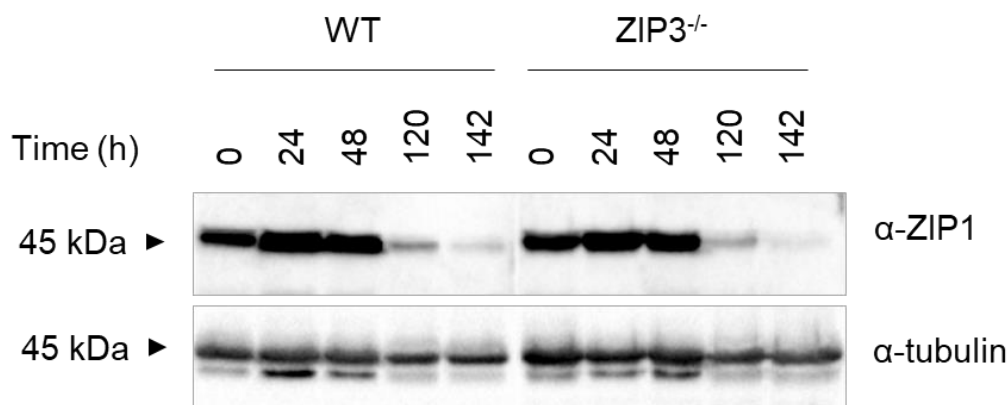


Fig. 15. *LiZIP1* expression pattern along the WT and *ZIP3^{-/-}* promastigote growth curve. *ZIP1* expression levels were analysed by western blotting. Membranes were hybridized with α -ZIP1 (upper panel). Loading control (lower panel) was performed with α -tubulin. Parasites were synchronized prior to the beginning of the experiments and, at day 0, cells were seeded at 10^6 cells/mL and allowed to grow for 120h. Parasites samples for protein analysis were harvested at the indicated time-points.

Analysis of ZIP1 expression along promastigote growth led to two conclusions: first, expression of the ZIP1 protein in both cell lines is higher in the lag and early log phases, diminishing as parasites enter the stationary phase. This is in line with the hypothesis of ZIP1 acting as a low-affinity transporter, being expressed and conceivably exerting its function as a zinc importer when the substrate is abundant in the culture medium¹⁹⁹. Secondly, no differences in ZIP1 expression could be detected between the two genomic backgrounds. Thus, if ZIP1 functions as an alternative zinc transporter, it does not seem to be upregulated under zinc limitation, nor is does it appear to compensate ZIP3 absence in *ZIP3^{-/-}* cells.

4.2.2 CRISPR-Cas9-mediated ablation of *LiZIP1*

To get further insight on *LiZIP1* function, a CRISPR-Cas9-based strategy to produce *L. infantum* homozygous knockout mutants for this protein was designed. It is of note that *LiZIP1* is encoded by two tandem genes in chromosome 31, and that this chromosome is tetraploid^{246,247}; thus, eight copies of the ZIP1 ORF exist in the *L. infantum* genome.

The strategy was applied to WT, *LiZIP3*^{-/-} parasites, and to the same cell lines previously complemented with an episome expressing ZIP1. The latter were included so that abrogation of all *LiZIP1* chromosomal copies could be achieved even in the case of *LiZIP1* essentiality in either or both genetic backgrounds, ruling out technical problems as the reason for a hypothetical strategy failure.

The general strategy followed to delete the *LiZIP1* locus is depicted in Fig. 16. Briefly, the aim was to excise >5000 bp by inducing two Cas9-mediated double stranded breaks (DSBs), targeted by two different sgRNAs, one upstream and another downstream of each *LiZIP1* locus. To efficiently repair the two DSBs through homologous directed repair (HDR), donor DNA cassettes flanked by short homology arms to the targeted regions were simultaneously supplied. These donor DNAs carried drug resistance genes, facilitating the selection of recombinant cells.

Generation of WT and *ZIP3*^{-/-} promastigote lines carrying the Cas9 nuclease, the T7 RNA polymerase and a vector for episomic expression of *LiZIP1*

As detailed in the Introduction section, the sgRNAs are transcribed *in vivo* by the T7 RNA polymerase from PCR-generated templates. Hence, cell lines constitutively expressing the Cas9 nuclease and the T7 RNA polymerase had first to be produced. To generate these lines, WT and *LiZIP3*^{-/-} promastigotes were transfected with the pTB007 plasmid²³⁸ carrying the Cas9 nuclease, the T7 RNA polymerase and a hygromycin resistance gene. Hygromycin-resistant parasites (WT_pTB007, *ZIP3*^{-/-}_pTB007) were then used to generate promastigotes ectopically expressing *LiZIP1*. To that end, the pXGZIP1 plasmid²⁴⁴ (Fig. S7) was transfected into the WT_pTB007 and *ZIP3*^{-/-}_pTB007 parasite lines. Hygromycin-/G418-resistant parasites were analyzed by western blotting with an anti-ZIP1 antibody to confirm protein overexpression (Fig. 17).



Fig. 16. Schematic representation of the LiZIP1 locus targeting, deletion and substitution by a donor template carrying a drug resistance gene, using CRISPR-Cas9, in *L. infantum*. The DNA target sequences, the 5'-gRNA (left), the 3'-gRNA (right), and the sequences of the homology sequences flanking the donor DNA template are specified. Primers used to diagnose allele replacement are represented.

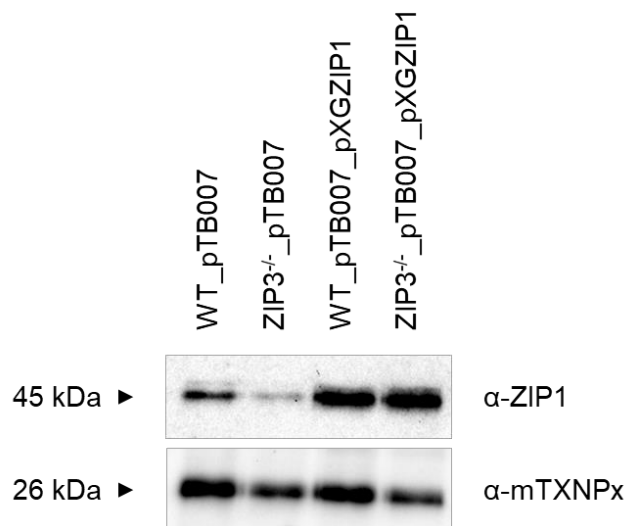


Fig. 17. WT and ZIP3^{-/-} parasites carrying the pXGZIP1 episome are able to overexpress LiZIP1. ZIP1 expression levels were analysed by western blotting. Membranes were hybridized with α-ZIP1 (upper panel). Loading control (lower panel) was performed with α-mTXNPx. Parasites were synchronized, seeded at 1x10⁶ cells/mL, and allowed to grow in liquid culture medium for 48h prior to being harvested for protein analysis

The four different produced cell lines will be, from now on, designated WT, ZIP3^{-/-}, WT_pXGZIP1 and ZIP3^{-/-}_pXGZIP1.

Single guide RNA and donor DNA design and production

The next step to produce *LiZIP1*-null cells was the design of sgRNAs targeting the *LiZIP1* locus. The part of a sgRNA that confers the specificity to the CRISPR-Cas9 system is the gRNA and, hence, its design is critical and obeys to specific rules. First, the gRNA-targeted sequence should immediately precede a 5'-NGG-3' PAM; second, to minimize the off-target activity of Cas9, the gRNA sequence should be highly matched with the target sequence. Furthermore, the target DNA should be as unique as possible in the genome²⁴⁸.

The two gRNAs designed to abrogate *LiZIP1* expression are presented in Fig. 16. One, the 5'-gRNA (P9), targets a region upstream of the first *ZIP1* gene (LinJ.31.3190), and the other, the 3'-gRNA (P10), targets a region downstream of the second *ZIP1* gene (LinJ.31.3180). Synthesis of a template sequence comprising a T7 RNA polymerase promoter and the gRNA 20-bp sequence, followed by a chimeric crRNA:tracrRNA sequence allows, upon T7 RNA polymerase transcription, formation of the complete sgRNA sequence *in vivo*²³⁸.

In order to enhance the efficiency of *LiZIP1* locus ablation and to allow an easy selection of successfully mutated parasites, donor DNA fragments containing drug-resistance markers, flanked by short homology arms, were designed. These donor DNAs consisted of a puromycin-/blastidicin-resistance cassette flanked by a 30-nt left arm complementary to the region immediately upstream of the DSB on the DNA sequence targeted by the 5'-gRNA

(P12), and a 30-nt right arm complementary to the region immediately downstream of the DSB on the DNA sequence targeted by the 3'-sgRNA (P13) (Fig. 16).

Upon PCR synthesis (Fig. S8), the two templates for 5'-sgRNA (P9+P11) and 3'-sgRNA (P10+P11) expression, plus the customized donors (amplified from the pTPuro/pTBlast plasmids using the primer pair P12+P13) were electroporated into the four parasite lines. Before this transfection, hygromycin concentration was increased to 50 µg/mL, to raise the copy number of the pTB007 plasmid and thus maximize the DSB-generation activity by Cas9.

In a first attempt to knockout *LIZIP1* two different donors, one carrying a puromycin resistance gene (PURO^R) and the other a blasticidin resistance gene (BSD^R), were provided to the parasites. Transfected parasites were allowed to recover in liquid culture or in agar plates, with the appropriate drugs (puromycin/blasticidin for the non-complemented cell lines, puromycin/blasticidin/G418 for the pXGZIP1-complemented cell lines). Only parasites from the ZIP3^{-/-} and ZIP3^{-/-}_pXGZIP1 background recovered from the drug selection in liquid culture. However, genomic analysis of both cell lines showed that no successful integration of either drug cassettes in the *locus* was achieved (data not shown).

A dual-drug strategy is useful to rapidly select homozygous knockout parasites when the target gene is in a diploid chromosome. However, as previously mentioned, *LIZIP1* is found in a tetraploid chromosome, obliging integration of four donor DNA molecules in the four *loci*. To enhance the probabilities of recovering recombinant parasites, a second attempt to ablate *LIZIP1*, using PURO^R-donors only, was performed. If puromycin-resistant parasites were recovered, and these still retained one or more *ZIP1 loci*, a second round of transfection with the BSD^R-donor would follow. This sequential selection should theoretically allow production of *LIZIP1*-null parasites, at least in the pXGZIP1-complemented lines.

Transfected parasites were plated in agar plates containing ~2x (35 µg/mL) the amount of puromycin routinely used. Transfectants were also allowed to recover in liquid cultures in the presence of ~2x or ~4x (60 µg/mL) puromycin. The use of higher drug concentrations aimed at facilitating the selection of parasites with multiple successfully replaced *loci*. Puromycin selection resulted solely in the recovery of parasites of the ZIP3^{-/-} background in liquid culture. As abovementioned, the drug-resistant polyclonal cultures could correspond to four phenotypes: replacement of one *LIZIP1 locus* by the donor in one chromosome, in two chromosomes, in three chromosomes or in all four chromosomes. A series of PCR diagnostic analysis was performed to discriminate between these possibilities. The results were not compatible with the integration of the marker in the targeted site (data not shown).

4.2.3 Characterization of *LZIP2*

The single copy gene LinJ.33.3350 encodes a putative iron and zinc transporter, named *LZIP2*. Similarly to *LZIP1* and *LZIP3*, the (predicted) 37 kDa ZIP2 protein holds most of the characteristics of ZIP members, namely the signature ZIP family and the histidine-rich motif in the variable region between TMDs III and IV²⁴⁴. However, opposing to the predicted topologies of *LZIP1* and *LZIP3*²⁴⁴, as well as to what is described for most of the ZIP family protein members⁵², the *LZIP2* topology prediction, using several available softwares, only presents seven TMDs instead of eight (See Fig. 23).

Contrary to *LZIP1*, neither information regarding location of *LZIP2* nor an efficient antibody for this protein were reported so far. Fusing a fluorescent protein to mark *LZIP2 in situ* should assist studies of its expression pattern and on resolving its subcellular location.

CRISPR-Cas9-mediated tagging of LiZIP2

CRISPR-Cas9-mediated endogenous tagging of *LZIP2* was conducted to investigate its definite subcellular localization. The strategy consisted on the introduction of a cassette coding the mNeonGreen fluorescent protein at either the N- or the C-terminus of ZIP2 (Fig. 18 and Fig. 19, respectively) in WT_pTB007 cells (See Section 4.2.2). This cassette also carried a drug-resistance gene (BSD^R) to facilitate selection of recombinant parasites, and three myc epitopes to simplify detection of fusion proteins²³⁸.

To generate *L. infantum* promastigotes expressing an endogenously N-terminally tagged *LZIP2* protein, a 5'-sgRNA (P28) to guide the Cas9 endonuclease to a region upstream the ZIP2 ORF was first designed (Fig. 18) Secondly, the flanking sequences of the donor DNA fragment that promote homologous recombination (P25 and P26) were designed in such a way that the cassette would be in frame in the ZIP2 protein (*i.e.*, the ATG triplet of ZIP2 would be removed in the recombinant cells).

Similarly, to generate *L. infantum* cells expressing an endogenously C-terminally tagged protein, a 3'-sgRNA (P27) to guide Cas9 to a region downstream the ZIP2 ORF (Fig. 19) was first designed. The flanking sequences of the donor DNA fragment (P23 and P24) were designed in such a way that the cassette would be in frame with the ZIP2 protein (*i.e.*, the STOP codon of ZIP2 would be removed in the recombinant cells).

The N-terminal tagging was expected to result in the production of a 67.5 kDa mNeonGreen-*LZIP2* fusion protein. In the case of C-terminal tagging, the *LZIP2*-mNeonGreen fusion protein was predicted to weight 62.82 kDa.

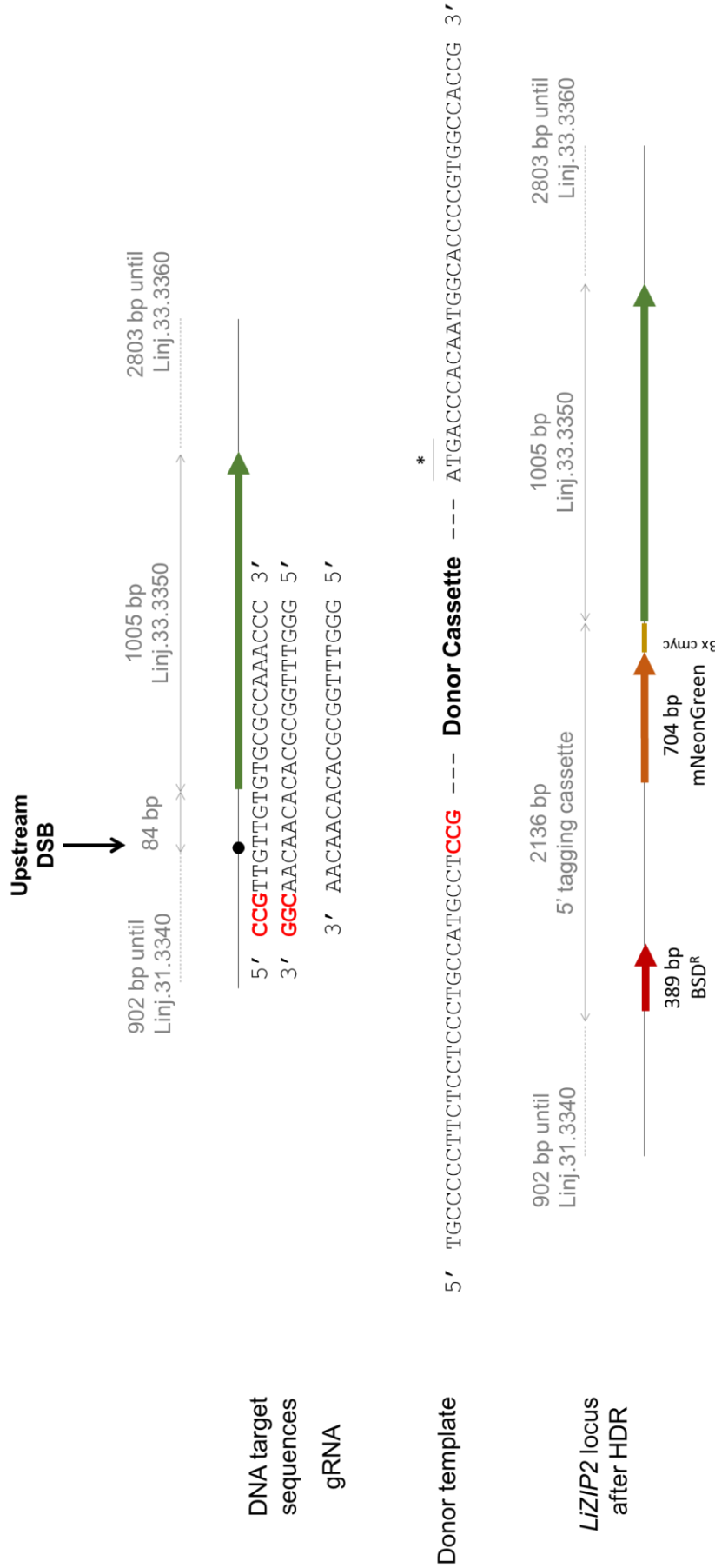


Fig. 18. Schematic representation of the knock-in of a mNeonGreen-carrying cassette at the N-terminus of LiZIP2, using CRISPR-Cas9, in *L. infantum*. The DNA target sequence, the 5'-gRNA, and the sequences of the homology sequences flanking the donor DNA template are specified. Primers used to diagnose cassette integration are represented.

^RLiZIP2 ATG codon

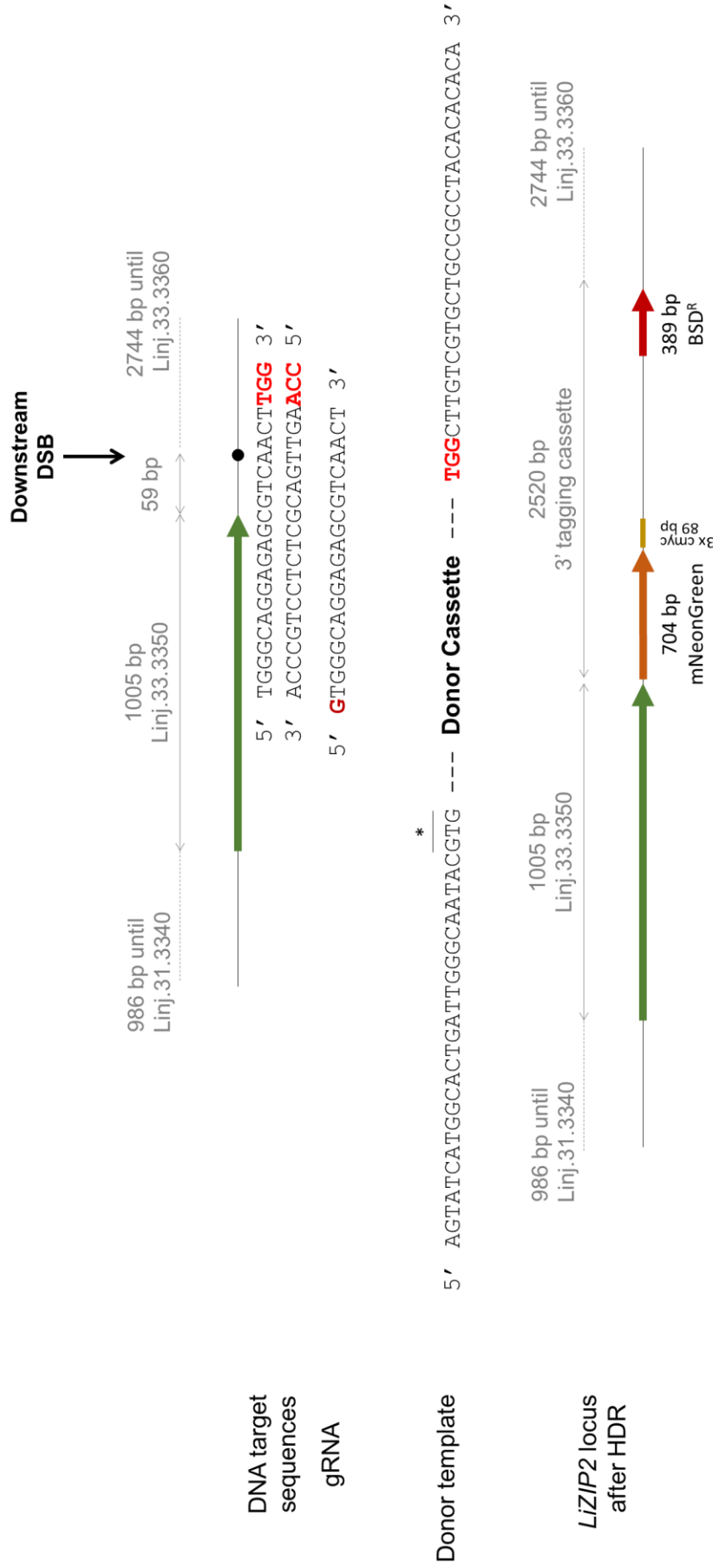


Fig. 19. Schematic representation of the knock-in of a mNeonGreen-carrying cassette at the C-terminus of LiZIP2, using CRISPR-Cas9, in *L. infantum*. The DNA target sequence, the 3'-gRNA, and the sequences of the homology sequences flanking the donor DNA template are specified. Primers used to diagnose cassette integration are represented. * triplet before LiZIP2 STOP codon

WT_pTB007 cells were transfected with the sgRNA and donor DNA cassette molecules for N-terminal (Fig. 18, Fig. S8) and C-terminal (Fig. 19, Fig. S9) tagging, and parasites were allowed to recover in liquid culture and in agar plates, with the appropriate drug (Blasticidin).

Analysis of the drug-selected cultures by immunofluorescence microscopy showed the following: first, most of the parasites exhibited no fluorescence at all (Fig. 20 A-D). Secondly, in the few parasites where the mNeonGreen signal was visible, this was dispersed throughout the parasites' cytoplasm, including the flagella, and not confined to membranar systems (Fig. 20A, B, C, D, and inset B1 and D1). This suggested that although mNeonGreen fluorescence was observable in some cells, it was likely that it was not the result of the expression of a *LiZIP2*-mNeonGreen chimera.

Western blot analysis using an α -myc antibody showed that the tagged protein being produced by these parasites did not have the expected size, migrating at around 40 kDa instead of around 65 kDa (Fig. 20F). Additionally, it was observed that N-terminally-tagged parasites expressed significantly higher levels of this 40 kDa α -myc-recognized protein, comparing with the C-terminally-tagged cells.

Genomic analysis of recovered parasites using primers specific for the mNeonGreen ORF and the *LiZIP2* ORF (P30+P31 for N-terminal integration diagnosis and P29+P32 for C-terminal integration diagnosis) showed that no successful integration of the cassette in the target *locus*, either at the N- or at the C-terminus, was achieved (data not shown). The absence of correct integration clarified the aberrant results observed in the immunofluorescence and western blot analyses.

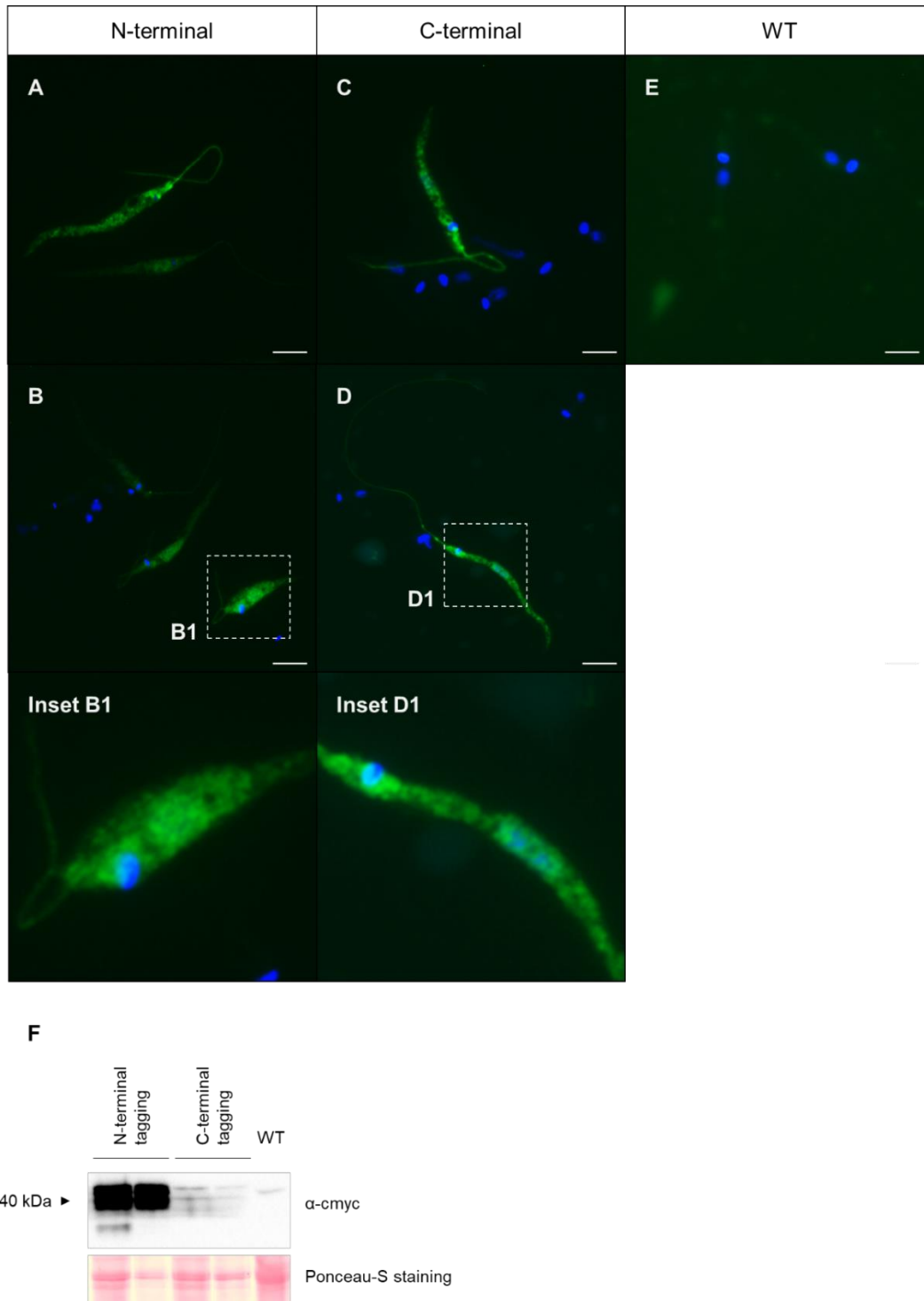


Fig. 20. Production of mNeonGreen-LiZIP2 and LiZIP2-mNeonGreen chimeras was unsuccessful. Panel A, B (63x objective) and inset B1 show immunofluorescence analysis of blasticidin-resistant polyclonal parasite cultures transfected with the 5'-sgRNA and the donor DNA template designed to promote the mNeonGreen cassette integration at the N-terminal of LiZIP2. Panel C, D (63x objective) and inset D1 show immunofluorescence analysis of blasticidin-resistant polyclonal parasite cultures transfected with the 3'-sgRNA and the donor DNA template designed to promote the mNeonGreen cassette integration at the C-terminal of LiZIP2. Panel E shows WT parasites used as control. Parasites were fixated with 4% PFA and stained with DAPI (blue). Images were acquired with the Zeiss Axio Imager Z1. Bar scale corresponds to 10 μ m. (E) Protein analysis by western blotting of parasite samples harvested from the blasticidin-resistant polyclonal cultures. WT parasite protein sample was used as control. Membrane was hybridized with an α -myc antibody. Lower panel shows the Ponceau-S staining of the same membrane.

4.2.4 Overexpression analysis

As an alternative approach to understand the contribution of *LZIP1* and *LZIP2* to *L. infantum* metal acquisition, the influence of protein overexpression on zinc internalization was addressed. The parasite lines included in these analyses were WT_pXGZIP1 (Fig. 17), WT_pXGZIP2, WT and ZIP3^{-/-}. Additionally, ZIP3^{-/-}_pXGZIP1 parasites (Fig. 17) were studied, to understand if ZIP1 overexpression in the ZIP3^{-/-} background alters zinc internalization dynamics.

Parasites were grown in normal media and, at defined time points, a part of the culture was supplemented with 50 µM ZnCl₂. Aliquots were harvested before and 24h after culture partition, without or with zinc supplementation (Fig. 21A). Cellular zinc content was then analysed by Inductively Coupled Plasma Mass Spectrometry (ICP-MS).

As shown in Fig. 21B, no differences in zinc content were found among the cell lines when grown in normal conditions (without zinc supplementation) in any time point. Parasites grown in zinc-supplemented media also showed no differences in the first three analysed time-points (24h w/Zn, 24h + 24h w/ Zn, 72h+ 24h w/Zn).

LZIP1 overexpression in WT cells only seems to impact zinc internalization when the metal is added to stationary-phase parasites (96h+24h w/ Zn), as there was a significant increase in zinc content comparatively to the WT background ($P \leq 0.05$). However, at the same conditions, the zinc content of ZIP3^{-/-}_pXGZIP3 parasites does not differ from that of ZIP3^{-/-} cells, suggesting that *LZIP1* overexpression in this background does not revert its zinc acquisition defect upon zinc supplementation. Given the contrasting data, a more detailed analysis is required to conclude about the role of *LZIP1* on *Leishmania* zinc internalization processes.

Parasites carrying an ectopic copy of *LZIP2* showed similar internalized zinc levels comparatively with WT, upon zinc supplementation to stationary phase cells. The fact that the presence of the pXGZIP2 plasmid had no visible impact on zinc content in these experiments does not discard the hypothesis of *LZIP2* influencing zinc uptake. It is possible that the absence of differences arises from the *LZIP2* protein not being correctly expressed from the vector, which cannot be ascertained due to the absence of an efficient antibody.

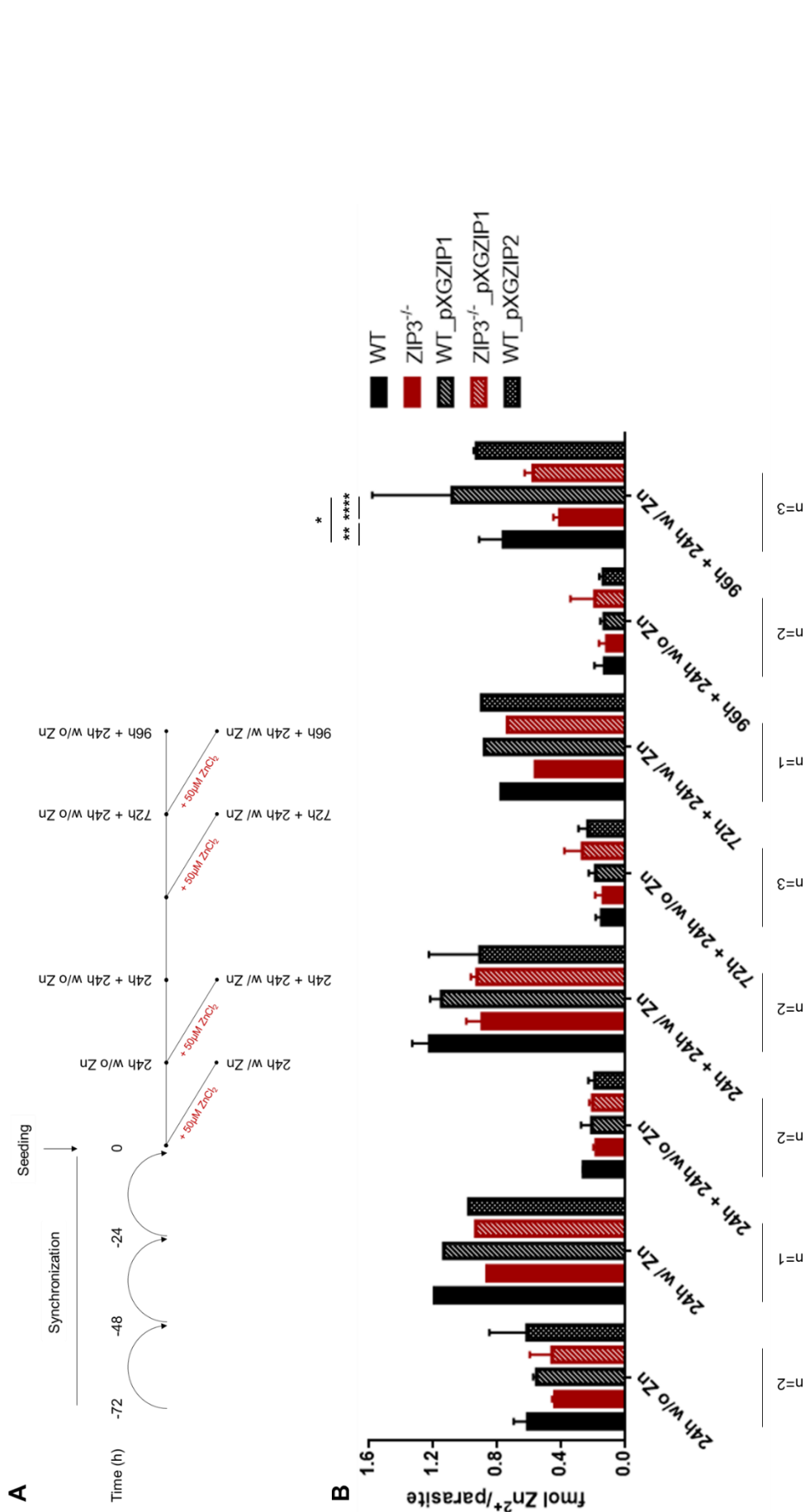


Fig. 21. Zinc content analysis of LiZIP1- and LiZIP2-overexpressing parasites. (A) Schematic representation of the experimental design. Parasites were synchronized and seeded at 1×10^6 in normal RPMI culture media. At defined time points, 5 mL of the original culture were transferred to a new flask and supplemented with $50 \mu\text{M ZnCl}_2$. Parasite samples for ICP-MS analysis were harvested before and 24h after culture partition, with or without zinc supplementation. (B) Zinc content of parasites at defined time points, measured by ICP-MS. Depicted in the figure is the number of independent measures performed for each time point (n). Stars represent significant differences ($^*P \leq 0.05$, $^{**}P \leq 0.01$, $^{***}P \leq 0.0001$), analysed by Two-way ANOVA with Tukey multiple comparison test. In the cases where $n \geq 2$, data represent the mean \pm SD from the indicated number of independent experiments.

4.3 Addressing the role of *LZIP3* in the course of an infection of an animal model

Ablation of the *ZIP3 loci* in *L. infantum* provided a model to study the importance of this protein both *in vitro* and *in vivo*. Following the extensive characterization of the ZIP3 transporter in the promastigote stage (Section 1), it was utterly relevant to address the significance of ZIP3 for *Leishmania* survival and virulence upon infection of a mammalian host.

The macrophage environment in which the amastigote stage lives may present or impose nutrient restrictions to *Leishmania*, namely of zinc. In these severe conditions, expression of high-affinity zinc transporters as *LZIP3* might constitute an advantage to intramacrophagic pathogens, providing a means to compete for the metal and survive. If this was the case, *LZIP3* could be regarded as a virulence factor, similarly to what is reported about zinc uptake systems in other human pathogens (Table 2).

Rodents, such as C57BL/6 mice, are usually used as models of visceral leishmaniasis. In the latter strain, parasite replication shows different kinetics in the main affected organs – the liver and the spleen. In a typical intravenous infection with *L. infantum*, amastigotes replicate swiftly in the liver in the first 20-28 days, followed by a rapid decrease in parasite burden in the following weeks due to the establishment of an effective immune response. Even so, parasites are never entirely eliminated in this organ. In contrast, the infection in the spleen progresses slower than that in the liver. In this organ, protozoans replicate up to a point where parasite burden reaches a plateau, whose level is reported to persist chronically²⁴⁹.

To analyse the relevance of ZIP3 in an *in vivo* situation, the capacity of parasites devoid of ZIP3 to thrive in both the liver and the spleen of C57BL/6 mice was compared to that of WT. The ZIP3^{-/-}_pXGZIP3 revertant strain was included so that any observed phenotype could be ascribed to the absence of the zinc transporter. The parasite burden in the liver and in the spleen at different days post-infection (dpi) was analysed by limiting dilution, as routinely performed in the lab (See Materials and Methods).

Fig. 22A shows that, in the hepatic tissue, the infection progressed analogously independently of the parasite line. All lines displayed the normal parasite burden kinetics, *i.e.*, fast replication from the first time point (7 dpi) to the second (21 dpi), followed by a containment phase (56 dpi and 91 dpi). Nevertheless, at 21 dpi, a statistically significant difference was detected between WT and ZIP3^{-/-} parasites ($P \leq 0.01$). Of note, this difference can be ascribed to the fact that, in one of the three independent experiments

performed, *L*ZIP3^{-/-}-infected mice showed a reduced parasite burden when compared to the other two experiments and to the total number of WT-infected mice. Additionally, at 21 dpi a difference between the revertant strain ZIP3^{-/-}_pXGZIP3 and WT ($P \leq 0.05$) parasites was observed. An intermediate phenotype is commonly observed when infecting mice with complemented lines, though.

Regarding the spleen (Fig 22B), ZIP3^{-/-} and ZIP3^{-/-}_pXGZIP3 parasites were able to infect this organ to the same extent as WT, at the earlier stages of infection (7 dpi). However, from this point onwards, differences between the parasite burden levels of the three parasite lines progressively increased. The divergence of parasite burden is already visible at 21 dpi, where ZIP3^{-/-} parasites replicated less than the WT ($P \leq 0.05$) and the revertant strain. At 56 dpi, there is a clear discrepancy between animals infected with WT and ZIP3^{-/-} parasites ($P \leq 0.0001$), since WT parasite burden was sustained, and ZIP3^{-/-} infection decreased. Noteworthy, the revertant strain was able to progressively prosper in the organ up to this later stage of infection, increasingly thriving as WT cells and clearly diverging from ZIP3^{-/-} parasites ($P \leq 0.001$). Parasite burden declination in ZIP3^{-/-}-infected animals continued until the last analysed time point (91 dpi).

The depression in ZIP3^{-/-} parasite burden observed in the spleen throughout the *in vivo* infection mirrors the phenotype of this cell line when cultured *in vitro* in zinc limiting conditions (Fig. 5). This observation, plus the fact that the phenotype was reverted in the ZIP3^{-/-}_pXGZIP3 add-back strain, suggests that the splenic environment has less zinc available for parasites to acquire when compared to the liver, resulting in a deleterious effect upon cells that do not possess the high affinity zinc transporter.

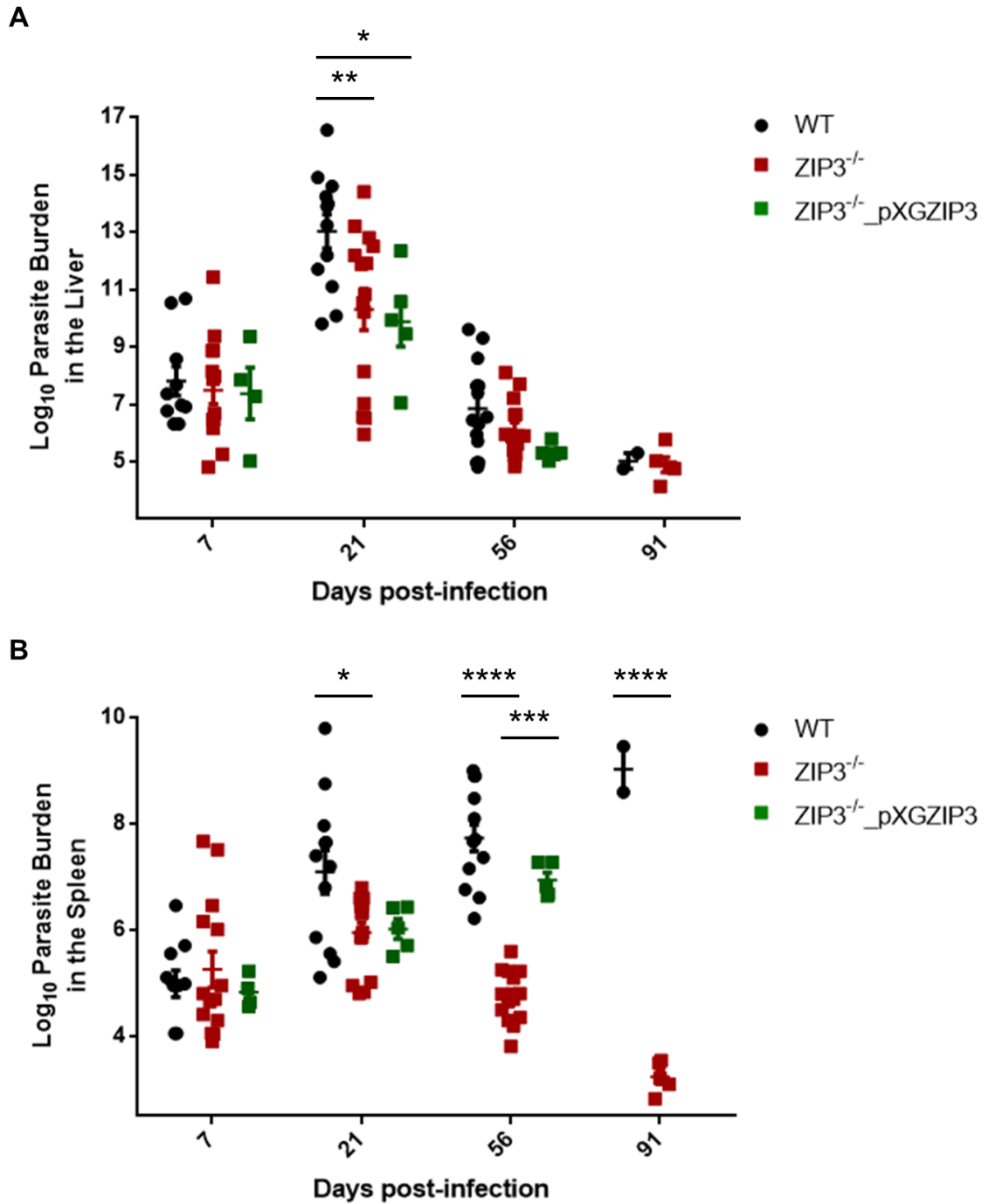


Fig. 22. LiZIP3 expression is essential for full infectivity of *Leishmania infantum* in the spleen. Graphic representation of the log₁₀ parasite burden in animals infected with WT (black circles, each representing one animal), ZIP3^{-/-} (red squares, each representing one animal) and ZIP3^{-/-}_pXGZIP3 (green squares, each represents one animal) parasites. Promastigotes were inoculated intravenously into C57BL/6 mice. At defined days post-infection, parasite burden was determined by limiting dilution as the number of parasites per gram of liver (A) or spleen (B). Stars represent significant differences (*P ≤ 0.05, **P ≤ 0.01, ***P ≤ 0.001, ****P ≤ 0.0001), analysed by Two-way ANOVA with Sidak multiple comparison test. Data represents the mean ± SEM of 3 independent experiments (involving a total of 37 animals infected with WT parasites, 48 animals infected with ZIP3^{-/-} parasites and 14 animals infected with ZIP3^{-/-}_pXGZIP3 parasites). From the three experiments, only one included ZIP3^{-/-}_pXGZIP3-infected animals.

Chapter 5: Discussion

The absence of effective human vaccines, the limitations presented by the available therapeutic arsenal (including toxicity, lack of efficiency and economic unsustainability to the highly affected 3rd world population), and the emergence of drug-resistant parasites are major handicaps for clinical management of the leishmaniases²⁵⁰. To approach this human and veterinary predicament with innovative and more efficient therapeutics, a better understanding of the biological differences between parasites and hosts, as well as of the pathogen virulence mechanisms and the mammalian immune responses impacting on the disease course is required.

The first complete genome sequencing of a *Leishmania* parasite (*L. major*) was reported almost 15 years ago²⁵¹. Meanwhile, high quality, well-annotated genomes of other trypanosomatids have also been released. The plethora of information therein collected facilitated subsequent genomic, transcriptomic and proteomic studies, bringing new insights on the protozoan biology, and on the molecular complexity beneath parasite-host-vector interactions¹⁷⁸. Namely, the subsequent identification of a cohort of cell surface transporters is greatly advancing the understanding about how *Leishmania* exploits the host to meet its own nutritional needs¹¹.

The concept of zinc homeostasis is indissociable from the understanding of transporters governing intracellular metal availability, ZIP family proteins being one of the more relevant players defining this fine balance. To pursue how *Leishmania* parasites cope with environmental differences in what concerns zinc availability and how they preserve zinc homeostasis, this thesis focused on the study of three zinc transporters, *LZIP1*, *LZIP2* and *LZIP3* for three main reasons:

- i) Trypanosomatids, unlike higher eukaryotes, co-transcribe functionally unrelated genes into polycistronic units²⁵²⁻²⁵⁴, leading one to question how these organisms achieve differential protein expression. In the context of trypanosomatid transporters whose expression is acutely tuned by substrate availability, studying *LZIP3* provides appealing, albeit challenging, opportunities to investigate the machineries behind gene and protein expression control in these organisms.
- ii) Ascertaining the role and spatio-temporal dynamics of *Leishmania* zinc transporters, namely of *LZIP1* and *LZIP2*, can offer new insights into the biology of these organisms. Specifically, acknowledging their expression pattern throughout the life cycle, sub-cellular location and substrates can provide important information on the zinc homeostatic network acting on *Leishmania*.
- iii) Study of membrane transporters at the interface between the parasite and the host can provide important information on how *Leishmania*, as well as other intracellular parasites,

can obtain essential nutrients and thrive in the mammalian host. Specifically, studies focusing on the *LZIP3* relevance to subvert host-imposed zinc nutritional immunity can render this protein a novel virulence factor expressed by *Leishmania*.

In summary, unravelling the parasite's requirement for zinc throughout its metabolically different life stages, together with insights on the molecular players triggered during the host-parasite "arms-of-race" for zinc in their symbiotic relationship and with epidemiological data, can support the combat to the debilitating and life threatening challenge imposed by *Leishmania* infection.

5.1 Phenotypic characterization of *LZIP3*^{-/-} parasites

The present study reports *in vitro* results on the characterization of previously generated homozygous knockout parasites for the *LZIP3*¹⁹⁸. The fact that *LZIP3*^{-/-} parasites were viable indicated that the protein was redundant and, thus, non-essential to promastigote stage parasites grown in standard conditions. Results from a previous (single) experiment hinted, however, that the transporter could become essential if zinc was rendered limiting. Hence, one of the objectives of this thesis entailed the in-depth analysis of *LZIP3*^{-/-} parasites. For this, a revertant strain (*i.e.*, re-introduction of the ZIP3 ORF in *LZIP3*^{-/-} parasites) had first to be generated.

Data obtained in this project showed that *LZIP3*^{-/-} present a consistent growth defect relatively to WT and complemented strains, whenever zinc became limited due to the introduction of a chelating agent (Fig. 5, Fig. 6, Fig. S3), but not when in sufficient/surplus conditions (Fig. 5). These results strongly suggest that *LZIP3* is crucial whenever the parasite is forced to scavenge the metal from a zinc-poor environment, which is in agreement with the pattern of expression of this protein (upregulated when the parasites face zinc limitation). It is conceivable that the protein supports parasite survival whenever it faces restriction of this essential nutrient in the insect vector and/or in the mammalian host. Metal availability in the sandfly's digestive tract is not known; yet, during metacyclogenesis, the synthesis of the zinc metalloprotease GP63 is augmented^{12,13}. Thus, it is possible that *Leishmania* might have to employ high-affinity zinc uptake systems to meet the high metal demand while differentiating on the vector. On the other hand, during infection of mammals, *LZIP3* seems to be employed by *Leishmania* to counteract nutritional immunity mechanisms of zinc limitation (discussed in section 5.3).

Characterization of the *LZIP3*^{-/-} mutants pointed towards a second important conclusion regarding *Leishmania* zinc metabolism: an alternative membrane zinc importer co-exists with *LZIP3* in these parasites. Such interpretation is in agreement with the observation that

LZIP3^{-/-} cells did not present any defect regarding their replication rate and morphology in standard growth conditions (Fig. 5). It is of note that, prior to the growth assays, parasites were synchronized through five daily passages in fresh culture medium. In these circumstances, cells were continuously facing zinc-replete environments. An alternative transporter would enable *LZIP3*^{-/-} parasites to acquire zinc and build storages that supported their growth in standard conditions similarly to WT cells (Fig. 5). The presence of an alternative transporter was also evidenced by the observation that *LZIP3*^{-/-} parasites continuously accumulate zinc when this is provided to the cells (Fig. 7B).

Evidence obtained during this project is compatible with the alternative zinc transporter possessing an affinity for the metal lower than that of *LZIP3*. In fact data shows that, when zinc is limited, as it is when TPEN is added to the medium, parasites grow only if they are capable of expressing *LZIP3* (*i.e.*, WT cells and the revertant strain *ZIP3*^{-/-}_{pXGZIP3} propagate but *LZIP3*^{-/-} parasites don't). This implies that, below a certain threshold of zinc (below the *K_m* of the transporter for zinc), the alternative importer is not able to complement the absence of the *LZIP3* function, likely because it is not functional in these conditions. However, when zinc bioavailability increases, the transporter is active and *LZIP3*^{-/-} parasites remain capable of accumulating the metal (as evidenced by analysis of their zinc content).

The finding that *L. infantum* promastigotes are able to express at least two zinc transporters can constitute a physiological advantage, as they provide parasites a means to adequately acquire zinc even in face of drastic environmental changes in nutrient availability¹⁹⁹. The presence of a second, low-affinity system would also be compatible with parasites allowing *LZIP3* abrogation through the CRISPR-Cas9 system under standard conditions¹⁹⁸.

5.2 Disclosing the second zinc transporter

Unveiling that *Leishmania* parasites express supplementary zinc transport system(s) other than *LZIP3* directed this project towards a second goal: to acknowledge the identity of the molecular players underlying the alternative zinc internalization in *L. infantum*. To tackle this question, two other ZIP family proteins identified in the genome of *L. infantum*, *LZIP1* and *LZIP2*, were considered.

LZIP1

Previous studies conducted at the Molecular Parasitology Group recognized that *LZIP1* is expressed at the parasite's cell membrane^{1,244}. However, its pattern of expression through a promastigote growth curve and its characterization as a transporter, in terms of both substrate and affinity, had not been yet established. Data obtained in this project indicates

that *LZIP1* is unlikely to be a high-affinity transporter, regardless of the metal it translocates to the parasite's cytosol. High-affinity transporters, as is *LZIP3*, are expressed mostly in the context of nutrient restriction¹⁹⁹, a situation that, in an *in vitro* promastigote culture, is met when cells reach stationary phase^{1,244}. Thus, the expression pattern of *LZIP1* (upregulated in the beginning of the growth curve and decreased in the end; See Fig. 15) seems incompatible with that of a high-affinity transport system. It is of note that analyses of the *Leishmania major* transcriptome showed that the homologous protein was downregulated in culture metacyclics^{255,256}, a finding in line with what was observed for *LZIP1*. Importantly, this places *LZIP1* as a candidate for the alternative zinc transport system, as the former is expected to be of lower affinity than *LZIP3*.

As a second step to understand if *LZIP1* could function as a second zinc transport mechanism in *L. infantum*, a CRISPR-Cas9-mediated strategy to produce *LZIP1* homozygous knockouts was designed. Knockout production was attempted in both WT and *LZIP3*^{-/-} parasites in parallel (and in the respective *LZIP1* episome-complemented cell lines) as the underlying hypothesis was that, if *LZIP1* was responsible for the preserved zinc internalization in the mutant cell line, its deletion would probably be possible in the former but unattainable in *LZIP3*-null parasites.

Since *L. infantum* presents eight copies of the *LZIP1* ORF, in two tandem copies in each of the tetraploid chromosome 31^{246,247}, abrogation of protein expression was expected to be challenging. This was due to the necessity of having, in the same cell, the generation of eight specific DSBs (with two different sgRNAs) and the promotion of four HR events (with four donor DNA cassette molecules) in order to delete all ORFs. However, by means of the recently described high-throughput CRISPR-Cas9 genome editing toolkit, multiplex ablation of four *loci* in one round of transfection was conceivable.

In a first attempt, the approach concealed a dual-drug strategy, *i.e.*, the promotion of HDR with DNA donor cassettes containing two different drug resistance genes. This strategy was unsuccessful, and the original methodology was reformulated. The new protocol used donor DNA cassettes carrying only one drug resistance gene were provided to the parasites. This rationale should raise the probabilities of successful HDR at the four *loci*, as fewer different DNA molecules had to meet in the same cell in order to efficiently produce eight DSBs and promote HR with four donor DNA cassettes. Unfortunately, even with the described optimization, successful generation of *LZIP1* homozygous knockouts was not achieved. Due to time constraints, no further efforts to produce such knockouts were carried out. As technical issues underlying the strategy failure cannot be discarded, a third attempt to

abrogate *LiZIP1*, using a donor DNA cassette carrying only one drug resistance gene, ought to be performed anon.

The third approach to investigate if *LiZIP1* could act as a zinc transporter focused on the use of cell lines overexpressing this protein. The reasoning was that, if that function was provided by *LiZIP1*, overexpression could impact cellular zinc content comparatively to WT cells. Unfortunately, data obtained in these experiments (Fig. 21) did not allow solid conclusions, as significant differences were only noticed between WT and WT_pXGZIP1 cells, when zinc was provided to stationary-phase parasites. The fact that an analogous difference was not perceivable when comparing ZIP3^{-/-} and ZIP3^{-/-}_pXGZIP3 cells raised serious doubts regarding the role of *LiZIP1* as the alternative zinc transporter.

It should be noted that zinc measurements were performed 24h upon metal addition to the cultures. It is possible that, during this period, zinc homeostasis mechanisms are triggered (e.g. zinc exporters), precluding the definition of a possible zinc import activity for *LiZIP1*. Conceivably more informative is a strategy comparing the kinetics of zinc internalization of *LiZIP1*-overexpressing parasites *versus* WT cells at shorter time periods after zinc addition (as performed for the zinc content comparison of WT and *LiZIP3*^{-/-} cells; See Fig. 7B).

LiZIP2

The second protein that was considered as an alternative zinc transporter in *L. infantum* parasites was *LiZIP2*. Contrarily to *LiZIP1*, no antibody could be produced for *LiZIP2*, and no information regarding the protein's expression pattern and intracellular localization was available.

One of the keys to understand a protein's function is to resolve its intracellular localization. However, the existing molecular tools for protein localization in some systems, namely in *Leishmania*, lagged behind the large datasets that were generated in the post-genomic era, leaving a great number of genes of interest with minimal annotation, and without the needed validation of localization and function. Tagging a gene of interest at its endogenous *locus*, resorting to plasmid-based approaches, depend on laborious and time-consuming cloning methods. The recent optimizations reported for CRISPR-Cas9-mediated genome editing in trypanosomatids offer the possibility to tag trypanosomatid proteins at either terminus employing only rapidly produced PCR-amplified donor DNA cassettes, that carry small epitopes, fluorescent proteins and drug-selectable markers to determine protein localization and, hence, provide insight into its function²⁴⁰. Hence, this project set to simultaneously introduce a small epitope (c-myc) and a fluorescent tag (mNeonGreen) in the *LiZIP2 locus* at both the N- and the C-terminus, using this genome editing toolkit²³⁸.

Efforts to tag *LIZIP2* were unproductive, as parasites correctly expressing *LIZIP2*-mNeonGreen fusion proteins were not obtained (Fig. 20). Although fluorescence microscopy analysis of polyclonal populations showed cells exhibiting green fluorescence, these were only a small fraction of the total cells. Additionally, the green signal was dispersed throughout the cytosol instead of confined to membranar systems, which is not compatible with proper expression of the *LIZIP2* chimera, a fact corroborated by western blotting analysis. Genetic analysis of these parasites also indicated that the donor DNA cassette was not introduced in the correct site. Since cells were drug resistant, it is possible that the mNeonGreen fluorescence and cmc signal resulted from off-target integration. Furthermore, in some cells, donor DNA cassettes might have integrated the correct location, in frame with the *LIZIP2* ORF, but the protein subsequently degraded. For certain proteins, the addition of an N- or C-terminal tag can disrupt proper folding, processing or localization of the fusion protein, leading to protein degradation, and this could be the case of *LIZIP2*. In fact, comparative analysis of the predicted topology of *LIZIP2* and its N-terminally and C-terminally tagged counterparts (Fig. 23) corroborate this hypothesis, since i) mNeonGreen might be too large (~27 kDa) to be suitable for *LIZIP2* tagging, a relatively small protein (~35 kDa) and ii) the N- and C-termini of *LIZIP2* are short, hence fusing mNeonGreen to these sites might destabilize the protein conformation and impede its correct localization at a membranar system. Future knock-in strategies will exploit the integration of smaller tags/epitopes.

As discussed for *LIZIP1*, a *LIZIP2* overexpression-based approach was also conducted to gain insight on a possible function of this protein regarding zinc uptake. However, as for the former, no robust conclusions could be drawn since the presence of a vector carrying a *LIZIP2* ORF had no visible impact on cellular zinc content. As discussed for *LIZIP1*, a second zinc internalization assay, concealing the measurement of zinc content at shorter time intervals upon metal supplementation, will be performed in the near future. Nevertheless, it is important to outline that, as no antibody to determine if *LIZIP2* is indeed overexpressed exists, the possibility of the protein not being produced from the episome cannot be discarded.

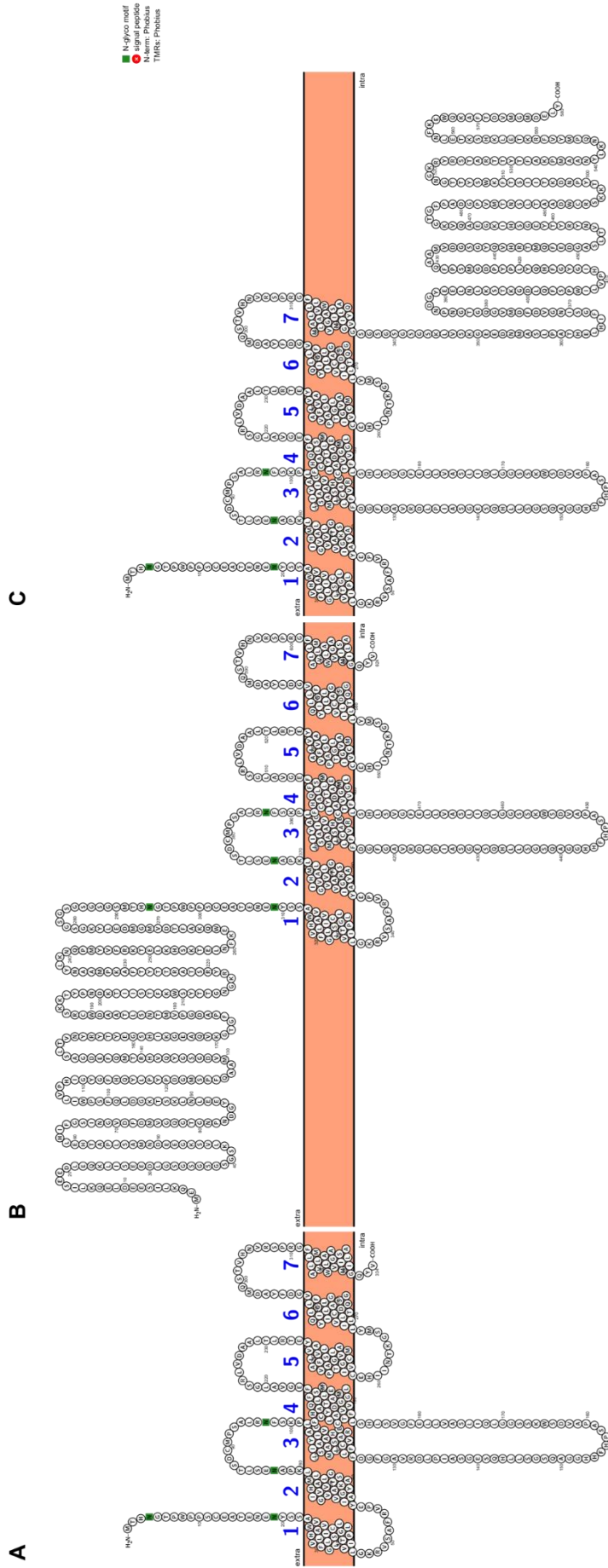


Fig. 23. Predicted topologies of the LiZIP2 protein and of the mNeonGreen-tagged LiZIP2 proteins. (A) Topology of WT LiZIP2. (B) Topology of LiZIP2 tagging with mNeonGreen, at the N-terminus of the protein. Protein topologies predicted using the Protter software

5.3 Addressing the role of *LIZIP3* in the course of an infection of an animal model

The successful production of *Leishmania infantum* parasites devoid of the only zinc high-affinity transporter characterized so far, *LIZIP3*, allowed an extensive characterization of the importance of this protein at the parasite's promastigote stage in *in vitro* assays. Following this, the present project set to establish how *LIZIP3* absence impacts the course of an infection on a mammalian host.

The results presented in this Thesis strongly suggest that the murine spleen can become, throughout the course of the disease, a zinc-limiting environment. Indeed, *LIZIP3*^{-/-} parasites presented no disadvantage in earlier phases of infection of this organ, suggesting that, in this period, either/both i) alternative zinc uptake systems are adequate or ii) existing intracellular zinc stores are sufficient to sustain parasite growth. Later on, however, mechanisms of nutrient withholding likely take place as a means to control the infection. As a matter of fact, contrary to WT and the revertant strain, *LIZIP3*^{-/-} parasites were not able to thrive in the spleen at later stages of infection, rendering the high-affinity zinc transporter essential when plausible changes in the immune environment are triggered. Remarkably, the infection kinetics of WT (and the revertant strain) *versus* *LIZIP3*^{-/-} parasites in the spleen is akin of the respective growth curves of the promastigote lines in the presence of the zinc chelator TPEN. This parallelism strongly corroborates that the deleterious phenotype observed *in vivo* may be related with zinc deprivation.

The absence of differences between the three parasite lines throughout the hepatic infection course suggests that parasites do not face zinc starvation in this organ, or at least not to the same extent as in the spleen. It is possible that the immunological players acting at the liver and the spleen may differ in what concerns innate nutritional availability. As though as an organ *per se* the liver presents higher zinc content⁸¹ than the spleen (both at steady-state⁸¹ and, importantly, in the context of infections¹¹²⁻¹²⁰), it remains to be cleared if the same is translated to the intramacrophagic milieu.

It should not be discarded that, as described for other infectious agents¹³⁹⁻¹⁴², the host cells might harness toxicity of other metals, such as copper, in the spleen. This would avert zinc internalization by lower affinity systems, and elevate the importance of prevailing high-affinity transporters, as *LIZIP3*. It is also conceivable that both mechanisms (zinc deprivation and heavy metal intoxication) may coexist.

Data obtained in this thesis points towards a nutritional immunity strategy the mammalian host may employ to curtail pathogen access to zinc, halting *Leishmania* infection. Albeit this

process is already extensively characterized as a control mechanism against other pathogens, including intracellular microorganisms^{150,151,161,167-169,173,176}, no information regarding *in vivo* macrophagic zinc withholding from *Leishmania* amastigotes was reported so far. Of note, upregulation of metallothionein genes has been recorded in the context of *in vitro* macrophage infections with *L. amazonensis*, *L. major* and *L. infantum*⁶⁷⁻⁶⁹, although a connection to zinc sequestration was not referred.

In summary, this Thesis conceals the first report on zinc-related nutritional immunity mechanisms acting on an *in vivo* *Leishmania* infection, as well as the primary proof of *LZIP3* being a disease progression determinant, by thwarting the host-imposed zinc starvation. Strategies targeting *LZIP3* as a virulence factor, reinforcing the macrophage's metal depletion defences, or the concomitant accomplishment of both, should appraise the emergence of innovative immune- or chemotherapeutic-based approaches to impair *Leishmania* infection.

Chapter 6: Final considerations and future work

Pathogens such as *Leishmania* depend on efficient acquisition of essential nutrients, such as transition metals, to survive, replicate and establish disease within their hosts. This necessity can be regarded as a vulnerability passive of being explored by the disease control fields. In line with this, the discovery of essential factors underlying the parasite's nutritional contingency, as it seems to be the case of *LiZIP3*, can be relevant for the development of new therapeutics.

Similarly, disclosing pathways employed by the host to control the disease, namely in terms of nutrient withholding, can lead to promising disease control modalities. Host-directed therapies may incite the interest of the pharmaceutical field, as macrophages are the host cells of various viral, bacterial, fungal and protozoan pathogens with major global health impact. It is possible that these pathogenic microorganisms have evolved analogous intracellular survival strategies to counteract the same innate nutritional immunity defenses, paving the way to the yet unexplored concept of pan-intracellular pathogen therapies.

Future work following on this thesis will attempt to integrate the responses of both infected animal models and of *Leishmania*, to resolve a holistic model describing how the host modulates nutrient accessibility during infection and how the pathogen responds to these changes (Fig. 24). For this, two major lines of investigation will be pursued:

- i) **To characterize the molecular mechanisms underlying zinc limitation during a *Leishmania* mammalian infection.** Defining the molecular basis of the unveiled zinc nutritional immunity defences amastigotes face in the mammalian host is of utter importance, not only in the context of the leishmaniases, but also because the mechanisms may be transversal to other infections. For this, studies on the expression of macrophage zinc metabolism-related proteins (transporters and chelators) in the spleen and liver at different times upon infection, as well as on the metal content of reticuloendothelial organs, in the blood and in macrophages isolated from the organs of infected animals, will follow. The results should retrieve important insights on the immunological orchestration of zinc homeostasis at the infected macrophage level and infer on the importance of *Leishmania* adaptation in order to sustain long-term infection.
- ii) **To unravel the other components of the zinc acquisition/homeostatic machinery of *Leishmania*, including zinc-sensing proteins that regulate *LiZIP3* response to zinc.** Further efforts to elucidate the role of other zinc transporters present in the genome of *Leishmania*, namely *LiZIP1* and *LiZIP2*, should be carried out. Furthermore, as *LiZIP3* is hypothesized to be essential for

the parasite to cope with zinc fluctuations in its mammalian host, it would be important to identify the sensing machinery responsible for *LZIP3* modulation by zinc. Of note, is possible that the same molecular players regulating *LZIP3* expression control other *Leishmania* zinc-responsive genes. These investigations should allow a clearer perception of the zinc homeostatic network operating in this organism, as well as on the environmental/nutritional sensing mechanisms in trypanosomatids, a field largely unexplored.

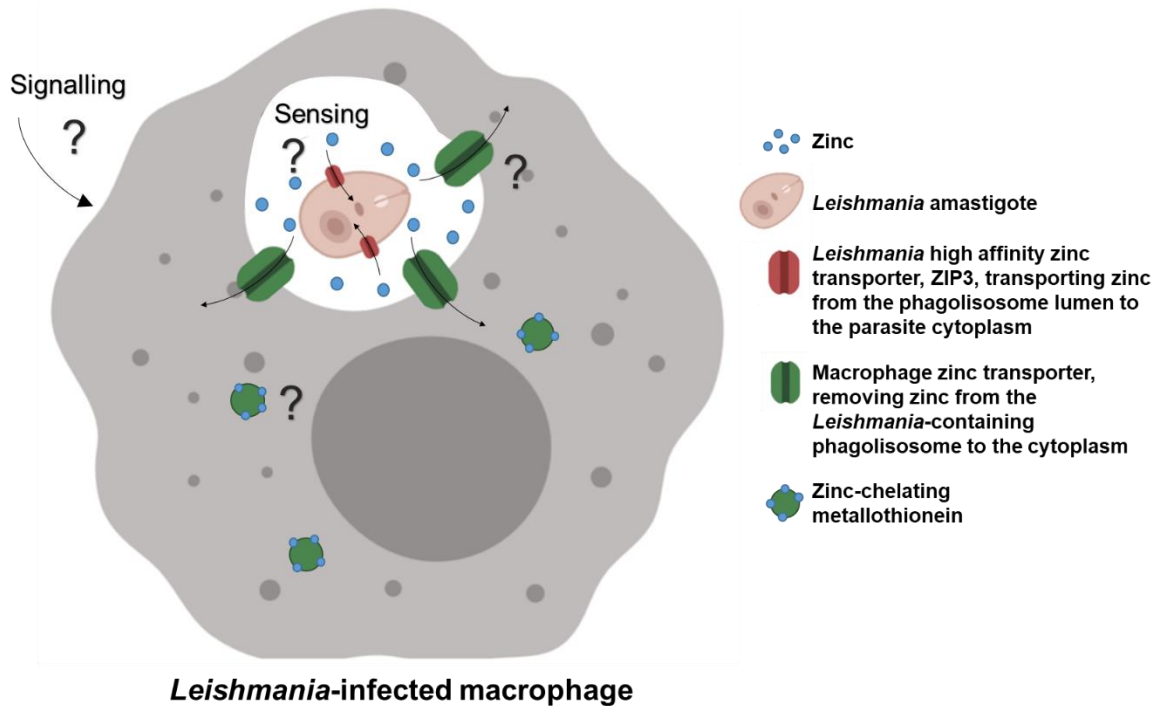


Fig. 24. Schematic representation of the mechanisms that might take place during *Leishmania* intramacrophagic infection, as well as of the proposed areas of future research aiming to unveil the processes underlying the “fight over zinc” at the amastigote-macrophage interface (not to scale).

Chapter 7: References

- 1 Carvalho, S. *et al.* LiZIP3 is a cellular zinc transporter that mediates the tightly regulated import of zinc in *Leishmania infantum* parasites. *Molecular microbiology* **96**, 581-595, doi:10.1111/mmi.12957 (2015).
- 2 Alvar, J. *et al.* Leishmaniasis worldwide and global estimates of its incidence. *PloS one* **7**, e35671, doi:10.1371/journal.pone.0035671 (2012).
- 3 Du, R., Hotez, P. J., Al-Salem, W. S. & Acosta-Serrano, A. Old World Cutaneous Leishmaniasis and Refugee Crises in the Middle East and North Africa. *PLoS neglected tropical diseases* **10**, e0004545, doi:10.1371/journal.pntd.0004545 (2016).
- 4 Al-Salem, W., Herricks, J. R. & Hotez, P. J. A review of visceral leishmaniasis during the conflict in South Sudan and the consequences for East African countries. *Parasit Vectors* **9**, 460, doi:10.1186/s13071-016-1743-7 (2016).
- 5 Berry, I. & Berrang-Ford, L. Leishmaniasis, conflict, and political terror: A spatio-temporal analysis. *Soc Sci Med* **167**, 140-149, doi:10.1016/j.socscimed.2016.04.038 (2016).
- 6 Kaye, P. & Scott, P. Leishmaniasis: complexity at the host-pathogen interface. *Nature reviews. Microbiology* **9**, 604-615, doi:10.1038/nrmicro2608 (2011).
- 7 Conceicao-Silva, F., Leite-Silva, J. & Morgado, F. N. The Binomial Parasite-Host Immunity in the Healing Process and in Reactivation of Human Tegumentary Leishmaniasis. *Front Microbiol* **9**, 1308, doi:10.3389/fmicb.2018.01308 (2018).
- 8 Chappuis, F. *et al.* Visceral leishmaniasis: what are the needs for diagnosis, treatment and control? *Nature reviews. Microbiology* **5**, 873-882, doi:10.1038/nrmicro1748 (2007).
- 9 Savoia, D. Recent updates and perspectives on leishmaniasis. *Journal of infection in developing countries* **9**, 588-596, doi:10.3855/jidc.6833 (2015).
- 10 Sinha, P. K. & Bhattacharya, S. Single-dose liposomal amphotericin B: an effective treatment for visceral leishmaniasis. *The Lancet. Global health* **2**, e7-8, doi:10.1016/S2214-109X(13)70151-7 (2014).
- 11 Landfear, S. M. Nutrient transport and pathogenesis in selected parasitic protozoa. *Eukaryotic cell* **10**, 483-493, doi:10.1128/EC.00287-10 (2011).
- 12 Lima, A. K. C., Elias, C. G. R., Souza, J. E. O., Santos, A. L. S. & Dutra, P. M. L. Dissimilar peptidase production by avirulent and virulent promastigotes of *Leishmania braziliensis*: inference on the parasite proliferation and interaction with macrophages. *Parasitology* **136**, 1179-1191, doi:10.1017/S0031182009990540 (2009).
- 13 Seay, M. B., Heard, P. L. & Chaudhuri, G. Surface Zn-proteinase as a molecule for defense of *Leishmania mexicana amazonensis* promastigotes against cytolysis inside macrophage phagolysosomes. *Infection and immunity* **64**, 5129-5137 (1996).
- 14 Saini, S., Bharati, K., Shaha, C. & Mukhopadhyay, C. K. Zinc depletion promotes apoptosis-like death in drug-sensitive and antimony-resistance *Leishmania donovani*. *Sci Rep-Uk* **7**, doi:10.1038/S41598-017-10041-6 (2017).
- 15 Kumari, A. *et al.* Intracellular zinc flux causes reactive oxygen species mediated mitochondrial dysfunction leading to cell death in *Leishmania donovani*. *PloS one* **12**, doi:10.1371/journal.pone.0178800 (2017).
- 16 Hood, M. I. & Skaar, E. P. Nutritional immunity: transition metals at the pathogen-host interface. *Nature reviews. Microbiology* **10**, 525-537, doi:10.1038/nrmicro2836 (2012).
- 17 Maret, W. Zinc biochemistry: from a single zinc enzyme to a key element of life. *Advances in nutrition* **4**, 82-91, doi:10.3945/an.112.003038 (2013).
- 18 Berg, J. M. & Shi, Y. The galvanization of biology: a growing appreciation for the roles of zinc. *Science* **271**, 1081-1085 (1996).

- 19 Gaither, L. A. & Eide, D. J. Eukaryotic zinc transporters and their regulation. *Biometals : an international journal on the role of metal ions in biology, biochemistry, and medicine* **14**, 251-270 (2001).
- 20 Andreini, C., Banci, L., Bertini, I. & Rosato, A. Counting the zinc-proteins encoded in the human genome. *J Proteome Res* **5**, 196-201, doi:10.1021/pr050361j (2006).
- 21 Andreini, C., Bertini, I. & Rosato, A. Metalloproteomes: a bioinformatic approach. *Acc Chem Res* **42**, 1471-1479, doi:10.1021/ar900015x (2009).
- 22 Yamasaki, S. *et al.* Zinc is a novel intracellular second messenger. *J Cell Biol* **177**, 637-645, doi:10.1083/jcb.200702081 (2007).
- 23 Kim, A. M. *et al.* Zinc sparks are triggered by fertilization and facilitate cell cycle resumption in mammalian eggs. *ACS Chem Biol* **6**, 716-723, doi:10.1021/cb200084y (2011).
- 24 Liang, X., Dempsey, R. E. & Burdette, S. C. Zn(2+) at a cellular crossroads. *Curr Opin Chem Biol* **31**, 120-125, doi:10.1016/j.cbpa.2016.02.008 (2016).
- 25 Andreini, C., Bertini, I., Cavallaro, G., Holliday, G. L. & Thornton, J. M. Metal ions in biological catalysis: from enzyme databases to general principles. *J Biol Inorg Chem* **13**, 1205-1218, doi:10.1007/s00775-008-0404-5 (2008).
- 26 Maret, W. Zinc and sulfur: a critical biological partnership. *Biochemistry* **43**, 3301-3309, doi:10.1021/bi036340p (2004).
- 27 Vallee, B. L. & Auld, D. S. Active-site zinc ligands and activated H₂O of zinc enzymes. *Proceedings of the National Academy of Sciences of the United States of America* **87**, 220-224 (1990).
- 28 Krezel, A. & Maret, W. The biological inorganic chemistry of zinc ions. *Arch Biochem Biophys* **611**, 3-19, doi:10.1016/j.abb.2016.04.010 (2016).
- 29 Kochanczyk, T., Drozd, A. & Krezel, A. Relationship between the architecture of zinc coordination and zinc binding affinity in proteins--insights into zinc regulation. *Metallomics* **7**, 244-257, doi:10.1039/c4mt00094c (2015).
- 30 Maret, W. New perspectives of zinc coordination environments in proteins. *J Inorg Biochem* **111**, 110-116, doi:10.1016/j.jinorgbio.2011.11.018 (2012).
- 31 Chevion, M., Korbashi, P., Katzhandler, J. & Saltman, P. Zinc--a redox-inactive metal provides a novel approach for protection against metal-mediated free radical induced injury: study of paraquat toxicity in *E. coli*. *Advances in experimental medicine and biology* **264**, 217-222, doi:10.1007/978-1-4684-5730-8_35 (1990).
- 32 Bray, T. M. & Bettger, W. J. The physiological role of zinc as an antioxidant. *Free Radic Biol Med* **8**, 281-291, doi:10.1016/0891-5849(90)90076-u (1990).
- 33 Powell, S. R. The antioxidant properties of zinc. *J Nutr* **130**, 1447S-1454S, doi:10.1093/jn/130.5.1447S (2000).
- 34 Maret, W. & Vallee, B. L. Thiolate ligands in metallothionein confer redox activity on zinc clusters. *Proceedings of the National Academy of Sciences of the United States of America* **95**, 3478-3482, doi:10.1073/pnas.95.7.3478 (1998).
- 35 Irving, H. & Williams, R. J. P. 637. The stability of transition-metal complexes. *Journal of the Chemical Society (Resumed)*, 3192-3210, doi:10.1039/JR9530003192 (1953).
- 36 Reyes-Caballero, H. *et al.* The metalloregulatory zinc site in *Streptococcus pneumoniae* AdcR, a zinc-activated MarR family repressor. *J Mol Biol* **403**, 197-216, doi:10.1016/j.jmb.2010.08.030 (2010).
- 37 Guerra, A. J., Dann, C. E., 3rd & Giedroc, D. P. Crystal structure of the zinc-dependent MarR family transcriptional regulator AdcR in the Zn(II)-bound state. *J Am Chem Soc* **133**, 19614-19617, doi:10.1021/ja2080532 (2011).
- 38 Eijkelkamp, B. A. *et al.* Extracellular zinc competitively inhibits manganese uptake and compromises oxidative stress management in *Streptococcus pneumoniae*. *PLoS one* **9**, e89427, doi:10.1371/journal.pone.0089427 (2014).

- 39 Broun, E. R., Greist, A., Tricot, G. & Hoffman, R. Excessive zinc ingestion. A reversible
cause of sideroblastic anemia and bone marrow depression. *JAMA* **264**, 1441-1443 (1990).
- 40 Valko, M. *et al.* Free radicals and antioxidants in normal physiological functions and
human disease. *Int J Biochem Cell Biol* **39**, 44-84, doi:10.1016/j.biocel.2006.07.001 (2007).
- 41 Jomova, K. & Valko, M. Advances in metal-induced oxidative stress and human disease.
Toxicology **283**, 65-87, doi:10.1016/j.tox.2011.03.001 (2011).
- 42 Maret, W. Zinc coordination environments in proteins as redox sensors and signal
transducers. *Antioxid Redox Signal* **8**, 1419-1441, doi:10.1089/ars.2006.8.1419 (2006).
- 43 Foster, A. W., Osman, D. & Robinson, N. J. Metal Preferences and Metallation. *Journal of
Biological Chemistry* **289**, 28095-28103, doi:10.1074/jbc.R114.588145 (2014).
- 44 Blaby-Haas, C. E. & Merchant, S. S. Lysosome-related Organelles as Mediators of Metal
Homeostasis. *Journal of Biological Chemistry* **289**, 28129-28136,
doi:10.1074/jbc.R114.592618 (2014).
- 45 Krezel, A. & Maret, W. Zinc-buffering capacity of a eukaryotic cell at physiological pZn. *J
Biol Inorg Chem* **11**, 1049-1062, doi:10.1007/s00775-006-0150-5 (2006).
- 46 Colvin, R. A. *et al.* Insights into Zn²⁺ homeostasis in neurons from experimental and
modeling studies. *Am J Physiol Cell Physiol* **294**, C726-742, doi:10.1152/ajpcell.00541.2007
(2008).
- 47 Finney, L. A. & O'Halloran, T. V. Transition metal speciation in the cell: insights from the
chemistry of metal ion receptors. *Science* **300**, 931-936, doi:10.1126/science.1085049
(2003).
- 48 Outten, C. E. & O'Halloran, T. V. Femtomolar sensitivity of metalloregulatory proteins
controlling zinc homeostasis. *Science* **292**, 2488-2492, doi:10.1126/science.1060331
(2001).
- 49 Vinkenborg, J. L. *et al.* Genetically encoded FRET sensors to monitor intracellular Zn²⁺
homeostasis. *Nature methods* **6**, 737-740, doi:10.1038/nmeth.1368 (2009).
- 50 Porcheron, G., Garenaux, A., Proulx, J., Sabri, M. & Dozois, C. M. Iron, copper, zinc, and
manganese transport and regulation in pathogenic Enterobacteria: correlations between
strains, site of infection and the relative importance of the different metal transport
systems for virulence. *Frontiers in cellular and infection microbiology* **3**, 90,
doi:10.3389/fcimb.2013.00090 (2013).
- 51 Mocchegiani, E., Malavolta, M., Marcellini, F. & Pawelec, G. Zinc, oxidative stress, genetic
background and immunosenescence: implications for healthy ageing. *Immunity & ageing :
I & A* **3**, 6, doi:10.1186/1742-4933-3-6 (2006).
- 52 Eide, D. J. in *Zinc Finger Proteins: From Atomic Contact to Cellular Function* (eds Shiro
Iuchi & Natalie Kuldell) 261-264 (Springer US, 2005).
- 53 Kolaj-Robin, O., Russell, D., Hayes, K. A., Pembroke, J. T. & Soulimane, T. Cation Diffusion
Facilitator family: Structure and function. *Febs Lett* **589**, 1283-1295,
doi:10.1016/j.febslet.2015.04.007 (2015).
- 54 Pyle, C. J. *et al.* Elemental Ingredients in the Macrophage Cocktail: Role of ZIP8 in Host
Response to Mycobacterium tuberculosis. *International journal of molecular sciences* **18**,
doi:10.3390/ijms18112375 (2017).
- 55 Patzer, S. I. & Hantke, K. The ZnuABC high-affinity zinc uptake system and its regulator Zur
in Escherichia coli. *Molecular microbiology* **28**, 1199-1210, doi:10.1046/j.1365-
2958.1998.00883.x (1998).
- 56 Hantke, K. Bacterial zinc uptake and regulators. *Current opinion in microbiology* **8**, 196-
202, doi:10.1016/j.mib.2005.02.001 (2005).
- 57 Dintilhac, A. & Claverys, J. P. The adc locus, which affects competence for genetic
transformation in Streptococcus pneumoniae, encodes an ABC transporter with a putative
lipoprotein homologous to a family of streptococcal adhesins. *Res Microbiol* **148**, 119-131,
doi:10.1016/S0923-2508(97)87643-7 (1997).

- 58 Kehres, D. G., Zaharik, M. L., Finlay, B. B. & Maguire, M. E. The NRAMP proteins of *Salmonella typhimurium* and *Escherichia coli* are selective manganese transporters involved in the response to reactive oxygen. *Molecular microbiology* **36**, 1085-1100, doi:10.1046/j.1365-2958.2000.01922.x (2000).
- 59 Makui, H. *et al.* Identification of the *Escherichia coli* K-12 Nramp orthologue (MntH) as a selective divalent metal ion transporter. *Molecular microbiology* **35**, 1065-1078, doi:10.1046/j.1365-2958.2000.01774.x (2000).
- 60 Braymer, J. J. & Giedroc, D. P. Recent developments in copper and zinc homeostasis in bacterial pathogens. *Curr Opin Chem Biol* **19**, 59-66, doi:10.1016/j.cbpa.2013.12.021 (2014).
- 61 Eide, D. J. Zinc transporters and the cellular trafficking of zinc. *Biochimica et biophysica acta* **1763**, 711-722, doi:10.1016/j.bbamcr.2006.03.005 (2006).
- 62 Coyle, P., Philcox, J. C., Carey, L. C. & Rofe, A. M. Metallothionein: the multipurpose protein. *Cell Mol Life Sci* **59**, 627-647 (2002).
- 63 Krezel, A. & Maret, W. Thionein/metallothionein control Zn(II) availability and the activity of enzymes. *J Biol Inorg Chem* **13**, 401-409, doi:10.1007/s00775-007-0330-y (2008).
- 64 Krezel, A. & Maret, W. Dual nanomolar and picomolar Zn(II) binding properties of metallothionein. *J Am Chem Soc* **129**, 10911-10921, doi:10.1021/ja071979s (2007).
- 65 Ghoshal, K. & Jacob, S. T. Regulation of metallothionein gene expression. *Prog Nucleic Acid Res Mol Biol* **66**, 357-384 (2001).
- 66 Emeny, R. T., Kasten-Jolly, J., Mondal, T., Lynes, M. A. & Lawrence, D. A. Metallothionein differentially affects the host response to *Listeria* infection both with and without an additional stress from cold-restraint. *Cell Stress Chaperones* **20**, 1013-1022, doi:10.1007/s12192-015-0630-z (2015).
- 67 Chaussabel, D. *et al.* Unique gene expression profiles of human macrophages and dendritic cells to phylogenetically distinct parasites. *Blood* **102**, 672-681, doi:10.1182/blood-2002-10-3232 (2003).
- 68 Ettinger, N. A. & Wilson, M. E. Macrophage and T-cell gene expression in a model of early infection with the protozoan *Leishmania chagasi*. *PLoS neglected tropical diseases* **2**, e252, doi:10.1371/journal.pntd.0000252 (2008).
- 69 Fernandes, M. C. *et al.* Dual Transcriptome Profiling of *Leishmania*-Infected Human Macrophages Reveals Distinct Reprogramming Signatures. *mBio* **7**, doi:10.1128/mBio.00027-16 (2016).
- 70 Christensen, S. M. *et al.* Meta-transcriptome Profiling of the Human-*Leishmania braziliensis* Cutaneous Lesion. *PLoS neglected tropical diseases* **10**, e0004992, doi:10.1371/journal.pntd.0004992 (2016).
- 71 Raulin, J. Etudes clinique sur la vegetation. *Annales des Sciences Naturelle: Botanique* **11**, 93-299 (1869).
- 72 Maze, P. Influences respectives des elements de la solution mineral du mais. *Annales de l'Institut Pasteur* **28**, 21-69 (1914).
- 73 Todd, W. R., Elvejheim, C. A. & Hart, E. B. Zinc in the nutrition of the rat. *American Journal of Physiology* **107**, 146-156 (1934).
- 74 O'Dell, B. L., Newberne, P. M. & Savage, J. E. Significance of dietary zinc for the growing chicken. *J Nutr* **65**, 503-518, doi:10.1093/jn/65.4.503 (1958).
- 75 Prasad, A. S., Miale, A., Jr., Farid, Z., Sandstead, H. H. & Schulert, A. R. Zinc metabolism in patients with the syndrome of iron deficiency anemia, hepatosplenomegaly, dwarfism, and hypogonadism. *J Lab Clin Med* **61**, 537-549 (1963).
- 76 Prasad, A. S., Halsted, J. A. & Nadimi, M. Syndrome of iron deficiency anemia, hepatosplenomegaly, hypogonadism, dwarfism and geophagia. *Am J Med* **31**, 532-546 (1961).
- 77 Whittaker, P. Iron and zinc interactions in humans. *Am J Clin Nutr* **68**, 442S-446S, doi:10.1093/ajcn/68.2.442S (1998).

- 78 King, J. C., Shames, D. M. & Woodhouse, L. R. Zinc homeostasis in humans. *J Nutr* **130**, 1360S-1366S, doi:10.1093/jn/130.5.1360S (2000).
- 79 Lu, J., Stewart, A. J., Sadler, P. J., Pinheiro, T. J. & Blindauer, C. A. Albumin as a zinc carrier: properties of its high-affinity zinc-binding site. *Biochem Soc Trans* **36**, 1317-1321, doi:10.1042/bst0361317 (2008).
- 80 Scott, B. J. & Bradwell, A. R. Identification of the serum binding proteins for iron, zinc, cadmium, nickel, and calcium. *Clin Chem* **29**, 629-633 (1983).
- 81 Mertz, W. & Underwood, E. J. *Trace elements in human and animal nutrition*. 5th edn, (Academic Press, 1986).
- 82 Keilin, D. & Mann, T. Carbonic anhydrase. *Nature* **144**, 442-443 (1939).
- 83 Vallee, B. L. & Falchuk, K. H. The biochemical basis of zinc physiology. *Physiol Rev* **73**, 79-118, doi:10.1152/physrev.1993.73.1.79 (1993).
- 84 Rink, L. & Gabriel, P. Zinc and the immune system. *P Nutr Soc* **59**, 541-552, doi:10.1017/S0029665100000781 (2000).
- 85 Fraker, P. J., Gershwin, M. E., Good, R. A. & Prasad, A. Interrelationships between zinc and immune function. *Fed Proc* **45**, 1474-1479 (1986).
- 86 Subramanian Vignesh, K., Landero Figueroa, J. A., Porollo, A., Caruso, J. A. & Deepe, G. S., Jr. Zinc sequestration: arming phagocyte defense against fungal attack. *PLoS pathogens* **9**, e1003815, doi:10.1371/journal.ppat.1003815 (2013).
- 87 Shankar, A. H. & Prasad, A. S. Zinc and immune function: the biological basis of altered resistance to infection. *Am J Clin Nutr* **68**, 447S-463S, doi:10.1093/ajcn/68.2.447S (1998).
- 88 Haase, H. & Rink, L. Multiple impacts of zinc on immune function. *Metallomics* **6**, 1175-1180, doi:10.1039/c3mt00353a (2014).
- 89 Nylen, S. & Eidsmo, L. Tissue damage and immunity in cutaneous leishmaniasis. *Parasite Immunol* **34**, 551-561, doi:10.1111/pim.12007 (2012).
- 90 Souza, M. A. *et al.* American tegumentary leishmaniasis: cytokines and nitric oxide in active disease and after clinical cure, with or without chemotherapy. *Scand J Immunol* **76**, 175-180, doi:10.1111/j.1365-3083.2012.02717.x (2012).
- 91 Scott, P. & Novais, F. O. Cutaneous leishmaniasis: immune responses in protection and pathogenesis. *Nat Rev Immunol* **16**, 581-592, doi:10.1038/nri.2016.72 (2016).
- 92 Kumar, A. *et al.* Leishmania infection activates host mTOR for its survival by M2 macrophage polarization. *Parasite Immunol* **40**, e12586, doi:10.1111/pim.12586 (2018).
- 93 Mesquita, I. *et al.* The impact of IL-10 dynamic modulation on host immune response against visceral leishmaniasis. *Cytokine* **112**, 16-20, doi:10.1016/j.cyto.2018.07.001 (2018).
- 94 Rodrigues, V., Cordeiro-da-Silva, A., Laforge, M., Silvestre, R. & Estaquier, J. Regulation of immunity during visceral Leishmania infection. *Parasit Vectors* **9**, 118, doi:10.1186/s13071-016-1412-x (2016).
- 95 Sprietsma, J. E. Zinc-controlled Th1/Th2 switch significantly determines development of diseases. *Medical hypotheses* **49**, 1-14 (1997).
- 96 Wirth, J. J., Fraker, P. J. & Kierszenbaum, F. Zinc requirement for macrophage function: effect of zinc deficiency on uptake and killing of a protozoan parasite. *Immunology* **68**, 114-119 (1989).
- 97 James, S. J., Swendseid, M. & Makinodan, T. Macrophage-mediated depression of T-cell proliferation in zinc-deficient mice. *J Nutr* **117**, 1982-1988, doi:10.1093/jn/117.11.1982 (1987).
- 98 Karl, L., Chvapil, M. & Zukoski, C. F. Effect of zinc on the viability and phagocytic capacity of peritoneal macrophages. *Proc Soc Exp Biol Med* **142**, 1123-1127, doi:10.3181/00379727-142-37190 (1973).
- 99 Chvapil, M. *et al.* Effect of zinc on peritoneal macrophages in vitro. *Infection and immunity* **16**, 367-373 (1977).

- 100 Prasad, A. S. Zinc in human health: effect of zinc on immune cells. *Mol Med* **14**, 353-357, doi:10.2119/2008-00033.Prasad (2008).
- 101 Fischer Walker, C. & Black, R. E. Zinc and the risk for infectious disease. *Annu Rev Nutr* **24**, 255-275, doi:10.1146/annurev.nutr.23.011702.073054 (2004).
- 102 Black, R. E. Zinc deficiency, infectious disease and mortality in the developing world. *J Nutr* **133**, 1485S-1489S, doi:10.1093/jn/133.5.1485S (2003).
- 103 Subramanian Vignesh, K. & Deepe, G. S., Jr. Immunological orchestration of zinc homeostasis: The battle between host mechanisms and pathogen defenses. *Arch Biochem Biophys* **611**, 66-78, doi:10.1016/j.abb.2016.02.020 (2016).
- 104 Weinberg, E. D. Nutritional immunity. Host's attempt to withhold iron from microbial invaders. *JAMA* **231**, 39-41, doi:10.1001/jama.231.1.39 (1975).
- 105 Brown, J. S. & Holden, D. W. Iron acquisition by Gram-positive bacterial pathogens. *Microbes Infect* **4**, 1149-1156 (2002).
- 106 Schaible, U. E. & Kaufmann, S. H. Iron and microbial infection. *Nature reviews. Microbiology* **2**, 946-953, doi:10.1038/nrmicro1046 (2004).
- 107 Nairz, M., Schroll, A., Sonnweber, T. & Weiss, G. The struggle for iron - a metal at the host-pathogen interface. *Cellular microbiology* **12**, 1691-1702, doi:10.1111/j.1462-5822.2010.01529.x (2010).
- 108 Hammer, N. D. & Skaar, E. P. Molecular mechanisms of *Staphylococcus aureus* iron acquisition. *Annual review of microbiology* **65**, 129-147, doi:10.1146/annurev-micro-090110-102851 (2011).
- 109 Weinberg, E. D. Iron availability and infection. *Biochimica et biophysica acta* **1790**, 600-605, doi:10.1016/j.bbagen.2008.07.002 (2009).
- 110 Skaar, E. P. The battle for iron between bacterial pathogens and their vertebrate hosts. *PLoS pathogens* **6**, e1000949, doi:10.1371/journal.ppat.1000949 (2010).
- 111 Kehl-Fie, T. E. & Skaar, E. P. Nutritional immunity beyond iron: a role for manganese and zinc. *Curr Opin Chem Biol* **14**, 218-224, doi:10.1016/j.cbpa.2009.11.008 (2010).
- 112 Milanino, R., Marrella, M., Gasperini, R., Pasqualicchio, M. & Velo, G. Copper and zinc body levels in inflammation: an overview of the data obtained from animal and human studies. *Agents and actions* **39**, 195-209, doi:10.1007/bf01998974 (1993).
- 113 Lichten, L. A. & Cousins, R. J. Mammalian zinc transporters: nutritional and physiologic regulation. *Annu Rev Nutr* **29**, 153-176, doi:10.1146/annurev-nutr-033009-083312 (2009).
- 114 Sobocinski, P. Z., Canterbury, W. J., Jr., Mapes, C. A. & Dinterman, R. E. Involvement of hepatic metallothioneins in hypozincemia associated with bacterial infection. *Am J Physiol* **234**, E399-406, doi:10.1152/ajpendo.1978.234.4.E399 (1978).
- 115 Kushner, I. The phenomenon of the acute phase response. *Annals of the New York Academy of Sciences* **389**, 39-48, doi:10.1111/j.1749-6632.1982.tb22124.x (1982).
- 116 Aydemir, T. B. et al. Zinc transporter ZIP14 functions in hepatic zinc, iron and glucose homeostasis during the innate immune response (endotoxemia). *PLoS one* **7**, e48679, doi:10.1371/journal.pone.0048679 (2012).
- 117 Liuzzi, J. P. et al. Interleukin-6 regulates the zinc transporter Zip14 in liver and contributes to the hypozincemia of the acute-phase response. *Proceedings of the National Academy of Sciences of the United States of America* **102**, 6843-6848, doi:10.1073/pnas.0502257102 (2005).
- 118 Gaetke, L. M., McClain, C. J., Talwalkar, R. T. & Shedlofsky, S. I. Effects of endotoxin on zinc metabolism in human volunteers. *Am J Physiol* **272**, E952-956, doi:10.1152/ajpendo.1997.272.6.E952 (1997).
- 119 Cousins, R. J. & Leinart, A. S. Tissue-specific regulation of zinc metabolism and metallothionein genes by interleukin 1. *Faseb J* **2**, 2884-2890, doi:10.1096/fasebj.2.13.2458983 (1988).

- 120 Cousins, R. J., Liuzzi, J. P. & Lichten, L. A. Mammalian zinc transport, trafficking, and signals. *The Journal of biological chemistry* **281**, 24085-24089, doi:10.1074/jbc.R600011200 (2006).
- 121 Diaz-Ochoa, V. E., Jellbauer, S., Klaus, S. & Raffatellu, M. Transition metal ions at the crossroads of mucosal immunity and microbial pathogenesis. *Frontiers in cellular and infection microbiology* **4**, 2, doi:10.3389/fcimb.2014.00002 (2014).
- 122 Corbin, B. D. *et al.* Metal chelation and inhibition of bacterial growth in tissue abscesses. *Science* **319**, 962-965, doi:10.1126/science.1152449 (2008).
- 123 Moroz, O. V. *et al.* Structure of the human S100A12-copper complex: implications for host-parasite defence. *Acta crystallographica. Section D, Biological crystallography* **59**, 859-867, doi:10.1107/s0907444903004700 (2003).
- 124 Brodersen, D. E., Nyborg, J. & Kjeldgaard, M. Zinc-binding site of an S100 protein revealed. Two crystal structures of Ca²⁺-bound human psoriasin (S100A7) in the Zn²⁺-loaded and Zn²⁺-free states. *Biochemistry* **38**, 1695-1704, doi:10.1021/bi982483d (1999).
- 125 Moroz, O. V., Blagova, E. V., Wilkinson, A. J., Wilson, K. S. & Bronstein, I. B. The crystal structures of human S100A12 in apo form and in complex with zinc: new insights into S100A12 oligomerisation. *J Mol Biol* **391**, 536-551, doi:10.1016/j.jmb.2009.06.004 (2009).
- 126 Glaser, R. *et al.* Antimicrobial psoriasin (S100A7) protects human skin from *Escherichia coli* infection. *Nature immunology* **6**, 57-64, doi:10.1038/ni1142 (2005).
- 127 Goyette, J. & Geczy, C. L. Inflammation-associated S100 proteins: new mechanisms that regulate function. *Amino acids* **41**, 821-842, doi:10.1007/s00726-010-0528-0 (2011).
- 128 Brinkmann, V. *et al.* Neutrophil extracellular traps kill bacteria. *Science* **303**, 1532-1535, doi:10.1126/science.1092385 (2004).
- 129 Lusitani, D., Malawista, S. E. & Montgomery, R. R. Calprotectin, an abundant cytosolic protein from human polymorphonuclear leukocytes, inhibits the growth of *Borrelia burgdorferi*. *Infection and immunity* **71**, 4711-4716, doi:10.1128/iai.71.8.4711-4716.2003 (2003).
- 130 Urban, C. F. *et al.* Neutrophil extracellular traps contain calprotectin, a cytosolic protein complex involved in host defense against *Candida albicans*. *PLoS pathogens* **5**, e1000639, doi:10.1371/journal.ppat.1000639 (2009).
- 131 McCormick, A. *et al.* NETs formed by human neutrophils inhibit growth of the pathogenic mold *Aspergillus fumigatus*. *Microbes Infect* **12**, 928-936, doi:10.1016/j.micinf.2010.06.009 (2010).
- 132 Damo, S. M. *et al.* Molecular basis for manganese sequestration by calprotectin and roles in the innate immune response to invading bacterial pathogens. *Proceedings of the National Academy of Sciences of the United States of America* **110**, 3841-3846, doi:10.1073/pnas.1220341110 (2013).
- 133 Malavia, D., Crawford, A. & Wilson, D. Nutritional Immunity and Fungal Pathogenesis: The Struggle for Micronutrients at the Host-Pathogen Interface. *Advances in microbial physiology* **70**, 85-103, doi:10.1016/bs.ampbs.2017.01.006 (2017).
- 134 Kitamura, H. *et al.* Toll-like receptor-mediated regulation of zinc homeostasis influences dendritic cell function. *Nature immunology* **7**, 971-977, doi:10.1038/ni1373 (2006).
- 135 Aydemir, T. B., Liuzzi, J. P., McClellan, S. & Cousins, R. J. Zinc transporter ZIP8 (SLC39A8) and zinc influence IFN-gamma expression in activated human T cells. *J Leukoc Biol* **86**, 337-348, doi:10.1189/jlb.1208759 (2009).
- 136 Mambula, S. S., Simons, E. R., Hastey, R., Selsted, M. E. & Levitz, S. M. Human neutrophil-mediated nonoxidative antifungal activity against *Cryptococcus neoformans*. *Infection and immunity* **68**, 6257-6264, doi:10.1128/iai.68.11.6257-6264.2000 (2000).
- 137 Lorenz, M. C., Bender, J. A. & Fink, G. R. Transcriptional response of *Candida albicans* upon internalization by macrophages. *Eukaryotic cell* **3**, 1076-1087, doi:10.1128/ec.3.5.1076-1087.2004 (2004).

- 138 Subramanian Vignesh, K., Landero Figueroa, J. A., Porollo, A., Caruso, J. A. & Deepe, G. S., Jr. Granulocyte macrophage-colony stimulating factor induced Zn sequestration enhances macrophage superoxide and limits intracellular pathogen survival. *Immunity* **39**, 697-710, doi:10.1016/j.immuni.2013.09.006 (2013).
- 139 Ward, S. K., Abomoelak, B., Hoyer, E. A., Steinberg, H. & Talaat, A. M. CtpV: a putative copper exporter required for full virulence of *Mycobacterium tuberculosis*. *Molecular microbiology* **77**, 1096-1110, doi:10.1111/j.1365-2958.2010.07273.x (2010).
- 140 White, C., Lee, J., Kambe, T., Fritsche, K. & Petris, M. J. A role for the ATP7A copper-transporting ATPase in macrophage bactericidal activity. *The Journal of biological chemistry* **284**, 33949-33956, doi:10.1074/jbc.M109.070201 (2009).
- 141 Shafeeq, S. *et al.* The cop operon is required for copper homeostasis and contributes to virulence in *Streptococcus pneumoniae*. *Molecular microbiology* **81**, 1255-1270, doi:10.1111/j.1365-2958.2011.07758.x (2011).
- 142 Wolschendorf, F. *et al.* Copper resistance is essential for virulence of *Mycobacterium tuberculosis*. *Proceedings of the National Academy of Sciences of the United States of America* **108**, 1621-1626, doi:10.1073/pnas.1009261108 (2011).
- 143 McDevitt, C. A. *et al.* A molecular mechanism for bacterial susceptibility to zinc. *PLoS pathogens* **7**, e1002357, doi:10.1371/journal.ppat.1002357 (2011).
- 144 Wagner, D. *et al.* Elemental analysis of *Mycobacterium avium*-, *Mycobacterium tuberculosis*-, and *Mycobacterium smegmatis*-containing phagosomes indicates pathogen-induced microenvironments within the host cell's endosomal system. *Journal of immunology* **174**, 1491-1500, doi:10.4049/jimmunol.174.3.1491 (2005).
- 145 Botella, H., Stadthagen, G., Lugo-Villarino, G., de Chastellier, C. & Neyrolles, O. Metallobiology of host-pathogen interactions: an intoxicating new insight. *Trends Microbiol* **20**, 106-112, doi:10.1016/j.tim.2012.01.005 (2012).
- 146 Botella, H. *et al.* Mycobacterial p(1)-type ATPases mediate resistance to zinc poisoning in human macrophages. *Cell Host Microbe* **10**, 248-259, doi:10.1016/j.chom.2011.08.006 (2011).
- 147 Lemire, J. A., Harrison, J. J. & Turner, R. J. Antimicrobial activity of metals: mechanisms, molecular targets and applications. *Nature reviews. Microbiology* **11**, 371-384, doi:10.1038/nrmicro3028 (2013).
- 148 Ong, C. L., Gillen, C. M., Barnett, T. C., Walker, M. J. & McEwan, A. G. An antimicrobial role for zinc in innate immune defense against group A streptococcus. *J Infect Dis* **209**, 1500-1508, doi:10.1093/infdis/jiu053 (2014).
- 149 Hood, M. I. *et al.* Identification of an *Acinetobacter baumannii* zinc acquisition system that facilitates resistance to calprotectin-mediated zinc sequestration. *PLoS pathogens* **8**, e1003068, doi:10.1371/journal.ppat.1003068 (2012).
- 150 Kim, S., Watanabe, K., Shirahata, T. & Watarai, M. Zinc uptake system (*znuA* locus) of *Brucella abortus* is essential for intracellular survival and virulence in mice. *J Vet Med Sci* **66**, 1059-1063, doi:10.1292/jvms.66.1059 (2004).
- 151 Yang, X., Becker, T., Walters, N. & Pascual, D. W. Deletion of *znuA* virulence factor attenuates *Brucella abortus* and confers protection against wild-type challenge. *Infection and immunity* **74**, 3874-3879, doi:10.1128/iai.01957-05 (2006).
- 152 Davis, L. M., Kakuda, T. & DiRita, V. J. A *Campylobacter jejuni* *znuA* orthologue is essential for growth in low-zinc environments and chick colonization. *Journal of bacteriology* **191**, 1631-1640, doi:10.1128/jb.01394-08 (2009).
- 153 Ho, T. D., Davis, B. M., Ritchie, J. M. & Waldor, M. K. Type 2 secretion promotes enterohemorrhagic *Escherichia coli* adherence and intestinal colonization. *Infection and immunity* **76**, 1858-1865, doi:10.1128/iai.01688-07 (2008).
- 154 Gabbianelli, R. *et al.* Role of *ZnuABC* and *ZinT* in *Escherichia coli* O157:H7 zinc acquisition and interaction with epithelial cells. *BMC Microbiol* **11**, 36, doi:10.1186/1471-2180-11-36 (2011).

- 155 Sabri, M., Houle, S. & Dozois, C. M. Roles of the Extraintestinal Pathogenic *Escherichia coli* ZnuACB and ZupT Zinc Transporters during Urinary Tract Infection. *Infection and immunity* **77**, 1155-1164, doi:10.1128/iai.01082-08 (2009).
- 156 Gunasekera, T. S., Herre, A. H. & Crowder, M. W. Absence of ZnuABC-mediated zinc uptake affects virulence-associated phenotypes of uropathogenic *Escherichia coli* CFT073 under Zn(II)-depleted conditions. *FEMS Microbiol Lett* **300**, 36-41, doi:10.1111/j.1574-6968.2009.01762.x (2009).
- 157 Moreau, G. B., Qin, A. & Mann, B. J. Zinc Acquisition Mechanisms Differ between Environmental and Virulent *Francisella* Species. *Journal of bacteriology* **200**, doi:10.1128/JB.00587-17 (2018).
- 158 Lewis, D. A. *et al.* Identification of the znuA-encoded periplasmic zinc transport protein of *Haemophilus ducreyi*. *Infection and immunity* **67**, 5060-5068 (1999).
- 159 Rosadini, C. V., Gawronski, J. D., Raimunda, D., Arguello, J. M. & Akerley, B. J. A novel zinc binding system, ZevAB, is critical for survival of nontypeable *Haemophilus influenzae* in a murine lung infection model. *Infection and immunity* **79**, 3366-3376, doi:10.1128/IAI.05135-11 (2011).
- 160 Stahler, F. N. *et al.* The novel *Helicobacter pylori* CznABC metal efflux pump is required for cadmium, zinc, and nickel resistance, urease modulation, and gastric colonization. *Infection and immunity* **74**, 3845-3852, doi:10.1128/IAI.02025-05 (2006).
- 161 Corbett, D. *et al.* Two zinc uptake systems contribute to the full virulence of *Listeria monocytogenes* during growth in vitro and in vivo. *Infection and immunity* **80**, 14-21, doi:10.1128/IAI.05904-11 (2012).
- 162 Murphy, T. F. *et al.* Role of the zinc uptake ABC transporter of *Moraxella catarrhalis* in persistence in the respiratory tract. *Infection and immunity* **81**, 3406-3413, doi:10.1128/IAI.00589-13 (2013).
- 163 Grover, A. & Sharma, R. Identification and characterization of a major Zn(II) resistance determinant of *Mycobacterium smegmatis*. *Journal of bacteriology* **188**, 7026-7032, doi:10.1128/JB.00643-06 (2006).
- 164 Garrido, M. E. *et al.* The high-affinity zinc-uptake system znuACB is under control of the iron-uptake regulator (*fur*) gene in the animal pathogen *Pasteurella multocida*. *FEMS Microbiol Lett* **221**, 31-37, doi:10.1016/S0378-1097(03)00131-9 (2003).
- 165 Nielubowicz, G. R., Smith, S. N. & Mobley, H. L. Zinc uptake contributes to motility and provides a competitive advantage to *Proteus mirabilis* during experimental urinary tract infection. *Infection and immunity* **78**, 2823-2833, doi:10.1128/IAI.01220-09 (2010).
- 166 Ammendola, S. *et al.* High-affinity Zn²⁺ uptake system ZnuABC is required for bacterial zinc homeostasis in intracellular environments and contributes to the virulence of *Salmonella enterica*. *Infection and immunity* **75**, 5867-5876, doi:10.1128/iai.00559-07 (2007).
- 167 Campoy, S. *et al.* Role of the high-affinity zinc uptake znuABC system in *Salmonella enterica* serovar typhimurium virulence. *Infection and immunity* **70**, 4721-4725, doi:10.1128/iai.70.8.4721-4725.2002 (2002).
- 168 Huang, K. *et al.* Investigation of the Role of Genes Encoding Zinc Exporters *zntA*, *zitB*, and *fiEF* during *Salmonella Typhimurium* Infection. *Front Microbiol* **8**, 2656, doi:10.3389/fmicb.2017.02656 (2017).
- 169 Liu, J. Z. *et al.* Zinc sequestration by the neutrophil protein calprotectin enhances *Salmonella* growth in the inflamed gut. *Cell Host Microbe* **11**, 227-239, doi:10.1016/j.chom.2012.01.017 (2012).
- 170 Grim, K. P. *et al.* The Metallophore Staphylopin Enables *Staphylococcus aureus* To Compete with the Host for Zinc and Overcome Nutritional Immunity. *mBio* **8**, e01281-01217, doi:10.1128/mBio.01281-17 (2017).

- 171 Bayle, L. *et al.* Zinc uptake by *Streptococcus pneumoniae* depends on both AdcA and AdcAll and is essential for normal bacterial morphology and virulence. *Molecular microbiology* **82**, 904-916, doi:10.1111/j.1365-2958.2011.07862.x (2011).
- 172 Tedde, V., Rosini, R. & Galeotti, C. L. Zn²⁺ Uptake in *Streptococcus pyogenes*: Characterization of *adcA* and *lmb* Null Mutants. *PloS one* **11**, e0152835, doi:10.1371/journal.pone.0152835 (2016).
- 173 Bobrov, A. G. *et al.* Zinc transporters YbtX and ZnuABC are required for the virulence of *Yersinia pestis* in bubonic and pneumonic plague in mice. *Metallomics* **9**, 757-772, doi:10.1039/c7mt00126f (2017).
- 174 Moreno, M. A. *et al.* The regulation of zinc homeostasis by the ZafA transcriptional activator is essential for *Aspergillus fumigatus* virulence. *Molecular microbiology* **64**, 1182-1197, doi:10.1111/j.1365-2958.2007.05726.x (2007).
- 175 Crawford, A. C. *et al.* Biphasic zinc compartmentalisation in a human fungal pathogen. *PLoS pathogens* **14**, e1007013, doi:10.1371/journal.ppat.1007013 (2018).
- 176 Citiulo, F. *et al.* *Candida albicans* scavenges host zinc via Pra1 during endothelial invasion. *PLoS pathogens* **8**, e1002777, doi:10.1371/journal.ppat.1002777 (2012).
- 177 Schneider, R. d. O. *et al.* Zap1 Regulates Zinc Homeostasis and Modulates Virulence in *Cryptococcus gattii*. *PloS one* **7**, e43773, doi:10.1371/journal.pone.0043773 (2012).
- 178 Cantacessi, C., Dantas-Torres, F., Nolan, M. J. & Otranto, D. The past, present, and future of *Leishmania* genomics and transcriptomics. *Trends in parasitology* **31**, 100-108, doi:10.1016/j.pt.2014.12.012 (2015).
- 179 Peacock, C. S. *et al.* Comparative genomic analysis of three *Leishmania* species that cause diverse human disease. *Nature genetics* **39**, 839-847, doi:10.1038/ng2053 (2007).
- 180 Fernandez-Martin, K. G. *et al.* Genome-wide identification, in silico characterization and expression analysis of ZIP-like genes from *Trichomonas vaginalis* in response to Zinc and Iron. *Biometals : an international journal on the role of metal ions in biology, biochemistry, and medicine* **30**, 663-675, doi:10.1007/s10534-017-0034-x (2017).
- 181 Sahu, T. *et al.* ZIPCO, a putative metal ion transporter, is crucial for *Plasmodium* liver-stage development. *EMBO Mol Med* **6**, 1387-1397, doi:10.15252/emmm.201403868 (2014).
- 182 Chasen, N. M., Stasic, A. J., Asady, B., Coppens, I. & Moreno, S. N. J. The Vacuolar Zinc Transporter TgZnT Protects *Toxoplasma gondii* from Zinc Toxicity. *mSphere* **4**, doi:10.1128/mSphere.00086-19 (2019).
- 183 Huynh, C., Sacks, D. L. & Andrews, N. W. A *Leishmania amazonensis* ZIP family iron transporter is essential for parasite replication within macrophage phagolysosomes. *The Journal of experimental medicine* **203**, 2363-2375, doi:10.1084/jem.20060559 (2006).
- 184 Jacques, I., Andrews, N. W. & Huynh, C. Functional characterization of LIT1, the *Leishmania amazonensis* ferrous iron transporter. *Molecular and biochemical parasitology* **170**, 28-36, doi:10.1016/j.molbiopara.2009.12.003 (2010).
- 185 Docampo, R., de Souza, W., Miranda, K., Rohloff, P. & Moreno, S. N. J. Acidocalcisomes - Conserved from bacteria to man. *Nature Reviews Microbiology* **3**, 251-261, doi:10.1038/nrmicro1097 (2005).
- 186 Docampo, R. & Moreno, S. N. J. Acidocalcisome: A novel Ca²⁺ storage compartment in trypanosomatids and apicomplexan parasites. *Parasitology today* **15**, 443-448, doi:Doi 10.1016/S0169-4758(99)01531-8 (1999).
- 187 LeFurgey, A., Ingram, P. & Blum, J. J. Compartmental responses to acute osmotic stress in *Leishmania* major result in rapid loss of Na⁺ and Cl⁻. *Comp Biochem Phys A* **128**, 385-394, doi:Doi 10.1016/S1095-6433(00)00319-6 (2001).
- 188 Lefurgey, A., Ingram, P. & Blum, J. J. Elemental Composition of Polyphosphate-Containing Vacuoles and Cytoplasm of *Leishmania-Major*. *Molecular and biochemical parasitology* **40**, 77-86, doi:Doi 10.1016/0166-6851(90)90081-V (1990).

- 189 Dvorak, J. A., Engel, J. C., Leapman, R. D., Swyt, C. R. & Pella, P. A. Trypanosoma cruzi: elemental composition heterogeneity of cloned stocks. *Molecular and biochemical parasitology* **31**, 19-26, doi:[https://doi.org/10.1016/0166-6851\(88\)90141-7](https://doi.org/10.1016/0166-6851(88)90141-7) (1988).
- 190 Scott, D. A., Docampo, R., Dvorak, J. A., Shi, S. & Leapman, R. D. In Situ Compositional Analysis of Acidocalcisomes in Trypanosoma cruzi. *Journal of Biological Chemistry* **272**, 28020-28029, doi:10.1074/jbc.272.44.28020 (1997).
- 191 Miranda, K., Benchimol, M., Docampo, R. & de Souza, W. The fine structure of acidocalcisomes in Trypanosoma cruzi. *Parasitol Res* **86**, 373-384, doi:DOI 10.1007/s004360050682 (2000).
- 192 Viegas, M. Study of a *Leishmania infantum* zinc transporter - what is its role in zinc homeostasis? *MSc thesis, Faculdade de Ciências da Universidade do Porto, Porto*.
- 193 Ramos, A. S. Study of the regulation of a zinc transporter in *Leishmania infantum*. *MSc thesis, Faculdade de Ciências da Universidade do Porto, Porto*.
- 194 Peng, D., Kurup, S. P., Yao, P. Y., Minning, T. A. & Tarleton, R. L. CRISPR-Cas9-mediated single-gene and gene family disruption in Trypanosoma cruzi. *mBio* **6**, e02097-02014, doi:10.1128/mBio.02097-14 (2015).
- 195 Lander, N., Li, Z. H., Niyogi, S. & Docampo, R. CRISPR/Cas9-Induced Disruption of Paraflagellar Rod Protein 1 and 2 Genes in Trypanosoma cruzi Reveals Their Role in Flagellar Attachment. *mBio* **6**, e01012, doi:10.1128/mBio.01012-15 (2015).
- 196 Sollelis, L. *et al.* First efficient CRISPR-Cas9-mediated genome editing in Leishmania parasites. *Cellular microbiology* **17**, 1405-1412, doi:10.1111/cmi.12456 (2015).
- 197 Zhang, W. W. & Matlashewski, G. CRISPR-Cas9-Mediated Genome Editing in Leishmania donovani. *mBio* **6**, e00861, doi:10.1128/mBio.00861-15 (2015).
- 198 Leão, T. CRISPR-Cas9-mediated ablation and functional analysis of the zinc transporter LiZIP3 in *Leishmania infantum*. *BSc report, Faculdade de Ciências da Universidade do Porto, Instituto de Ciências Biomédicas Abel Salazar, Porto*. (2016).
- 199 Eide, D. J. An "inordinate fondness for transporters" explained? *Science signaling* **5**, pe5, doi:10.1126/scisignal.2002837 (2012).
- 200 Mishra, J., Carpenter, S. & Singh, S. Low serum zinc levels in an endemic area of visceral leishmaniasis in Bihar, India. *The Indian journal of medical research* **131**, 793-798 (2010).
- 201 Jinek, M. *et al.* A programmable dual-RNA-guided DNA endonuclease in adaptive bacterial immunity. *Science* **337**, 816-821, doi:10.1126/science.1225829 (2012).
- 202 Cong, L. *et al.* Multiplex genome engineering using CRISPR/Cas systems. *Science* **339**, 819-823, doi:10.1126/science.1231143 (2013).
- 203 Makarova, K. S., Grishin, N. V., Shabalina, S. A., Wolf, Y. I. & Koonin, E. V. A putative RNA-interference-based immune system in prokaryotes: computational analysis of the predicted enzymatic machinery, functional analogies with eukaryotic RNAi, and hypothetical mechanisms of action. *Biology direct* **1**, 7, doi:10.1186/1745-6150-1-7 (2006).
- 204 Barrangou, R. *et al.* CRISPR provides acquired resistance against viruses in prokaryotes. *Science* **315**, 1709-1712, doi:10.1126/science.1138140 (2007).
- 205 Grissa, I., Vergnaud, G. & Pourcel, C. The CRISPRdb database and tools to display CRISPRs and to generate dictionaries of spacers and repeats. *BMC bioinformatics* **8**, 172, doi:10.1186/1471-2105-8-172 (2007).
- 206 Ishino, Y., Shinagawa, H., Makino, K., Amemura, M. & Nakata, A. Nucleotide sequence of the iap gene, responsible for alkaline phosphatase isozyme conversion in Escherichia coli, and identification of the gene product. *Journal of bacteriology* **169**, 5429-5433 (1987).
- 207 Bolotin, A., Quinquis, B., Sorokin, A. & Ehrlich, S. D. Clustered regularly interspaced short palindrome repeats (CRISPRs) have spacers of extrachromosomal origin. *Microbiology* **151**, 2551-2561, doi:10.1099/mic.0.28048-0 (2005).

- 208 Mojica, F. J., Diez-Villasenor, C., Garcia-Martinez, J. & Soria, E. Intervening sequences of regularly spaced prokaryotic repeats derive from foreign genetic elements. *Journal of molecular evolution* **60**, 174-182, doi:10.1007/s00239-004-0046-3 (2005).
- 209 Pourcel, C., Salvignol, G. & Vergnaud, G. CRISPR elements in *Yersinia pestis* acquire new repeats by preferential uptake of bacteriophage DNA, and provide additional tools for evolutionary studies. *Microbiology* **151**, 653-663, doi:10.1099/mic.0.27437-0 (2005).
- 210 Gee, K. R., Zhou, Z.-L., Qian, W.-J. & Kennedy, R. Detection and Imaging of Zinc Secretion from Pancreatic β -Cells Using a New Fluorescent Zinc Indicator. *Journal of the American Chemical Society* **124**, 776-778, doi:10.1021/ja011774y (2002).
- 211 Marraffini, L. A. & Sontheimer, E. J. CRISPR interference limits horizontal gene transfer in staphylococci by targeting DNA. *Science* **322**, 1843-1845, doi:10.1126/science.1165771 (2008).
- 212 Garneau, J. E. *et al.* The CRISPR/Cas bacterial immune system cleaves bacteriophage and plasmid DNA. *Nature* **468**, 67-71, doi:10.1038/nature09523 (2010).
- 213 Chao, Y. & Fu, D. Kinetic Study of the Antiport Mechanism of an *Escherichia coli* Zinc Transporter, ZitB. *Journal of Biological Chemistry* **279**, 12043-12050, doi:10.1074/jbc.M313510200 (2004).
- 214 Nishimasu, H. *et al.* Crystal structure of Cas9 in complex with guide RNA and target DNA. *Cell* **156**, 935-949, doi:10.1016/j.cell.2014.02.001 (2014).
- 215 Gasiunas, G., Barrangou, R., Horvath, P. & Siksnys, V. Cas9-crRNA ribonucleoprotein complex mediates specific DNA cleavage for adaptive immunity in bacteria. *Proceedings of the National Academy of Sciences of the United States of America* **109**, E2579-2586, doi:10.1073/pnas.1208507109 (2012).
- 216 Bottcher, R. *et al.* Efficient chromosomal gene modification with CRISPR/cas9 and PCR-based homologous recombination donors in cultured *Drosophila* cells. *Nucleic acids research* **42**, e89, doi:10.1093/nar/gku289 (2014).
- 217 Paix, A. *et al.* Scalable and versatile genome editing using linear DNAs with microhomology to Cas9 Sites in *Caenorhabditis elegans*. *Genetics* **198**, 1347-1356, doi:10.1534/genetics.114.170423 (2014).
- 218 Lin, S., Staahl, B. T., Alla, R. K. & Doudna, J. A. Enhanced homology-directed human genome engineering by controlled timing of CRISPR/Cas9 delivery. *eLife* **3**, e04766, doi:10.7554/eLife.04766 (2014).
- 219 Li, J. F. *et al.* Multiplex and homologous recombination-mediated genome editing in *Arabidopsis* and *Nicotiana benthamiana* using guide RNA and Cas9. *Nature biotechnology* **31**, 688-691, doi:10.1038/nbt.2654 (2013).
- 220 Xie, K. & Yang, Y. RNA-guided genome editing in plants using a CRISPR-Cas system. *Molecular plant* **6**, 1975-1983, doi:10.1093/mp/sst119 (2013).
- 221 Upadhyay, S. K., Kumar, J., Alok, A. & Tuli, R. RNA-guided genome editing for target gene mutations in wheat. *G3* **3**, 2233-2238, doi:10.1534/g3.113.008847 (2013).
- 222 Jia, H. & Wang, N. Targeted genome editing of sweet orange using Cas9/sgRNA. *PloS one* **9**, e93806, doi:10.1371/journal.pone.0093806 (2014).
- 223 Zhang, H. *et al.* The CRISPR/Cas9 system produces specific and homozygous targeted gene editing in rice in one generation. *Plant biotechnology journal* **12**, 797-807, doi:10.1111/pbi.12200 (2014).
- 224 Bassett, A. R., Tibbit, C., Ponting, C. P. & Liu, J. L. Highly efficient targeted mutagenesis of *Drosophila* with the CRISPR/Cas9 system. *Cell reports* **4**, 220-228, doi:10.1016/j.celrep.2013.06.020 (2013).
- 225 Gratz, S. J. *et al.* Genome engineering of *Drosophila* with the CRISPR RNA-guided Cas9 nuclease. *Genetics* **194**, 1029-1035, doi:10.1534/genetics.113.152710 (2013).
- 226 Hwang, W. Y. *et al.* Efficient genome editing in zebrafish using a CRISPR-Cas system. *Nature biotechnology* **31**, 227-229, doi:10.1038/nbt.2501 (2013).

- 227 Ota, S., Hisano, Y., Ikawa, Y. & Kawahara, A. Multiple genome modifications by the CRISPR/Cas9 system in zebrafish. *Genes to cells : devoted to molecular & cellular mechanisms* **19**, 555-564, doi:10.1111/gtc.12154 (2014).
- 228 Friedland, A. E. *et al.* Heritable genome editing in *C. elegans* via a CRISPR-Cas9 system. *Nature methods* **10**, 741-743, doi:10.1038/nmeth.2532 (2013).
- 229 Wang, H. *et al.* One-step generation of mice carrying mutations in multiple genes by CRISPR/Cas-mediated genome engineering. *Cell* **153**, 910-918, doi:10.1016/j.cell.2013.04.025 (2013).
- 230 Yang, H. *et al.* One-step generation of mice carrying reporter and conditional alleles by CRISPR/Cas-mediated genome engineering. *Cell* **154**, 1370-1379, doi:10.1016/j.cell.2013.08.022 (2013).
- 231 Cheng, A. W. *et al.* Multiplexed activation of endogenous genes by CRISPR-on, an RNA-guided transcriptional activator system. *Cell research* **23**, 1163-1171, doi:10.1038/cr.2013.122 (2013).
- 232 Ma, Y. *et al.* Heritable multiplex genetic engineering in rats using CRISPR/Cas9. *PLoS one* **9**, e89413, doi:10.1371/journal.pone.0089413 (2014).
- 233 Hu, X. *et al.* Heritable gene-targeting with gRNA/Cas9 in rats. *Cell research* **23**, 1322-1325, doi:10.1038/cr.2013.141 (2013).
- 234 Jinek, M. *et al.* RNA-programmed genome editing in human cells. *eLife* **2**, e00471, doi:10.7554/eLife.00471 (2013).
- 235 Mali, P. *et al.* RNA-guided human genome engineering via Cas9. *Science* **339**, 823-826, doi:10.1126/science.1232033 (2013).
- 236 Shen, B., Brown, K. M., Lee, T. D. & Sibley, L. D. Efficient gene disruption in diverse strains of *Toxoplasma gondii* using CRISPR/CAS9. *mBio* **5**, e01114-01114, doi:10.1128/mBio.01114-14 (2014).
- 237 Ghorbal, M. *et al.* Genome editing in the human malaria parasite *Plasmodium falciparum* using the CRISPR-Cas9 system. *Nature biotechnology* **32**, 819-821, doi:10.1038/nbt.2925 (2014).
- 238 Beneke, T. *et al.* A CRISPR Cas9 high-throughput genome editing toolkit for kinetoplastids. *Royal Society Open Science* **4**, 170095, doi:10.1098/rsos.170095 (2017).
- 239 Papadopoulou, B. & Dumas, C. Parameters controlling the rate of gene targeting frequency in the protozoan parasite *Leishmania*. *Nucleic acids research* **25**, 4278-4286 (1997).
- 240 Dean, S. *et al.* A toolkit enabling efficient, scalable and reproducible gene tagging in trypanosomatids. *Open biology* **5**, 140197, doi:10.1098/rsob.140197 (2015).
- 241 Calvo-Alvarez, E. *et al.* Appraisal of a *Leishmania major* strain stably expressing mCherry fluorescent protein for both in vitro and in vivo studies of potential drugs and vaccine against cutaneous leishmaniasis. *PLoS neglected tropical diseases* **6**, e1927, doi:10.1371/journal.pntd.0001927 (2012).
- 242 Peng, D. & Tarleton, R. EuPaGDT: a web tool tailored to design CRISPR guide RNAs for eukaryotic pathogens. *Microb Genom* **1**, e000033, doi:10.1099/mgen.0.000033 (2015).
- 243 Aslett, M. *et al.* TriTrypDB: a functional genomic resource for the Trypanosomatidae. *Nucleic acids research* **38**, D457-462, doi:10.1093/nar/gkp851 (2010).
- 244 Carvalho, S. Studies on metal acquisition systems in *Leishmania infantum*. *PhD thesis, Instituto de Ciências Biomédicas Abel Salazar, Porto.* (2015).
- 245 Buffet, P. A., Sulahian, A., Garin, Y. J., Nassar, N. & Derouin, F. Culture microtitration: a sensitive method for quantifying *Leishmania infantum* in tissues of infected mice. *Antimicrob Agents Chemother* **39**, 2167-2168, doi:10.1128/aac.39.9.2167 (1995).
- 246 Rogers, M. B. *et al.* Chromosome and gene copy number variation allow major structural change between species and strains of *Leishmania*. *Genome research* **21**, 2129-2142, doi:10.1101/gr.122945.111 (2011).

- 247 Dumetz, F. *et al.* Modulation of Aneuploidy in *Leishmania donovani* during Adaptation to Different In Vitro and In Vivo Environments and Its Impact on Gene Expression. *mBio* **8**, doi:10.1128/mBio.00599-17 (2017).
- 248 Mei, Y., Wang, Y., Chen, H., Sun, Z. S. & Ju, X. D. Recent Progress in CRISPR/Cas9 Technology. *Journal of genetics and genomics = Yi chuan xue bao* **43**, 63-75, doi:10.1016/j.jgg.2016.01.001 (2016).
- 249 Engwerda, C. R., Ato, M. & Kaye, P. M. Macrophages, pathology and parasite persistence in experimental visceral leishmaniasis. *Trends in parasitology* **20**, 524-530, doi:10.1016/j.pt.2004.08.009 (2004).
- 250 den Boer, M., Argaw, D., Jannin, J. & Alvar, J. Leishmaniasis impact and treatment access. *Clinical microbiology and infection : the official publication of the European Society of Clinical Microbiology and Infectious Diseases* **17**, 1471-1477, doi:10.1111/j.1469-0691.2011.03635.x (2011).
- 251 Ivens, A. C. *et al.* The genome of the kinetoplastid parasite, *Leishmania major*. *Science* **309**, 436-442, doi:10.1126/science.1112680 (2005).
- 252 El-Sayed, N. M. *et al.* Comparative genomics of trypanosomatid parasitic protozoa. *Science* **309**, 404-409, doi:10.1126/science.1112181 (2005).
- 253 Haile, S. & Papadopoulou, B. Developmental regulation of gene expression in trypanosomatid parasitic protozoa. *Current opinion in microbiology* **10**, 569-577, doi:10.1016/j.mib.2007.10.001 (2007).
- 254 Martinez-Calvillo, S., Vizuet-de-Rueda, J. C., Florencio-Martinez, L. E., Manning-Cela, R. G. & Figueroa-Angulo, E. E. Gene expression in trypanosomatid parasites. *Journal of biomedicine & biotechnology* **2010**, 525241, doi:10.1155/2010/525241 (2010).
- 255 Dillon, L. A. *et al.* Transcriptomic profiling of gene expression and RNA processing during *Leishmania major* differentiation. *Nucleic acids research* **43**, 6799-6813, doi:10.1093/nar/gkv656 (2015).
- 256 Inbar, E. *et al.* The Transcriptome of *Leishmania major* Developmental Stages in Their Natural Sand Fly Vector. *mBio* **8**, doi:10.1128/mBio.00029-17 (2017).

Chapter 8: Appendix

8.1 Supplementary Figures

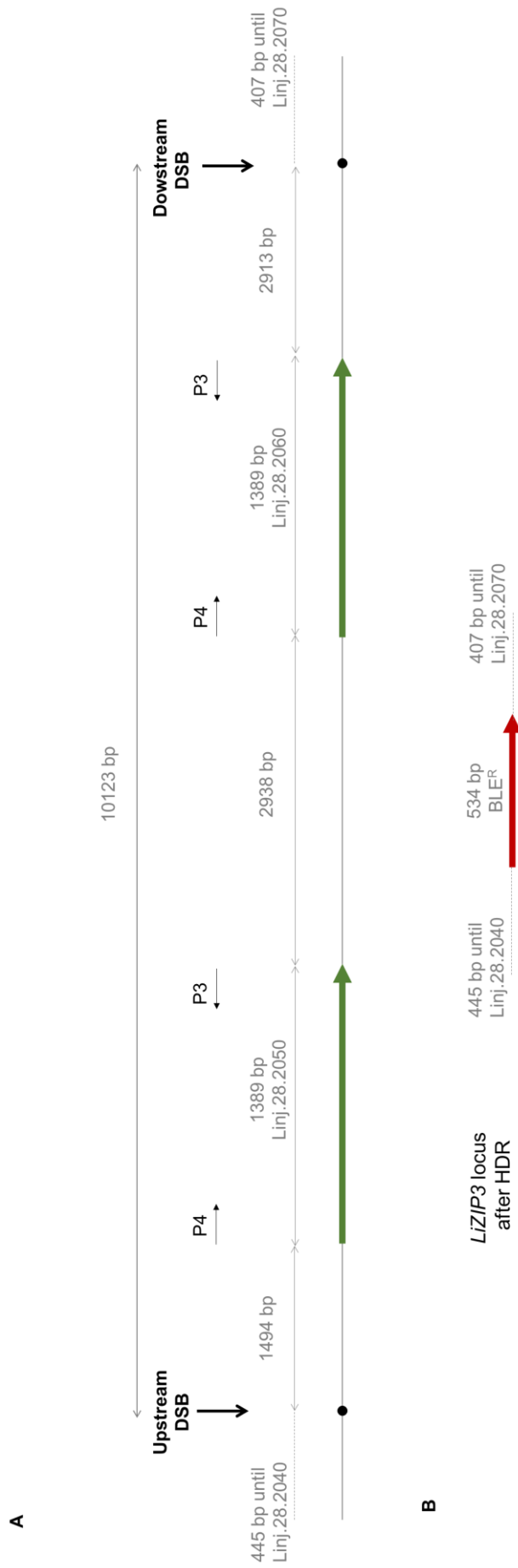


Fig. S 1. Schematic representation of the LiZIP3 locus targeting (A), deletion and substitution by a Ble cassette (B) using CRISPR-Cas9 in *L. infantum* (Leão, T. & Tomás, A.M., unpublished results). Primers used in this work are represented. The scheme is not drawn to scale. DSB: Double strand break; HDR: homologous directed recombination; BLE^R: Bleomycin

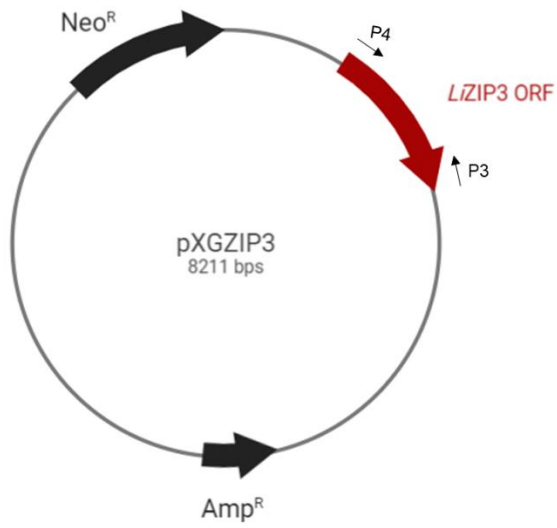


Fig. S 2. Schematic representation of the pXGZIP3 expression plasmid^{1,246}. The vector enables ectopic expression of LiZIP3. Neo^R: Neomycin resistance gene. Amp^R: Ampicillin resistance gene. The scheme is not drawn to scale.

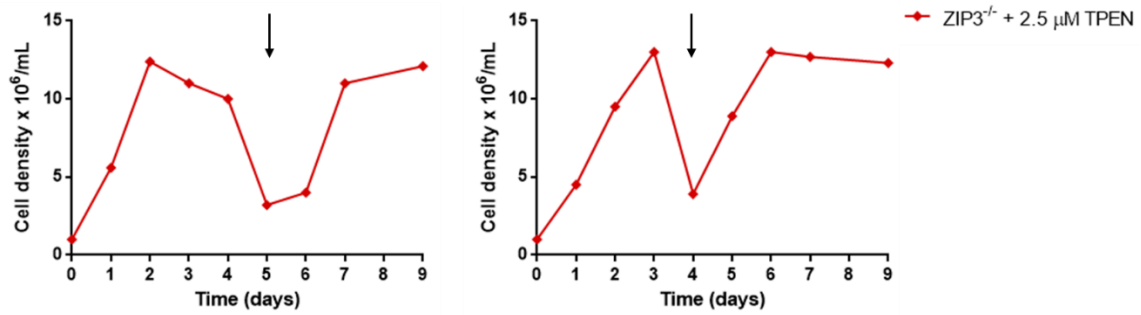


Fig. S 3. LiZIP3^{-/-} growth contraction in the presence of 2.5 μM TPEN is specifically due to zinc restriction. Growth curves of ZIP3^{-/-} promastigotes in the presence of 2.5 μM TPEN. Cultures were supplemented with 50 μM ZnCl₂ when cell density declined (arrow). After zinc supplementation, parasite growth resumed. Parasites were synchronized prior to the beginning of the experiment and, at day 0, cells were seeded at 10⁶ cells/mL. Cell counting was performed in the indicated time points. Two independent experiments are shown. See Fig. 2 and main text for additional information.

Disclosing the zinc acquisition and homeostatic machinery of *Leishmania* parasites

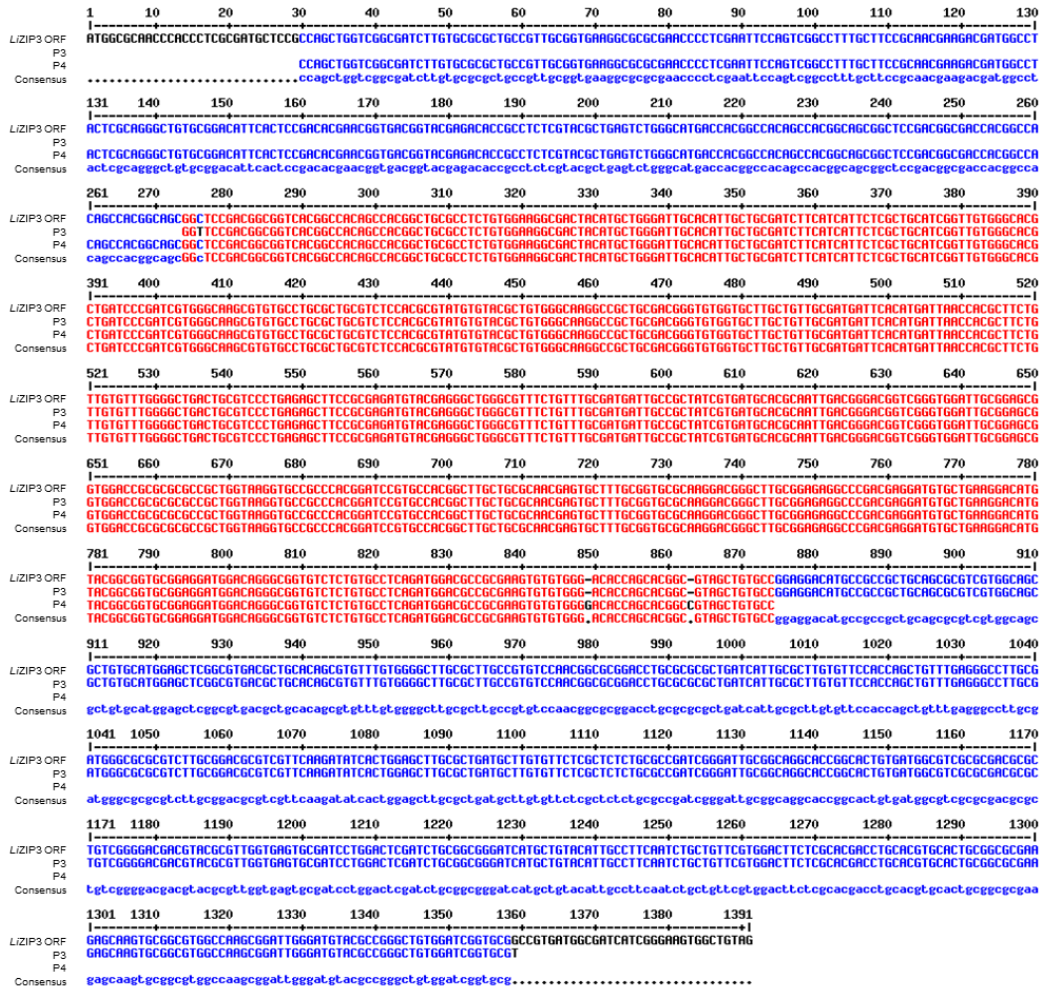


Fig. S 4. Sequencing results from the assembled pLEXSYZIP3 construct, using the primer pair P3+P4. The resulting sequence was compared to the LiZIP3 ORF. See Fig. 8 for primer location.

Disclosing the zinc acquisition and homeostatic machinery of *Leishmania* parasites

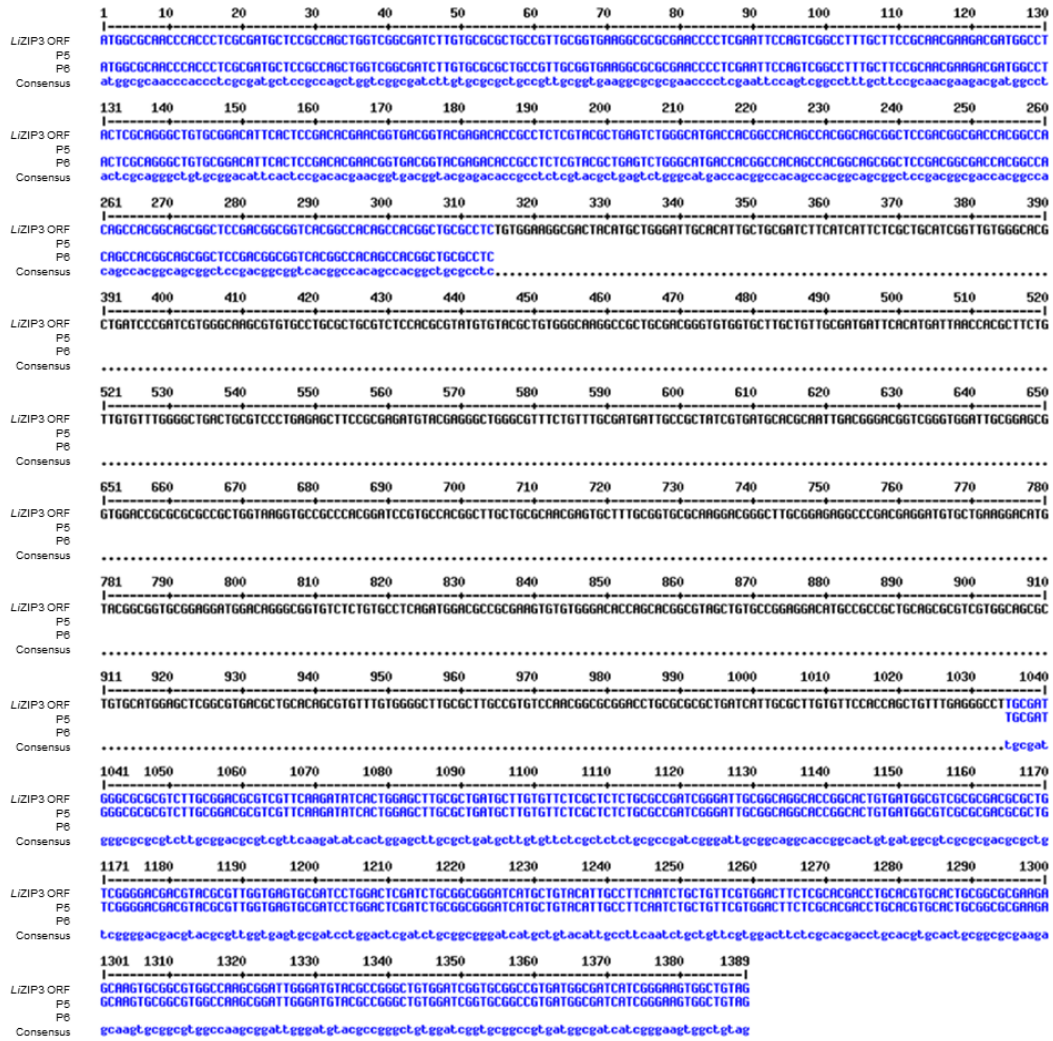


Fig. S 5. Sequencing results from the assembled pLEXSYZIP3 construct, using the primer pair P5+P6. The resulting sequence was compared to the LiZIP3 ORF. See Fig.8 for primer location.

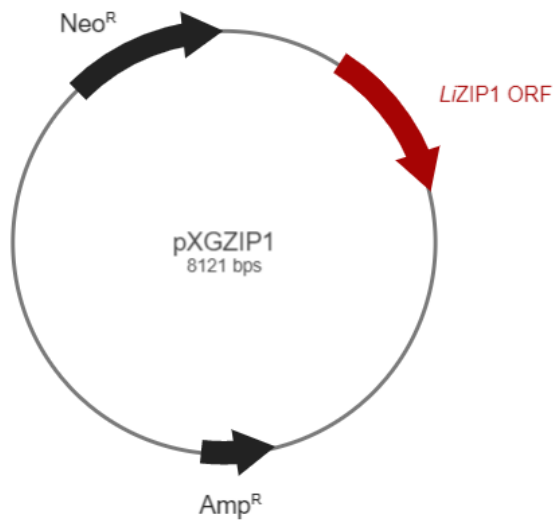


Fig. S 6. Schematic representation of the pXGZIP1 expression plasmid²⁴⁶. The vector enables ectopic expression of LiZIP1. *Neo^R*: Neomycin resistance gene. *Amp^R*: Ampicillin resistance gene. The scheme is not drawn to scale

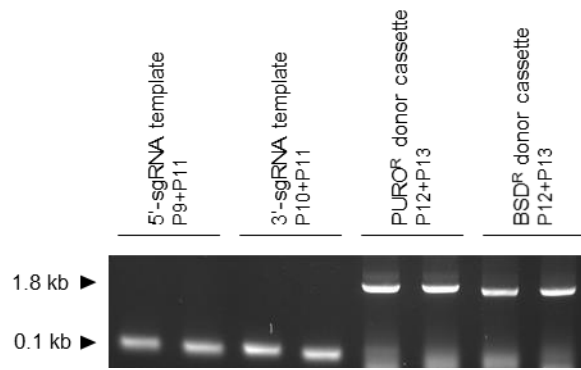


Fig. S 7. Gel electrophoresis of the sgRNAs and donor DNA cassettes used to abrogate the LiZIP1 locus. Primer pairs used in each PCR amplification are depicted.

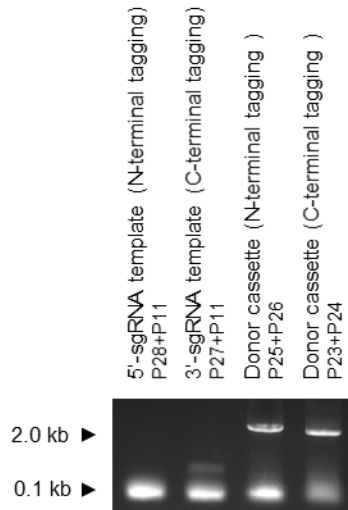


Fig. S 8. Gel electrophoresis of the sgRNAs and donor DNA cassettes used to knock-in the mNeonGreen-carrying cassette into the N-/C-terminus of LiZIP2. Primer pairs used in each PCR amplification are depicted.

8.2 Supplementary Tables

Table S 1. Oligonucleotides used in this work. Clamp sequences are indicated in lower case and restriction sites are in *italic*.

Primer ID	Lab List ID	Sequence	Purpose
P1	844	5' - <i>ggaagatct</i> ATGGCGCAACCCACCCTC - 3'	Sense primer to amplify the <i>LiZIP3</i> ORF from the pUC19_ZIP3 plasmid and clone into the pLEXSY_Hyg vector (introduces <i>Bgl</i> II restriction site)
P2	845	5' - <i>atttgcggccgc</i> CTACAGCCACTTCCCGATG - 3'	Antisense primer to amplify the <i>LiZIP3</i> ORF from the pUC19_ZIP3 plasmid and clone into the pLEXSY_Hyg vector (introduces <i>NofI</i> restriction site)
P3	204	5' - <i>tgctctaga</i> ATGGCGCAACCCACCCTC - 3'	Antisense primer annealing at the end of <i>LiZIP3</i> ORF. Used to sequence the pLEXSY_ZIP3 vector
P4	203	5' - <i>caccgctcag</i> CTACAGCCACTTCCCGATG - 3'	Sense primer annealing at the beginning of the <i>LiZIP3</i> ORF. Used to sequence the pLEXSY_ZIP3 vector
P5	219	5' - TGATCATTGGCGTTGTGT - 3'	Sense primer annealing at ~300 bp from the end of <i>LiZIP3</i> ORF. Used to sequence the pLEXSY_ZIP3 vector
P6	220	5' - TCGCAGCAATGTGCAATC - 3'	Antisense primer annealing at ~400 bp from the beginning of <i>LiZIP3</i> ORF. Used to sequence the pLEXSY_ZIP3 vector

Table S 2. Oligonucleotides used in this work. (continued).

Primer ID	Lab List ID	Sequence	Purpose
P7	260	5' - CCGAGGGCAAAGGAATAG - 3'	Sense primer annealing at the end of the <i>Hyg</i> resistance gene. Used to confirm cassette integration in the ribosomal locus
P8	872	5' - GATCCAGCTGCAGGTTTAC - 3'	Antisense primer annealing at the end of the <i>SSU</i> gene. Used to confirm cassette integration in the ribosomal locus
P9	854	5' - GAAATTAATACGACTCACTATAGGGCAG GGAGTGGGTGAATTAATG GTTTAGAGCTAG AAATAGC - 3'	Sense primer to amplify the 5'-sgRNA to perform the knockout of the <i>LiZiP1</i> locus
P10	855	5' - GAAATTAATACGACTCACTATAGGGTCT CAGGCTTGATGAGGTAGTTT TAG AGCTAG AAATAGC - 3'	Sense primer to amplify the 3'-sgRNA to perform the knockout of the <i>LiZiP1</i> locus
P11	786	5' - AAAAGCACCGACTCGGTGCCACTTTTTTC AAGTTGATAACGGACTAGCCCTATTTT AACT TGCTATTTCTAGCTCT AAAAC - 3'	Antisense primer comprising the scaffold to generate sgRNAs
P12	856	5' - CTCTCCCTCACTCTTGTCGGCCTACCTC ATGTATAATGCAGACCTGCTGC - 3'	Sense primer to amplify the drug resistance cassette from pT plasmids and insert in the <i>LiZiP1</i> locus. Includes the 5' homology flank

Table S 4. Oligonucleotides used in this work. (continued).

Primer ID	Lab List ID	Sequence	Purpose
P13	857	5' - CGACGTCCTCTATGATACGCGTACCCAT A C C C A A T T T G A G A G A C C T G T G C - 3'	Sense primer to amplify the drug resistance cassette from pT plasmids and insert in the <i>LiZIP1</i> locus. Includes the 3' homology flank
P14	192	5' - cggactagtATGGAGACGGCGAAACTG - 3'	Sense primer annealing at the beginning of the <i>LiZIP1</i> ORF
P15	193	5' - ccggaattcCTACAGCCAGTTGCCAC - 3'	Antisense primer annealing at the end of the <i>LiZIP1</i> ORF
P16	216	5' - AGCTGTTCCGAGGGCATGG - 3'	Sense primer annealing at ~350 bp from the end of <i>LiZIP1</i> ORF
P17	827	5' - GGCTGAGAAAGGGCGTCTT - 3'	Sense primer annealing at the 5' UTR of the first <i>LiZIP1</i> ORF
P18	826	5' - TAGTGCTACTCACCGCCACG - 3'	Antisense primer annealing at the 3' UTR of the second <i>LiZIP1</i> ORF

Table S 5. Oligonucleotides used in this work. (continued).

Primer ID	Lab List ID	Sequence	Purpose
P19	828	5' - GCCGAGGACATGGTGCATGA - 3'	Sense primer annealing at the end of the puromycin resistance gene (PURO) ORF
P20	829	5' - CTCGCGTAGCAAGACGAACC - 3'	Antisense primer annealing at the beginning of the puromycin resistance gene (PURO) ORF
P21	406	5' - TTCGTGAATTGCTGCCCTC - 3'	Sense primer annealing at the end of the blasticidin resistance gene (BSD) ORF
P22	425	5' - CGCTGGCGACGCTGTAG - 3'	Antisense primer annealing at the beginning of the blasticidin resistance gene (BSD) ORF
P23	830	5' - AGTATCATGGCAGTGGGCAATACG TGGTCTGTTAGTAGTGGT TCCGG - 3'	Sense primer to amplify the knock-in cassette from pPLOT-mNG-blast-blast plasmid and insert in the C-terminus of the <i>LiZiP2</i> ORF. Includes the 5' homology flank
P24	835	5' - TGTTGTGTAGGCGGAGCAGCACAAGC CACCAATTTGAGAGACCTGTGC - 3'	Antisense primer to amplify the knock-in cassette from PLOT-mNG-blast-blast plasmid and insert in the C-terminus of the <i>LiZiP2</i> ORF. Includes the 3' homology flank

Table S 7. Oligonucleotides used in this work. (continued).

Primer ID	Lab List ID	Sequence	Purpose
P25	837	5' - TGCCCCCTTCCTCCCTGCCATGCCTCC GGTATAATGCAGACCTGCTGC - 3'	Sense primer to amplify the knock-in cassette from pPLOT-mNG-blast-blast plasmid and insert in the N-terminus of the <i>LiZIP2</i> ORF. Includes the 5' homology flank
P26	838	5' - CGGTGGCCACGGGTGCCATTGTGGTC ATACTACCCGATCCTGATCCAG - 3'	Antisense primer to amplify the knock-in cassette from PLOT-mNG-blast-blast plasmid and insert in the N-terminus of the <i>LiZIP2</i> ORF. Includes the 3' homology flank
P27	836	5' - GAAATTAATACGACTCACTATAGTGCGC AGGAGAGCGTCAACTGTTTTAGAGCTAGAAA TAGC - 3'	Sense primer to amplify the 3'-sgRNA to perform the knock-in in the C-terminus of the <i>LiZIP2</i> ORF
P28	839	5' - GAAATTAATACGACTCACTATAGGGGTT TGCGGCACACAACAAGTTTTAGAGCTAGAAA TAGC - 3'	Sense primer to amplify the 5'-sgRNA to perform the knock-in in the N-terminus of the <i>LiZIP2</i> ORF
P29	239	5' - ccgcgcacafatgTTTTTCGATGGCTTTGGAG - 3'	Sense primer annealing at ~600 bp from the end of the <i>LiZIP2</i> ORF
P30	240	5' - caccgctcgagCTGCAAGCCACCACCTGC - 3'	Antisense primer annealing at ~500 bp from the beginning of the <i>LiZIP2</i> ORF

Table S 8. Oligonucleotides used in this work. (continued).

Primer ID	Lab List ID	Sequence	Purpose
P31	847	5' - ATGGGGATGGACGAATTG - 3'	Sense primer annealing at the end of the <i>mNeonGreen</i> ORF
P32	848	5' - TTCCTCACCTTTCGAGAC - 3'	Antisense primer annealing at the beginning of the <i>mNeonGreen</i> ORF